Apoptosis Regulation via the Mitochondrial Pathway: Membrane Response upon Apoptotic Stimuli

Marc Antoine Sani

Akademisk avhandling

Som med vederbörligt tillstånd av rektorsämbetet vid Umeå universitet för avläggande av filosofie doktorsexamen i kemi.
Framläggs till offentligt försvar i BiA201, Biologihuset, Fredagen den 7 november 2008, kl. 13.00, Umeå universitet.
Avhandlingen kommer att försvaras på engelska.

Fakultetsopponent: **Prof. Dr. Antoinette Killian**, Chemical Biology and Organic Chemistry, Department of Chemistry, Faculty of Science
Utrecht University, The Netherlands.

Ph.D. Dissertation, November 2008
Department of Chemistry
Umeå University

Organisation
Umeå University
Department of Chemistry
SE-901 87 Umeå

Université Bordeaux 1
Institut Européen de Chimie et
Biologie IECB,
UMR 5248 CBMN, 33607 Pessac,
France

Document type
DOCTORAL THESIS

Date of publication
17th October 2008

Author
Marc-Antoine Sani

Title
Apoptosis Regulation via the Mitochondrial Pathway: Membrane Response upon Apoptotic Stimuli

Abstract
The aim of this thesis was the investigation of the mitochondrial response mechanisms upon apoptotic stimuli. The specific objectives were the biophysical characterization of membrane dynamics and the specific roles of lipids in the context of apoptotic regulation occurring at the mitochondrion and its complex membrane systems.
The BH4 domain is an anti-apoptotic specific domain of the Bcl-2 protein. Solid phase peptide synthesis was used to produce large amount of the peptide for biophysical studies. A protocol has been established and optimized, guarantying the required purity for biophysical studies. In detail the purification by high performance liquid chromatography and the characterisation via mass spectroscopy are described. The secondary structure of BH4 changes significantly in the presence of lipid vesicles as observed by infrared spectroscopy and circular dichroism. The BH4 peptide aggregates at the membrane surface and inserts slightly into the hydrophobic part of the membrane. Using nuclear magnetic resonance (NMR) and calorimetry techniques, it could even be shown that the BH4 domain modifies the dynamic and organization of the liposomes which mimic a mitochondrial surface. The second study was on the first helix of the pro-apoptotic protein Bax. This sequence called Bax-α1 has the function to address the cytosolic Bax protein to the mitochondrial membrane upon activation. Once again a protocol has been established for the synthesis and purification of this peptide. The aim was to elucidate the key role of cardiolipin, a mitochondria-specific phospholipid, in the interaction of Bax-α1 with the mitochondrial membrane system. The NMR and circular dichroism studies showed that Bax-α1 interacts with the membrane models only if they contain the cardiolipin, producing a strong electrostatic lock effect which is located at the membrane surface.
Finally, a new NMR approach was developed which allows the investigation of the lipid response of isolated active mitochondria upon the presence of apoptotic stimuli. The goal was there to directly monitor lipid specific the occurring changes during these physiological activities.

Keywords
Apoptosis, BH4 peptide, Bax-α1 peptide, model membrane, cardiolipin, solid phase peptide synthesis, circular dichroism, solid-state nuclear magnetic resonance spectroscopy.

Language: English **ISBN** 978-91-7264-676-6 **Number of pages**: 45+13

N° d'ordre :

THESE

présentée à

L'UNIVERSITE DE BORDEAUX 1

ECOLE DOCTORALE DES SCIENCES CHIMIQUES

Par **Marc Antoine Sani**

POUR OBTENIR LE GRADE DE

DOCTEUR

SPECIALITE : CHIMIE-PHYSIQUE

****

Régulation de l'apoptose au niveau mitochondrial: Réponse membranaire à des stimuli apoptotiques

****

Soutenue le 7 Novembre 2008

Après avis de :

Mme Antoinette Killian	Professeur de l'Université d'Utrecht	Rapporteur
M. Simon Tuck	Professeur assistant de l'université d'Umeå	Rapporteur

Devant la commission d'examen formée de :

Mme Antoinette Killian	Professeur de l'Université d'Utrecht	Rapporteur
M. Simon Tuck	Professeur assistant de l'université d'Umeå	Rapporteur
M. Jean-Marie Schmitter	Professeur de l'Université de Bordeaux 1	Président
M. Erick J. Dufourc	Directeur de recherche CNRS	Directeur de Thèse
M. Gerhard Gröbner	Professeur de l'Université d'Umeå	Directeur de Thèse

-2008-

Résumé :

Le but de cette thèse est de montrer la réponse de la membrane mitochondriale au cours la régulation de l'apoptose en étudiant l'effet de domaines clés sur la dynamique membranaire et l'importance de la composition phospholipidiques des modèles utilisés.
Le domaine BH4 est la partie spécifique anti-apoptotique de la famille Bcl-2. La première étape a été de synthétiser le peptide par voie chimique en utilisant la synthèse peptidique en phase solide. Un protocole décrivant les étapes de purification par chromatographie liquide et de caractérisation par spectroscopie de masse, garantissant une pureté indispensable pour des études biophysiques, a été établi. La modification de la structure secondaire du peptide interagissant avec des vésicules a été étudiée par spectroscopie infrarouge ainsi que par dichroïsme circulaire. Le peptide s'agrège à la surface et s'insère peu profondément dans la partie hydrophobe de la membrane. En utilisant la résonance magnétique nucléaire (RMN) et la calorimétrie, il a été montré que le peptide BH4 modifie l'organisation et la dynamique des liposomes mimant la surface mitochondriale. La deuxième étude a porté sur la première hélice de la protéine pro-apoptotique Bax (Bax-α1) qui a la propriété de diriger la protéine cytosolique vers la mitochondrie. Un protocole de synthèse et purification a été à nouveau établi. Le but de cette étude est de démontrer le rôle de l'interaction spécifique entre la cardiolipine, un phospholipide uniquement présent dans la mitochondrie et le peptide Bax-α1. Les études RMN ont montré que Bax-α1 n'interagissait uniquement que si la cardiolipine était présente, produisant un fort effet électrostatique piégeant le peptide à la surface de la membrane.
Enfin, un nouveau protocole permettant d'étudier la réponse des lipides de mitochondries isolées toujours actives par RMN est présenté. Le but est de pouvoir directement observer les modifications subies par chaque phospholipide de la mitochondrie.

Mots clés :

Apoptose, peptide BH4, peptide Bax-α1, modèle de membrane, cardiolipine, synthèse peptidique en phase solide, dichroïsme circulaire, RMN des solides.

Apoptosis Regulation via the Mitochondrial Pathway: Membrane Response upon Apoptotic Stimuli

Marc Antoine Sani

Ph.D. Dissertation, November 2008
Department of Chemistry
Umeå University

We all labour against our own cure, for death is the cure of all diseases.
SIR THOMAS BROWNE

À mon rayon de soleil, merci de m'avoir supporté, de m'avoir attendu, notre vie commence enfin

Department of Chemistry
Umeå University
SE-90187 Umeå
Sweden

Front cover: adapted from http://microscopy.fsu.edu
ISBN 978-91-7264-676-6
Printed by Print och Media, Umeå University, Umeå

Publications and manuscripts list

I. **Synthesis and secondary structure in membranes of the Bcl-2 anti-apoptotic domain BH4.**
Khemtémourian L*, Sani MA*, Bathany K, Gröbner G, Dufourc EJ. *J Pept Sci. 2006 Jan;12(1):58-64.*

II. **Pro-apoptotic bax-alpha1 synthesis and evidence for beta-sheet to alpha-helix conformational change as triggered by negatively charged lipid membranes.**
Sani MA, Loudet C, Gröbner G, Dufourc EJ. *J Pept Sci. 2007 Feb;13(2):100-6.*

III. **Restriction of lipid motion in membranes triggered by beta-sheet aggregation of the anti-apoptotic BH4 domain.**
Sani MA, Castano S, Dufourc EJ, Gröbner G. *FEBS J. 2008 Feb;275(3):561-72.*

IV. **How does the Bax-α1 targeting sequence interact with mitochondrial membranes: The role of cardiolipin.**
Sani MA, Dufourc EJ, Gröbner G. *Submitted to BBA –biomembrane*

V. **Tracking lipid interactions in intact mitochondria under oxidative stress by ex vivo solid state ^{31}P NMR spectroscopy.**
Sani MA, Keech O, Gardeström P, Dufourc EJ, Gröbner G. *Submitted to Nature Methods*

* Authors contributed equally to this work

Reprints were made with kind permission from the publishers.

List of abbreviations

ACN	acetonitrile
ANT	adenine nucleotide translocase
Arg	arginine
ATP	adenosine triphosphate
ATR	attenuated total reflection
BH	Bcl2 homology
BSA	bovine serum albumine
CD	circular dichroism
C_P	heat capacity
CP	cross polarization
CS	contact site
CSA	chemical shift anisotropy
Cys	cysteine
DCM	dichloromethane
DIEA	diisopropylethyl amine
DMF	N,N-dimethylformamide
EDT	ethane-di-thiol
FID	free induction decay
HBTU	2-(1H-Benzotriazole-1-yl)-1,1 ,3,3-tetramethyluronium hexafluorophosphate
HOBt	1-hydroxybenzotriazole
HPLC	high performance liquid chromatography
IM	inner membrane
IMS	inter membrane space
IR	infrared
LUV	large unilamellar vesicle
MALDI-TOF	matrix-assisted laser desorption-ionisation time of flight
MAS	magic angle spinning
Met	methionine
MLV	multi lamellar vesicle
MMP	mitochondrial membrane permeabilization
MPT	mitochondrial permeability transition

NMP	N-methyl piperazine
NMR	nuclear magnetic resonance
OM	outer membrane
PC	phosphatidylcholine
PCD	programmed cell death
PE	phosphatidylethanolamine
PTPC	permeability transition pore complex
ROS	reactive oxygen species
Ser	serine
SPPS	solid phase peptide synthesis
SUV	small unilamellar vesicle
TES	triethylsilane
TFA	trifluoroacetic acid
TFE	trifluoroethanol
Thr	threonine
TIS	triisopropylsilane
TM	transmembrane
T_P	transition temperature
Trp	tryptophan
Tyr	tyrosine
VDAC	voltage-dependent anion channel
$\Delta\nu$	quadrupolar splitting

Tables of content

I Apoptosis via the mitochondrial pathway: Introduction

Definition and focus

June the 27th 2008

Apoptosis (Greek: *apo* - from, *ptosis* - falling) was distinguished from traumatic cell death by Ross Kerr while he was studying tissues using electron microscopy at the University of Queensland Pathology Department in Brisbane. Following the publication of these results, Kerr was invited to join Professor Alastair R Currie and his Ph.D. student Andrew Wyllie, at the University of Aberdeen to continue his research. In 1972, the trio published a seminal article in the British Journal of Cancer [1]. Kerr had originally used the term "programmed cell necrosis" to describe the phenomenon but in the 1972 article this process of natural cell death was called apoptosis. Kerr, Wylie and Currie credited Professor James Cormack (Department of Greek, University of Aberdeen) with suggesting the term apoptosis. In Greek, apoptosis means "dropping off" of petals or leaves from plants or trees. Cormack reintroduced the term for medical use as it had a medical meaning for the Greeks over two thousand years before. Hippocrates used the term to mean "the falling off of the bones". Galen extended its meaning to "the dropping of the scabs". Cormack was without any doubt aware of this usage when he suggested the name. The debate continues over the correct pronunciation, with opinions divided between a pronunciation with a silent p and the p spelt out, as in the original Greek. (**Wikipedia**)

Apoptosis in google: **10 300 000 hits**

Apoptosis in google scholar: **2 330 000 hits**

Apoptosis in PubMed: **147 668 hits**

Apoptosis in ISI web of knowledge: **>100 000 hits**

Apoptosis has become a major field of research because homeostasis is a vital regulation in every complex system (eukaryotic). However, one has to realize this complexity and an endless ocean to describe apoptosis. Therefore I will focus only on regulation of apoptosis via the mitochondrial pathway. It means that apoptosis has not occurred yet in the cell and little information on the up/down-regulation will be done: I will mainly describe what happens if the mitochondrion encounters apoptotic stimuli (why are they here, how they are generated, is not described). But for once let be impolite and talk first about the host before talking about the guests…

a) Mitochondria

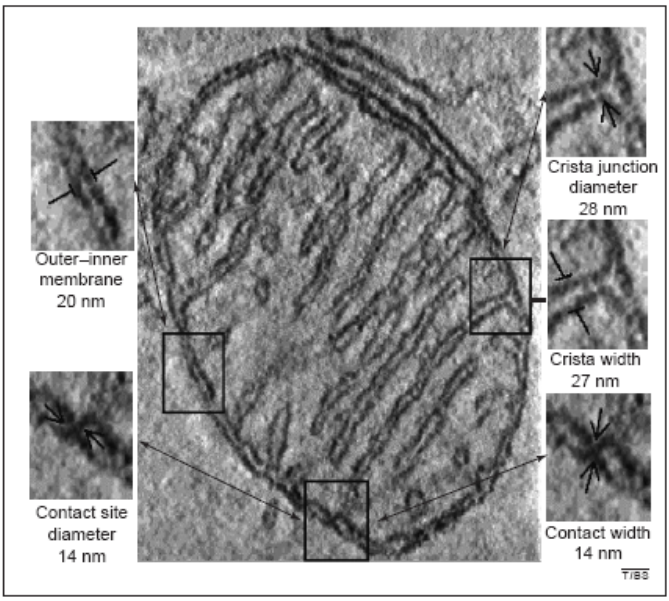

Figure 1 A single section through the 3D tomogram of a mitochondrion. (Adapted from Frey and Mannella, TIBS 2000 [2])

- Structure and internal organization

Mitochondria are present in varying numbers in any type of cell, for instance 1000 to 2000 mitochondria are contained in one rat liver cell which occupy roughly one fifth of the cell volume [3]. They are crucial organelles in the functioning of a cell. Their main task is to provide the energy (ATP), but they are also heavily involved in various signalling pathways including apoptosis. Mitochondria can be depicted as a cylinder of approximately 1µm diameter but they undergo strong morphological and size changes according to the cell development, metabolic state or alterations due to diseases. The mitochondrion contains an outer membrane (OM), an inner membrane (IM) and two internal compartments. Each compartment has a different lipid and protein composition, the protein machinery of the inner part being more strongly conserved along the cell types. It is noteworthy that mitochondria are inherited from the mother's ovum and do not replicate but rather partition before cell division by a complex coordinated machinery [4].

The outer membrane (OM)

It is a strainer. Indeed, large number of transport proteins (mainly porins, as the voltage-dependent anion channel (VDAC)) are present in the OM allowing molecules up to 5000 Daltons to translocate freely into the intermembrane space (IMS) [5]. Since most of the proteins are translated into the cytoplasm, protein transport is occurring specifically into different mitochondrial subunits mainly by TOM proteins complexes. Mitochondria even undergo fusion/fission via proteins (Fzo1) localized as well in the OM as in the IM. Many others proteins are not listed, and probably many still need to be identified but for the sake of brevity, this will not be presented here.

The OM is mainly composed of two phospholipids, phosphatidylcholine (PC) counting for 41 %w/w and phosphatidylethanolamine (PE) for 27% w/w, which confers a global neutral surface [6]. Whereas a significant amount of PE is present in the OM, well-known to favour hexagonal organization because of its surfactant packing parameter < 0.5, the OM displays a lamellar bilayer organization with an approximate thickness of 70Å [2]. There are controversial statements about the presence of the anionic cardiolipin there as a native phospholipid. Several studies have shown traces of cardiolipin in isolated outer membrane vesicles from different species (less than 5% at most). However, various groups have described the translocation of cardiolipin patches from the IM to the OM as a crucial event, especially in apoptosis [7; 8]. Indeed, cardiolipin is highly involved in the stabilization of membrane proteins and, as discussed below, the contact site formation between OM and IM. Then, the OM could expose highly negatively charged domains (containing cardiolipin), crucial in signalling, apoptosis regulation, etc…

The Intermembrane space (IMS)

Since the OM is highly permeable, the composition of the IMS resembles that of the cytosol, except for proteins of more than 5000 Da. A lot of enzymes, and various soluble proteins, such the apoptotic factors cytochrome C, pro-caspase, Diablo/SMAC, etc…, reside in the IMS. However, strong gradients of certain metabolites occur close to the inner membrane, required to keep the protein machinery going, such as the respiratory chain which needs proton, inorganic phosphates, ATP, etc.. The space between the two membranes is variable since mitochondria exhibit a strong morphological dynamics, but cryo-electron microscopy measured an averaged static value of 60Å [2].

The inner membrane (IM)

The proteins found in the IM have three main functions: oxidative phosphorylation of the electron-transport chain (complex I-IV, cytochromes, etc…), ATP synthesis (ATP synthase) and the transport of proteins that regulate the metabolic flux in the matrix (ANT, TIM, etc.). Additionally to PC (35% w/w) and PE (27%), the IM membranes contain a very specific "double" anionic phospholipid, cardiolipin (18%), which is intimately involved in many proteins stabilization and membrane structure formation [9; 10; 11]. The inner membrane contains in two different regions: the boundary inner membrane which adopts a lamellar structure similar to the OM with an identical thickness (70Å); and the cristae which are invaginations of the inner boundary membrane that protrude into the matrix. They are connected to the inner boundary membrane by narrow tubular structures (cristae junctions) of approximately 27nm width [2]. Interestingly, the morphology of the IM is highly regulative since gradients, metabolites flux and cytochrome C diffusions between compartments are restricted by the curvature. Likewise, the shape and the volume changes of cristae in response to alterations in osmotic or metabolic conditions is a vital mechanism.

The Matrix

The matrix contains a highly condensed mixture of many enzymes responsible for the oxidation of pyruvate and fatty acids, and for the citric acid cycle. It also contains the genetic material of mitochondria and the machinery for expression. In the respiratory process producing ATP, reactive oxygen species (ROS) are produced. They could be a source of damage for phospholipids and proteins but they are most often scavenged by proteins such SOD or glutathione proteins. ROS might play a role in apoptosis as apoptotic signal and/or important for mediating apoptotic proteins-phospholipids interactions.

The contact sites (CS)

Mitochondria undergo high trafficking between the cytosol and the matrix. If most of the time the translocation occurs via distinct transport proteins, some translocations occur simultaneously across the OM and the IM through region of contact between the two membranes. Furthermore, the fission-fusion process requires a close contact between the OM and the IM. Contact sites have been reported in all types of mitochondria and are stable complexes and not a partial fusion between the OM and the IM. Indeed, EM-microscopy reveals a contact thickness (~15nm) which is never below the sum of the IM and OM ones [11]. Their main function is to stabilize native pores connecting the cytosol directly to the matrix by

the association of VDAC, ANT, etc., known as the permeability transition pore complex (PTPC). They are also known to stabilize the cristae junction and might have other functions not identified yet. The PTPC has an important role for cytochrome C release in the apoptosis pathway [9; 10; 12].

The major feature of CS composition is the remarkable enrichment in cardiolipin content (~25% w/w) and in unsaturated phospholipids [6]. This means that CS have a pronounced dynamic and flexibility, allowing them to adapt quickly to shape variations or even facilitating the transfer of phospholipids from the IM to the OM. Indeed, cardiolipin patches have been identified in the OM, of course in low abundance, which sustains the signalling role of cardiolipin, and the close contact between the IM and the OM could provide the best candidate for their translocation.

- Apoptosis regulation via the mitochondrial pathway

Fundamental metabolic processes occur in mitochondria essential for the functioning of all eukaryotic cells. The striking observation that highlights the essential role of mitochondria in the intrinsic apoptosis pathway is the appearance of signs of disturbances long before any signs of apoptosis. This is not surprising because mitochondria contain various harmful molecules that can activate apoptosis via different pathways. Indeed, toxic compounds like ROS and apoptotic inducers proteins are released from the submitochondrial compartmentalization. Hence, mitochondrial membrane permeabilization (MMP) is a critical event and is the point of no return, and therefore lethal to the cell. Indeed, induction of MMP is sufficient to trigger apoptosis and pharmacological inhibitors preventing MMP stop the cell death [13; 14]. However, the regulation of MMP occurs via a broad spectrum of possibilities. Numerous pathological and physiological signals (calcium, reactive oxygen species, genotoxic stress, etc.) to stress response can trigger MMP putting mitochondria as an antenna for cell alterations [15; 16]. Of course, MMP can cause a deregulation of the energy production which is also a lethal event for the cell. MMP is a marker used in medicine for detection of apoptosis ex vivo in pathologies such as AIDS or leukaemia under chemotherapy [17; 18]. Also, several genetic diseases associated with cell disturbance have been linked to mutations in mitochondria genome or gene expressing mitochondrial proteins [19; 20]. Finally, various drugs have been developed that act on the MMP of mitochondria to stop or induce apoptosis and have been proved to be efficient, opening a huge field for disease treatments [13; 21; 22]. The MMP mechanism is not fully understood yet, especially how the OM, the IM or both of them

interact, and what complex protein machinery is involved in its regulation. More details will be discussed in the section II.b).

- The use of isolated mitochondria in apoptosis studies

Because there is much evidence of mitochondria's involvement in a wide range of cellular dysfunction, great efforts have been made to study this organelle in a great detail and depth. Of course, intact cells possess a complete set of factors that influence the apoptosis mechanism, but this is unfortunately also a major drawback. Indeed, the effect of one molecule could affect so many partners directly and/or indirectly that a specific molecular action is impossible to study. That is why one has to use model systems to provide a basic molecular understanding and then to try to make conclusions for the whole system. But here again, the connection between model system and intact system is always a problematic one. For instance, using model membrane mimicking mitochondrial domains to study the impact of apoptotic stimuli, such as protein domains, leads to a precise molecular view of any interactions occurring. However, the biological relevance of such studies may be questioned by the community of biologists. On the other hand, loading some drugs into living animals reveals the consequence of a complex interplay of numerous molecular mechanisms involved but fails to reveal any clear picture (That might explain the side effects of pills…). That is why a potential alternative is the use of *ex vivo* systems, here isolated mitochondria, to remove part of the unknown/uncontrolled side effects and to upgrade the basic lipid-peptide model. Many techniques have been developed to address important questions about the isolated mitochondria response during apoptosis stress. For instance, electron microscopy on isolated mitochondria revealed that MMP-induced cytochrome C release does not occur via mitochondrial swelling as it has been proposed [23]. However, the use of fluorescent probes trapped in the mitochondrial matrix, and quenchers such as Co^{2+}, provided evidence of a mitochondrial matrix swelling upon Ca^{2+} upload [24]. Again, this is a clear example of all the contradictory results existing and how sample preparation or the technique used affects results. Fluorescent probes added to proteins involved in apoptosis in order to monitor their targets/movements [25], effect of various stimuli as Ca^{2+} stress [26], membranes/proteins involved in the MMP [27] and many others studies are systematically performed on isolated mitochondria because they provide the closest "controlled" system to resolve molecular mechanisms as they might happen in a cell. Therefore, we tried to investigate the mitochondrial membrane of isolated mitochondria by non-invasive, high resolution solid-state ^{31}P NMR, and its response to calcium stress as a test (see V and MS V).

b) Bcl2 proteins regulation

The mitochondrial pathway of apoptosis is a central event in the managing of the homeostasis in living systems. By controlling the permeabilization of mitochondria, the Bcl2 family is the main regulator of the mitochondrial apoptosis activation [28; 29; 30]. The name-giving protein of this family, the Bcl-2 (B-Cell Lymphoma 2) proto-oncogene, was discovered to inhibit cell death rather than promote the cell proliferation [31]. Since then, many members of the Bcl2 family were found in mammals, well over twenty proteins classified in three functional groups.

- The Bcl2 family: function, location, structure

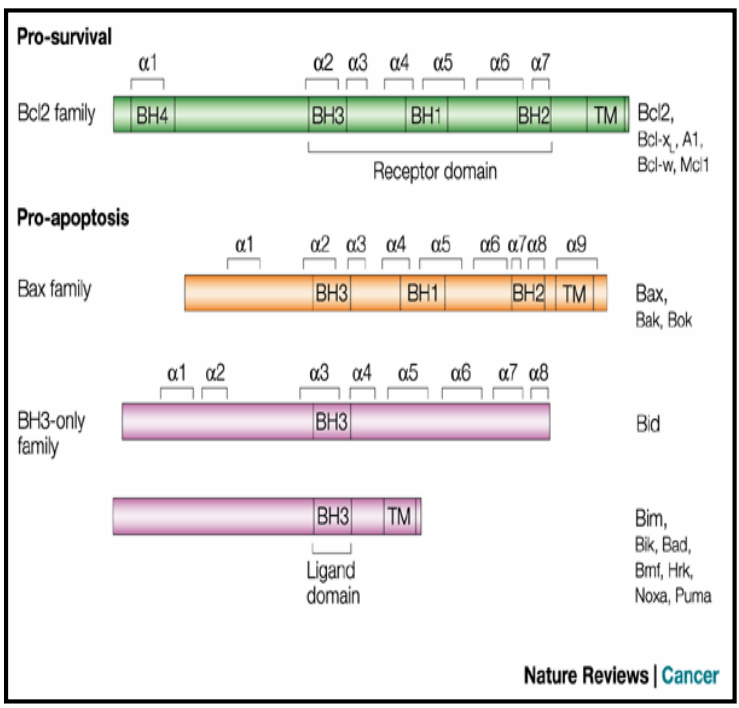

Figure 2. The apoptotic Bcl2 protein family with the sub populations and their important regulative domains (Adapted from Corry and Adams, Nature Review Cancer, 2002 [29])

The main feature of Bcl2 members is that they possess up to four conserved Bcl2 homology (BH) domains, all corresponding to α-helical segments, designated BH1 to BH4, which classify their functional group membership: the anti-apoptotic, the pro-apoptotic and the BH3-only proteins [28; 32]. All proteins of this family will not be described here, and the focus will be on the most effective and investigated one in mammals.

The pro-apoptotic tribe

Inactivation of pro-apoptotic proteins leads to severe impairment of apoptosis while addition to mitochondria induces cytochrome C release and apoptosis. Two main pro-apoptotic proteins, Bax and Bak, are essential for the induction of cell death. Bax is a native cytosolic protein while Bak is an integral mitochondrial membrane protein. Both, upon apoptotic stimuli, such as BH3-only proteins interaction (see below), will undergo a strong conformational change that will activate their pro-apoptotic activity at the mitochondrion. Bax, upon modification, will expose addressing (assumed to be its first helix) and anchoring (mainly its C-terminus) sequences to translocate and insert to the outer membrane of mitochondria [33]. Then it releases the cytochrome C by a mechanism that remains unclear, but seems to involve its homo-oligomerization, which triggers MMP. Both proteins are widely believed to be involved in the permeabilization of the outer membrane of mitochondria [34]. Pro-apoptotic proteins are composed of nine α-helical segments and exhibit three BH domains (BH1-3) and a transmembrane C-terminus (TM). This later, the α_9-helix, is hindered in a hydrophobic groove formed by BH1, BH2 and BH3 which is exposed upon activation. The BH1 and BH2 or more precisely $\alpha_{5\text{-}8}$-helices, are the pore/receptor formation domains. $\alpha_{2\text{-}4}$-helices are the ligand/receptor domain (where α_2 corresponds to BH3) [29]. The role as an addressing sequence of Bax-α_1 is still hardly debated.

The anti-apoptotic guardians

They are the inhibitors of apoptosis. Indeed, their overexpression prevents cytochrome C release and therefore apoptosis activation. Bcl2 and its closest homologues, Bcl-X_L and Bcl-w, are the main anti-apoptotic proteins. Bcl2 is an integral membrane protein, natively located in the OM, whereas Bcl-XL and Bcl-w are tightly associated with the mitochondria after activation upon cytotoxic signals [35]. Beside their main action of blocking cytochrome C release by a complex mechanism still not fully understood, they seem also to be important for the scavenging of reactive oxygen species, which are also involved in apoptosis regulation via protein/phospholipids peroxidation [36]. They have also the capacity to homo-oligomerize but

this function is not clear for their anti-apoptotic activity. Furthermore, they can block pro-apoptotic proteins activity by hetero-dimerizing via their BH3 domain but may also trap BH3-only proteins that allow pro-apoptotic proteins to homo-oligomerize or even release BH3-only proteins that will activate Bax prior translocation. That clearly shows why the regulation of apoptosis is a complex and unresolved mechanism with probably a multifaceted regulation [37]. Indeed, the anti-apoptotic proteins have a structure close to that of pro-apoptotic proteins except they have an additional BH4 domain. They are composed of seven α-helical segments where the α_1 is the BH4, $\alpha_{2\text{-}4}$ the ligand/receptor domain (α_2 corresponding to BH3), $\alpha_{5\text{-}7}$ the pore/receptor domain (containing BH1 and BH2) and have a TM segment at the C-terminus [29]. Their three-dimensional solution configuration resembles to pro-apoptotic proteins, with the hydrophobic groove hindered by the BH1-4 domains [38]. The BH4 domains appears only in anti-apoptotic proteins, furthermore it is the essential part for anti-apoptotic activity, as deletion of this domain transforms the protein to a pro-apoptotic protein [39]. Also this domain was found to interact/bind to various proteins involved in apoptosis such Raf1, Bad (BH3-only protein), etc. [40; 41].

The BH3-only mediators

Their main role is to associate with pro-apoptotic proteins, activating their functions, except maybe for Bid that interacts preferentially with contact site and cardiolipin prior to binding to Bax or Bak [10]. They promote Bax or Bak conformational change upon binding which then triggers the cytochrome C release [37]. They act at different levels or are specialized for different cells: Bid, indispensable for cell development, facilitates the deaths of hepatocytes [42]. Bim is essential for elimination of autoreactive lymphocytes and participates in neuronal death [43; 44]. Bad, and possibly Bid, bind to anti-apoptotic proteins neutralizing their functions [45]. They are all held by association with, for instance, microtubules (Bim) or 14-3-3 scaffold proteins (Bad) or are synthesized as a precursor that needs to be cleaved to be active (Bid to tBid) [46; 47; 48]. They all share the BH3 domain helical segment but the preferential binding is still unclear. Also, while the BH3 domain is supposed to be the specific site for homo/hetero-oligomerization of the Bcl2 family, BH3-only proteins cannot form homodimers. Bid and Bad lack a C-terminus transmembrane segment, and therefore are native cytosolic proteins while Bim possess the anchoring sequence but has not been found in a specific membrane location [32].

- Interplay at the mitochondrion

As partially described above, the Bcl2 family acts at the mitochondrion in order to regulate cytochrome C release, the univocal cell death sentence. However, the complex interplay between the Bcl2 proteins members themselves and with the mitochondrial membranes is far from clear to be identify, matter of disagreements, most likely due to many mechanisms involved according to the type of cell, the type of stimuli, the experimental setups and so on. So far, there are two main pathways discussed: the permeability transition pore complex (PTPC) dependent and PTPC-independent pathways.

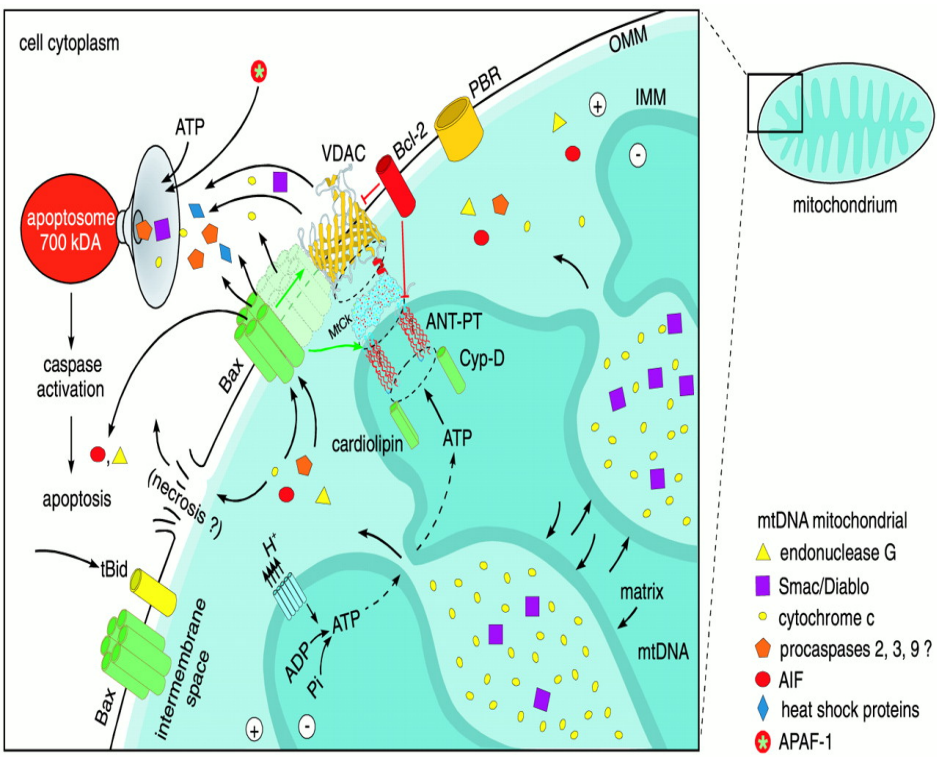

Figure 3 Regulation of the apoptotic activation at the mitochondrial level: Bcl2 protein family interplay and cytochrome C release. (Adapted from Mayer et al. News Physiol Sci, 2003 [30])

PTPC-dependent pathway

In this model, Bax and Bak interact with the VDAC (porins located in the OM), promoting its enlargement and opening, which involved the mitochondrial swelling and depolarization by osmotic shock and finally leads to OM disruption and cytochrome C release. Bcl-2, Bcl-XL and the corresponding anti-apoptotic BH4 peptide prevent such an event by closing the VDAC [49; 50]. Moreover, the role of the IM in the PTPC-dependent model is questioned but the IM seems to participate in the mitochondrial swelling. Indeed, at contact sites, VDAC and ANT, form supramolecular assemblies that link the matrix to the cytosol. When VDAC is in a lasting open state due to pro-apoptotic stimuli, the free passage of molecules <1.5 kDa through the ANT channel induces the osmotic swelling of the IM, which has by far a greater volume than the, OM and then triggers its disruption [51]. For example, Ca^{2+} overload is known to promote mitochondrial swelling by increasing the ANT conductivity, which in turn leads to an inward flux of protons and ions and osmotic shock. Furthermore, malfunction of the respiratory chain due to IM perturbation leads to increase production of reactive oxygen species (ROS). These harmful molecules can oxidize lipids and proteins, creating a total impairment of the mitochondria: In particular, by interacting with cardiolipin, it can weaken its tight binding with cytochrome C [52; 53].

PTPC-independent pathway

This model involves only the OM and the Bcl2 family. Upon apoptosis induction, Bax is activated (often by tBid BH3-only proteins) and translocated into the OM. Therefore, it undergoes strong oligomerization with itself or with Bak to form a large pore allowing the cytochrome C release [54]. tBid can also interact strongly with mitochondria via its affinity for cardiolipin [10]. An important role for mitochondrial lipids is emerging, where cardiolipin may have a central role. Indeed, Bcl2 proteins can alter the composition and curvature of the OM and there activate MMP. Furthermore, the membrane environment is essential for pro-apoptotic proteins conformational rearrangement and pore formation. The physical properties of the membrane (hydrophobic thickness, lateral pressure, electrostatic surface potential, etc.) are therefore crucial for the regulation of recruitment, insertion and oligomerization of proteins [55]. Cardiolipin appears to be the central, specific phospholipid involved in this regulation. For instance, Bax activation required cardiolipin, and tBid-mediated cardiolipin redistribution could induce Bax to bind and activate prior to pore formation [10; 12; 53; 55]. Therefore, cardiolipin could act as a signalling lipid, as we suggest (MS IV) by its affinity with the addressing sequence of Bax (Bax-α1). The anti-apoptotic proteins work here as

quenchers which can block Bax oligomerization, or the tBid association with cardiolipin[56]. However, Bcl-2 proteins, lacking their BH4 domains almost completely loose their anti-apoptotic function but still remain able to bind to various pro-apoptotic members, suggesting another function like acting directly onto VDAC, making the full story very complicated [57; 58].

At the end, it appears that both pathways may coexist depending on the Bax concentration present. Indeed, low amounts of Bax do not induce mitochondrial swelling and depolarization while they are detected above a certain threshold in isolated mitochondria [59]. It highlights the numerous problems studying studying this highly complex and interconnected mechanism of intrinsic apoptosis regulation.

- The use of Bcl protein in disease treatment

Knowing that nearly one million cells need to die each second in our body, a tight control is essential for our well being. The burst of knowledge about apoptosis, the main mechanism of cell homeostasis regulation, has allowed therapies to flourish. Indeed, a range of physiological pathologies (cancer, autoimmunity, infections, etc., for insufficient apoptosis; Ischemia, heart failure, neurodegeneration, etc., for excessive death) are directly connected with apoptosis deregulation and therefore apoptosis-based therapies have emerged [13]. Most of the effort is put into cancer research by looking for Bcl-2/Bcl-XL antagonists. The main principle is to block their BH3 binding site which would impair the hetero-dimerization with pro-apoptotic proteins [60]. Also, the anti-apoptotic activity of the BH4 domain alone was shown to prevent ischemia-reperfusion and protect cells from high exposure to irradiation [61; 62; 63]. Of course, many other potential targets in the apoptotic pathway are used, acting on caspases, APAF-1, mitochondria integrity and so on [13]. Anyway, the knowledge of the molecular mechanism of apoptotic regulation is still far to be fully understood, especially with the critical role of lipids emerging, and new considerations are each day made that can be important for improving the therapy efficiencies.

c) Aims and strategy

The goal of this thesis was to investigate the biophysical behavior of mitochondrial membranes in response to several important domains present in the Bcl2 family. The two main points of this thesis were to investigate how the overexpression of the anti-apoptotic specific domain of the human Bcl-2 protein affects the membrane behaviour and how the addressing sequence of the pro-apoptotic protein Bax, can recognize and target the

mitochondrial membrane surface. For these purposes, the first step was to produce pure peptides and then by using various biophysical techniques, to elaborate a molecular mechanism of action that could help to understand the biological processes happening during apoptosis. Finally, a NMR method for tracking the response of the lipid membrane matrix of living isolated mitochondria was set up for future investigations of apoptotic mechanisms which involve rearrangements of their phospholipid containing membranes.

II BH4, TAT-BH4 and Bax-α1 peptide production

a) Solid Phase Peptide Synthesis (SPPS)

- Chemistry

Solid-phase peptide synthesis (SPPS) was proposed first by R. Merrifield in 1963 [64] and is now the most common method used for peptide synthesis. SPPS allows the synthesis of natural peptides which are difficult to express in bacteria, the incorporation of unnatural amino acids and/or labelled amino acids and all synthetic peptides used in fundamental research. It is relatively cheap, fast and with a reasonable yield according to the length (100 a.a. great maximum) and hydrophobicity of the sequence.

The syntheses were carried out on an Applied Biosystems 433A Peptide Synthesizer (PE Biosystem, Courtaboeuf, France) using Fmoc [65] strategy. Small solid beads, the resin, are composed of a linker that is acid sensitive and preloaded with the C-terminus a.a. of the sequence synthesized. Indeed, unlike protein expression, the SPPS occurs from the C-terminus to the N-terminus. The peptide will remain covalently attached to the bead until cleaved by acetic acid (TFA). Small (tenfold molar excess of a.a. to resin) or medium (fourfold excess of a.a.) range scale were carried out.

Fastmoc chemistry was applied in four major automated steps per cycle:

i) After swelling using DCM the resin is deprotected of Fmoc groups by piperidine and N_2 agitation which forms carbamate salts and CO_2 as side products. Each deprotection step is monitored by conductivity measurement of carbamate salt formation.

ii) Activation of added amino acid (in cartridge) is done by HBTU/HOBt (37.9 g /13.6 g) in 200 ml of DMF addition. It forms an active ester which promotes little racemisation and then improves the yield.

iii) The amide link formation is done by coupling the deprotected part with the activated one with a solution of 35% DIEA in NMP.

iv) Since the presence of unreacted amino functions after coupling is unfortunate, capping procedure avoids the formation of deletion sequences. The capping will yield a truncated sequence which differs generally considerably from the final peptide and can be easily separated. Capping to prevent truncated peptide elongation is done using acetic anhydride/DIEA/HOBt (19 ml /9 ml /0,8 g) in 400 ml of NMP.

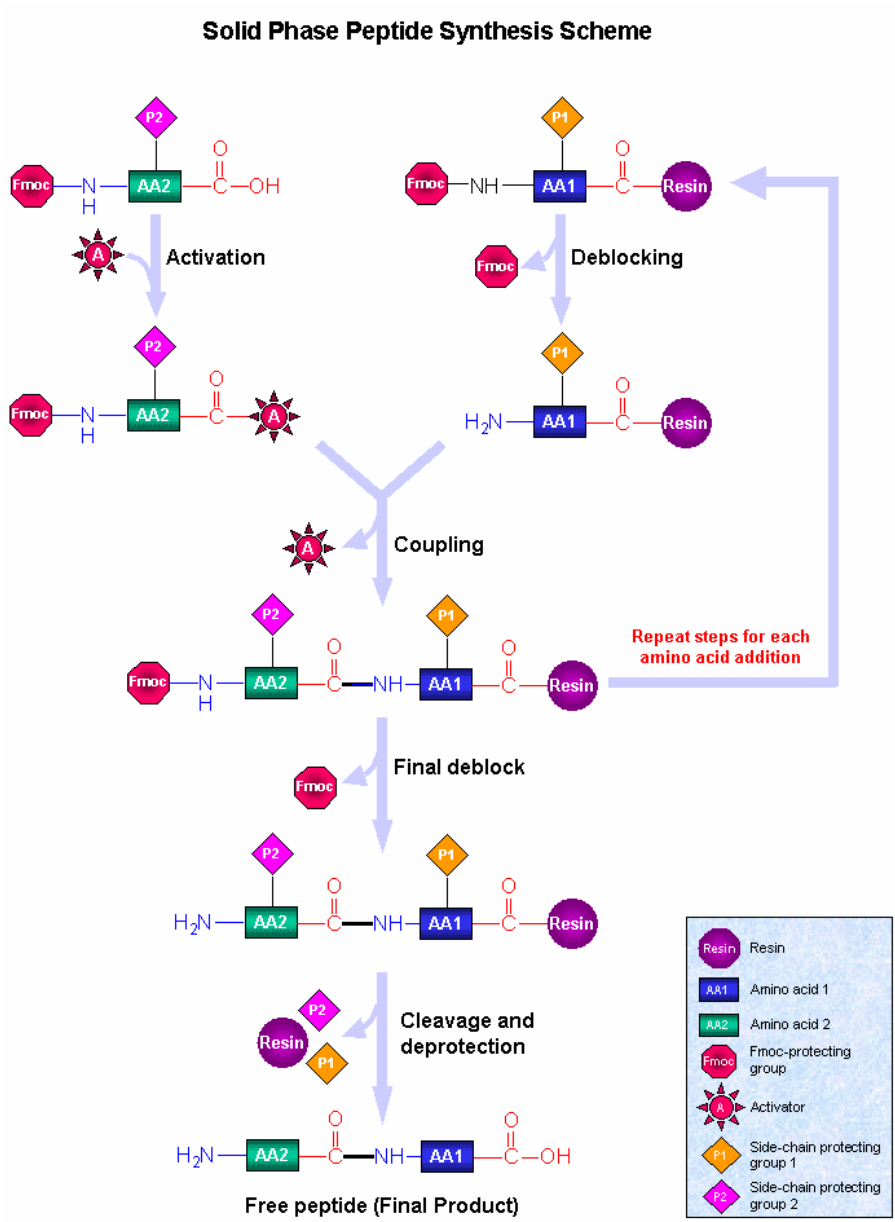

Figure 4 Solid phase peptide synthesis steps (Source: Sigma Aldrich)

- Cleavage

Concentrated TFA is used to perform the final cleavage of the crude peptide from the resin together with the removal of the side chain protecting groups. However, during the reaction, highly reactive carbocations are generated and it is necessary to trap them to avoid undesired reactions with sensitive amino acids such as Cys, Met, Ser, Thr, Trp or Tyr. This effect is obtained by the addition of scavengers to the cleavage solution.

Water is a moderately efficient scavenger and can be used as a single scavenger for the cleavage of peptides devoided of Cys, Met and Trp. EDT is the most common and efficient scavenger for peptides containing sensitive amino acids. The use of sulfur containing scavengers is recommended in the cleavage of sequences containing Met, Cys and Arg. Also silane derivatives (TES, TIS) can successfully replace the malodorous EDT. They show good efficacy in quenching carbocations in sequences containing Arg and Trp residues.

Cocktail compositions must be tried and compared for improving the qualitative and quantitative recovery before choosing the final one. Furthermore, the time evaluation of the cleavage must also be optimized, knowing that side reactions can arise from long exposure to strong acid environment.

The final step is the peptide precipitation by adding of cold diethyl ether and the cloudy aqueous phase is collected by centrifuging in a bench-top machine. After filtration of the supernatant, water is added to the crude product prior lyophilisation.

b) Purification (RP-HPLC) and characterization (MALDI-TOF)

- High Performance Liquid Chromatography (HPLC)

The coupling efficiency is not 100% and the final product is a crude mixture of pure, truncated and/or not totally deprotected peptides. Therefore, purification is required, especially when structural and functional studies of the peptide are involved. We used high performance liquid chromatography using reverse phase columns (RP-HPLC) which is a standard method for peptide purification. It was performed on a HPLC (Waters Alliance 2695) with photodiode array detector and using a semi-preparative Vydac (Hesperia, USA) C4 column (300 Å, 5 μm, 250x10 mn).

Basically, the sample is loaded in small volume according to the columns type (analytic 0.9mL, semi-preparative 1.8mL) to the stream of a mobile phase where electrostatic/hydrophobic interactions with the stationary phase promote, ideally, unique retention times for each specie. To improve the separation, gradient elution is performed,

where the mobile phase polarity varies by mixing water to, for instance, acetonitrile (ACN). The gradient separates the species as a function of their affinity for the mobile phase relatively to the stationary phase. The columns used in reversed phase chromatography have a silica stationary phase that has been treated with RMe_2SiOH, R being an alkyl group which gives the denotation as C4 ($R = C_4H_9$) or C18 ($R = C_{18}H_{37}$) to the columns. Therefore, retention time is longer for molecules which are more hydrophobic, and can be adjusted by the length of the R chain. In fact, the binding of the molecules to the stationary phase is proportional to the contact surface area around the non-polar segment of the molecule and the water solvent. Then, the retention can be decreased by adding less-polar solvent to reduce the interaction with water. Also, TFA (0.1%, vol/vol) is used as an ion-pairing agent and increases the sharpness and symmetry of peaks and may increase the peptide solubility. The detection is done by monitoring the absorbance at 280 nm if the sequence contains a tryptophan and/or tyrosine otherwise at 214 nm where the -CONH- amide bound absorbs.

- Matrix Assisted Laser Desorption/Ionisation mass spectroscopy coupled with Time-Of-Flight detector (MALDI-TOF)

In order to check if the removal of protecting groups is quantitative, and to identify the eluted fractions by HPLC which contain the pure product and even, in case of miracle or misfortune, if the purification step is not required, MALDI-TOF is commonly used. This work was done at the Mass Spectroscopy platform at IECB by Katell Bathany, under the supervision of Prof J.M. Schmitter. Nonetheless the basic principle will be briefly described.

Very small amounts of the peptide sample are dissolved in matrix solution composed of α-cyano-4-hydroxy-cinnamic acid in saturated solution of 50% ACN. The matrix is used to protect the biomolecule from being destroyed by direct laser beam and to facilitate desorption and ionization. An aliquot is air-dried on a target plate and the laser is fired at the crystals, where the matrix absorbs the laser energy and the peptide is ionized. Ions observed after this process consist of a neutral molecule [M] and an added ($[M+H]^+$) or removed ion. Multiply charged ions ($[M+nH]^{n+}$) can also be created, as a function of the matrix, the laser intensity and/or the voltage used. Time-of-flight detection used electric field to accelerate the ions produced and separate the molecules according to their mass-to-charge ratio (heavier particles reach lower speeds).

It is noteworthy that MALDI-TOF is not a quantitative method. Even the major peak may reflect the major population, homogeneity of the matrix, ionization and solubility parameters are very important issues. Salts and TFA are also a source of noise and insufficient ionization.

Also, the laser section is much smaller than the sample which required several shots because of the non-homogeneous repartition.

c) Trifluoroacetic acid (TFA) contamination

TFA is largely used during peptide synthesis and purification. While it is thought to be not dangerous for the peptide integrity, it can perturb several measurements. Indeed, it is a severe contaminant because it acts as a perfect counter-ion for basic amino-acids and therefore is removal by a simple freeze-drying method is often incomplete.

- Risk for experiments

First of all, is a dramatic error is mass weighing. As we measured (see Paper II and next section), around two counter ions per basic amino acid can be found which, depending on the number of basic a.a., could lead to serious miscalculation in molar concentration, peptide/lipid ratio, etc.

Also, TFA molecules can perturb several techniques. For instance, Infrared spectroscopy is very sensitive to TFA contamination because its signal appears in the peptide amide bounds region, which induces serious signal distortion. The baseline in MALDI can be seriously distorted and the molecule ionization greatly decreased.

Finally, it can severely decrease the pH of NMR sample because high concentration of peptide is often required, and the buffer strength should not perturb the lipid/peptide interactions. Moreover, TFA can degrade di-acyl-phospholipids into lyso-phospholipids which lead to isotropic phase formation.

- Detection and removal

We set up a quantitative NMR method to investigate the TFA contamination in peptide sample (see paper II). ^{19}F is a perfect reporter of TFA presence in sample since TFA possesses three fluorines while phospholipids or a.a. does not. Furthermore, fluorine is easy to detect using a single pulse NMR sequence since it has a high natural abundance (~100%) and high gyromagnetic ratio. Trifluoroethanol (TFE) is used as an internal reference, separated from the sample by a capillary, which allow quantitative measurement.

The removal is performed using a more convenient counter ion. The peptide was treated with HCl acid, which has a lower pKa value inducing reprotonation of TFA anions and can be easily removed by freeze-drying. Generally, a three fold molar excess provides a complete

removal. It is noteworthy that ice cooled solution and short incubation time have to be used to avoid any possible peptide degradation.

d) Results & Comments

Table 1 presents a summary of the synthesized peptides with their corresponding yield. The protocol descriptions are in paper I and II and will not be further discussed. It is noteworthy that work on TAT-BH4 is still on going and not enough data has been acquired to establish a manuscript yet. Data are just presented in here to discuss and to compare some difficulties in peptide production.

Table 1 **Summary of synthesized peptides**

	$BH4^{6-30}$	$BH4^{6-31}$	Bax^{14-38}	$TAT\text{-}BH4^{14-38}$
After synthesis[a] (mg)	250	250	900	500
After cleavage (mg)	135	188	250	250
After purification (mg)	1	67	85	-
Yield (after HPLC)[b] (%)	54 (-)	74 (36)	47 (12)	50 (-)

[a] All protected groups remain

[b] ~99% purity

The yield is representative for a good synthesis protocol but is never as high as theoretically expected. The coupling efficiency is usually close to 99%, which means that for a 25 a.a. long peptide, the yield must be $(0.99)^{25}$, so approximately 78%. First, it is evident that long peptide are therefore limited (50 a.a, 60%; 100 a.a., 37%), especially that 99% is a high coupling efficiency probability. Finally long sequences require a serious purification, according to the purity needed, which dramatically reduces the final yield (see III b) and table 1). Also, TFA contamination leads to severe miscalculation and can be harmful for sample preparation or measurement (see III c)).

SPPS is a good way to produce large amount of peptide but variation in the preparation (scale used, resin freshness, etc.), solvent quality or the peptide sequence hydrophobicity can induce huge difference in yield. For instance, as seen in paper I, the difference between $BH4^{6-30}$ and $BH4^{6-31}$ remains unclear. The first sequence was synthesized without a protected tryptophan, which led to a problem in the cleavage but no real explanation of the poor purification peptide recovery can be done. It might have been clogged in the columns, but no delayed releases have been monitored. However, this phenomenon was observed previously with a hydrophobic sequence (neu/erbB-2), which could explain that adding a charged a.a. (aspartic acid, D) has enhanced its solvability and purification. It must be noted that a thorough washing and equilibration was performed prior any injection day.
During this first synthesis period (BH4), I was not aware of the possible TFA contamination, and all the yields were established without TFA removal. However, the first NMR experiment showed lipid degradations, as formation of lyso-lipids. It was unlikely a peptide property but rather a contamination and consistent with this possibility, TFA was found to be present. Considering that BH4 contains five basic a.a., TFA counter ions are heavily bound to the peptide. For measurement in paper III, TFA was carefully removed. Bax^{14-38} synthesis was done without any special problems. The low yield is typical of a relatively hydrophobic sequence. Also, the detection using MALDI-TOF method is not always the best choice. Indeed, TAT-BH4 synthesis shows promising result on the HPLC chromatogram, with a large dominant peak. However, detection of this major component by MALDI-TOF was unsuccessful. Despite a preliminary TFA removal step, it appeared that strong TFA binding, since the full peptide contains thirteen basic a.a., induced a low desorption/ionization process. However, using the Edman sequencing method, the presence of TAT-BH4 was found rather pure.

These results demonstrate that the choice of a specific protocol, gradient, methods of detection, etc., must always be optimized because results cannot be predicted from a previous synthesis. Whereas some difficulties can be easily encountered, SPPS is able to produce quickly, with high purity and large amount of peptide which put it as the method of choice for studying small sequences.

III Interaction with membranes: methodology and applications

The importance of biomembranes is an emerging issue of scientific interest and nowadays many molecular mechanisms cannot be explained without considering the membranes. The biophysical study of lipid membranes allows therefore elucidating how membrane trafficking, signalling, protein folding or/and insertion, *etc.* can occur. Many techniques have been developed in order to describe at atomic and molecular resolution the functionality of biomembranes and their interaction with different stimuli. The core of my thesis was to investigate how the apoptotic peptides interact with membranes. Indeed, all the peptides used belong to proteins interacting with membranes. Therefore, the biological relevance of studying these peptides is directly linked to their membrane activity. First, membranes will likely promote structural change and organization of the peptide. Then, by reciprocity, the peptide will trigger membrane perturbations. This interplay has been studied with various biophysical techniques, which will briefly describe before jump to the results and discussion.

a) From the peptide side

- Circular dichroism spectroscopy (CD)

The circular dichroism technique is based on two principles: the chirality of the amide backbone and the light polarization. The natural amino acids have non-superimposable mirror image isomers, which mean they are chiral molecules and so optically active. When interacting with circular polarized light, the peptide backbone will not absorb homogeneously the left and right components of the radiation. This absorption is wavelength dependent (the 250-190nm range is commonly used) and enables classification of the peptide backbone conformation in four main secondary structures: α-helix, β-sheet, β-turn and random coil. Indeed, the CD spectrum of a protein or peptide is not a sum of the individual amino acid circular dichroism spectra, but is significantly influenced by the dihedral or torsion angles (the angle about the α-carbon and the nitrogen of the amide is known as φ (phi) while, the angle about the α-carbon and the carbon of the carbonyl is known as ψ (psi)) giving the three-dimension backbone structure of the macromolecule itself, as described by the Ramachandran plot [66]. Each structure has a specific CD signature and this can be used to distinguish structural elements and to follow changes in the structure upon interaction with membrane for instance.

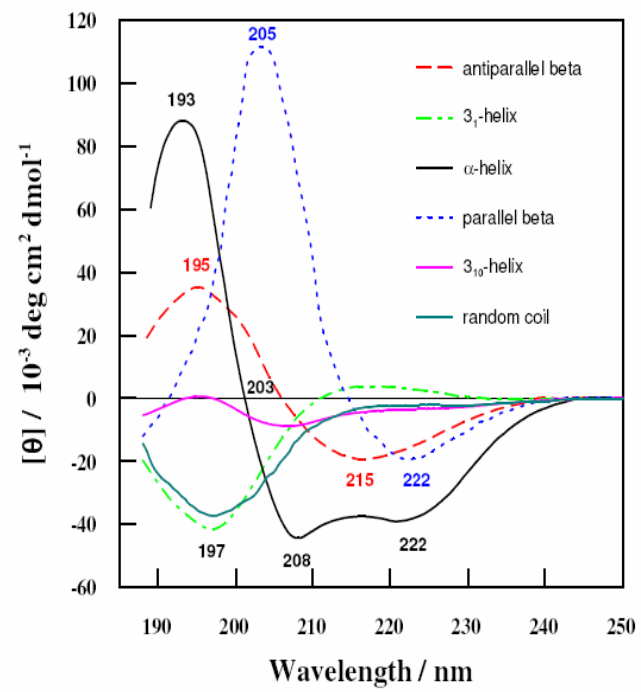

Figure 5 Typical lineshape of secondary structures obtain by CD (Courtesy from Karolinska Institute)

Finally, a short description of the secondary structure elements considered in our CD analysis.

α-helix: a right handed structure where each carbonyl is hydrogen bonded to the N-H group of the fourth peptide (i,i+4) bond along the chain. These hydrogen bonds run parallel to the backbone and fix the structure to a rigid rod shape. The length of an α-helix is 1.5Å per a.a.. It is worth noting that different helical structures are known, the π helix (i,i+5) or the 3_{10} (i,i+3) but they are rare and not as stable as the α-helix. It has two minima at 222nm and 208nm and a maximum 193nm.

β-sheet: the hydrogen bonding occurs interstrand and there are two kinds of association. The parallel β-sheets have the N-H groups of one strand establishing hydrogen bonds with the carbonyl groups in the backbone of the adjacent strands in the same direction. They are bent and have a i,i+2 distance of 6Å. In an antiparallel arrangement, the successive β strands alternate directions so that the N-terminus of one strand is adjacent to the C-terminus of the

opposite strand. This is the arrangement that produces the strongest inter-strand stability because it allows the inter-strand hydrogen bonds between carbonyls and amines to be planar, which are their preferred orientation. The parallel β-sheet has a broad minimum at 215nm and a broad maximum at 195nm while the anti-parallel β-sheet has a broad minimum at 222nm and a broad maximum at 205nm.

β-turn: often a single pair beta-sheet hydrogen bond formation between the carbonyl group and amide of the third peptide bond along the chain, which bends/turns the peptide backbone. Usually the sequence in this region contains glycine, providing almost no steric hindrance, and proline, to force the bend in the chain. It has a weak positive band a 225nm and minimum around 201nm.

Random coil: it is not a total unstructured structure since even arbitrary sequences of amino acids tend to exhibit some hydrogen bonds. It is more conceptualized as a fully stretch helix or a statistical coil but without any pattern. It has a minimum at 198nm

In order to obtain the percentage of secondary structure, the CDPro package developed by Woody and Seerama, was used for deconvolution [67; 68; 69]. It uses a fitting algorithm for extracting each secondary structure component from the experimental data. For this purpose, different set of proteins structure basis have been resolved by NMR or X-ray.

Of note, measurement of CD is complicated by the fact that typical aqueous buffer systems often absorb in the range where structural features exhibit differential absorption of circularly polarized light.

- Attenuated total reflection spectroscopy (ATR)

ATR allows secondary structure determination as well, but it can also provide the average orientation of the peptide relative to the membrane normal. Briefly, an IR radiation enters the crystal at a specific angle that provides the total internally reflection. It reflects through the crystal and penetrates "into" the sample (about 0.5 to 5μm depth) by a finite amount with each reflection along the top surface via the so-called "evanescent" wave. By shearing the sample at the crystal surface with a teflon tape, the membrane normal spontaneously orients parallel to the crystal. Then, absorptions due to molecular vibrations are recorded. The amide I band of peptides and proteins, which mainly involves the carbonyl stretching vibrations of the peptide backbone, is a sensitive marker of peptide secondary structure, as the vibrational frequency of each C=O bond depends on hydrogen bonding and the interactions between the amide units. Therefore, each secondary structure has a well defined absorption band which

can be deconvoluted. Furthermore, by using polarized IR, one can obtain the peptide averaged orientation. Parallel and perpendicular IR will be absorbed differently according to the peptide orientation in the oriented membrane. From the dichroic ratio between both absorptions, one can figure out the angle of the peptide along the membrane normal [70; 71].

b) From the lipid side

- Phospholipid bilayer polymorphism

The phospholipids in biological membrane are diverse. The complexity of these membranes determines the functionality of each specific membrane of cells, organelles, vesicles, etc. but also leads to severe difficulties when studying their behaviour. Therefore, one uses model membranes of well known phospholipid compositions to be able to explain the full molecular mechanism upon interaction with peptides for instance. The phospholipid structures are mainly composed of two hydrophobic acyl chains which can have different lengths and saturations and possess also specific polar headgroups (phosphatidylcholine and phosphatidylethanolamine most common to be found in nature). Of course, cardiolipin is a unique phospholipid having four acyl chains, linked two by two with a glycerol chain. The amphiphatic behaviour of phospholipids will spontaneously promote organization in an aqueous environment in order to minimize interactions of their hydrophobic fatty acid chains with water but enable hydrophilic interactions with the polar lipid headgroup region. The ratio between the hydrophobic and the polar volume, known as the packing parameter p ($p=v/a_0.l_c$; v volume of the headgroup, a_0 the interface area and l_c the acyl chain length), will predict the arrangement, called phase [72].

The typical organizations are:

$p<1/3$: micelle. They are small (<50Å) spheres where the hydrophobic chain are towards the interior avoiding contact with water.

$1/3<p<1/2$: hexagonal phase. A tubular organization where the water surrounds the tubes maintain together by hydrophobic chains continuous structure.

$1/2<p<1$: liposome. The lipids organize themselves as bilayer with a curvature radius forming a spherical shape. It is the most usual phase for mimicking the cell membranes. They will form multilamellar vesicles (MLVs) with an approximate range of diameter from 200nm to 800 nm but with extrusion technique, one can produce large unilamellar vesicles (LUVs), with radius fixed by the filters used or use of sonication, small unilamellar vesicles (SUVs), with a radius of ca. 50nm.

p≈1: planar lamellar phase. It is the same bilayer organization without the curvature constraint.

However, experimental conditions will also play a critical role in the lipid organization, like water content, ionic strength and addition of molecules like peptides.

The thermotropism of phospholipids is also often described as a phase. The dynamic of the acyl chains fluctuates according to the temperature. In the gel phase (L_{β}), the chains are rigid in a *trans* conformation and parallel to the bilayer normal or tilted ($L_{\beta'}$). When increasing the temperature, the chains are said to melt and *gauche-trans* isomerisation occurs. This phase is called the fluid phase L_{α}. In the fluid phase the bilayer thickness is reduced.

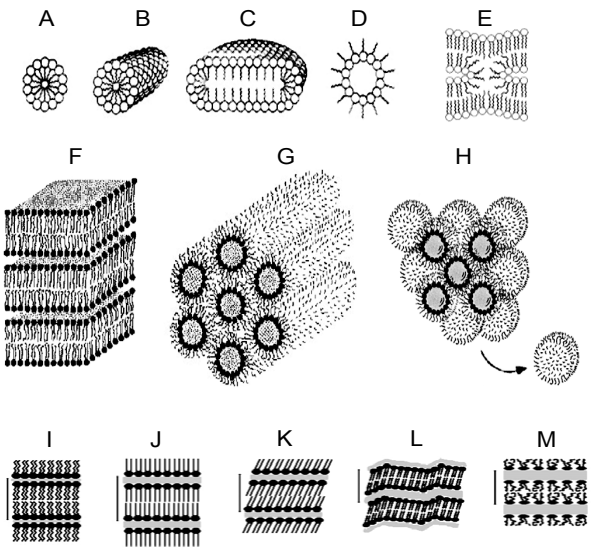

Figure 6 phospholipid arrangements and thermotropism: (A) Spherical micelle; (B) cylindrical micelles (tubules); (C) disks; (D) inverted micelles; (E) a fragment of a rhombohedral phase; (F) lamellae (G) inverted hexagonal phase; (H) inverted micellar cubic phase. Lamellar phases: (I) subgel, L_c; (J) gel, untilted chains, L_{β}; (K) gel, tilted chains, L_{β}; (L) rippled gel, $P_{\beta'}$; (H) liquid crystalline, L_{α}. (adapted from Koynova et al. WILEY ENCYCLOPEDIA OF CHEMICAL BIOLOGY, 2008)

- Nuclear magnetic resonance (NMR)

The nuclear magnetic resonance (NMR) principle is based on the electromagnetic properties of the nucleus: the nuclei posses a spin (I) associated with a magnetic moment that will orient in a magnetic field. At first, the spin will equilibrate within the magnetic field, populating 2I+1 energy states according to the Boltzman law. The resulting magnetization is oriented along the z axis of the spectrometer magnetic field ($\mathbf{B}_0$). A transition between these energy states occurs when the nuclei absorb or emit an electromagnetic radiation at their Larmor frequency (ω_0), which is specific according to the gyromagnetic ratio of the nucleus. Therefore, by using a radio frequency (r.f.) called $\mathbf{B}_1$ field, one can perturb the distribution of spins by switching their magnetization by an angle θ. The relaxation of perturbed system to its equilibrium state is then recorded and is called the free induction decay (FID), which after Fourier transformation gives the NMR spectrum. The longitudinal relaxation time (T_1) along the z axis and the transverse (T_2) along the xy plan are reflecting the molecular dynamic of the spin, T_1 being connected to the molecular environment at the nanosecond timescale and T_2 is sensitive to slower dynamic (up to millisecond) giving information on the collective motions of the spins. The interesting part for studying biomembrane is that phospholipids possess different spins located in the hydrophobic core or in the polar headgroup. Then using selective r.f. to excite the specific spin gives precious information of the membrane behaviour and response upon stress like when interacting with peptides and so on. In fact, without internal interaction, each spin of a given isotope would give the same signal and bring little information. Fortunately, coupling occurs between the spins and they feel their electromagnetic environment, providing a useful tool for biophysical investigation. In the results and discussion section, the chemical shift, the quadrupolar interaction and the magic angle spinning technique are the notion used and will be briefly described:

<u>The chemical shift</u>

The electronic density around the nuclei will modify (shield or deshield) the local magnetic field. Therefore, the spins which sense a different electronic environment will provide different resonance frequencies (in ppm), proportional to strength of $\mathbf{B}_0$. The frequency of a signal is known as its chemical shift. The chemical shift varies with the molecular orientation in the field, thus it is anisotropic. The anisotropy will induce line broadening of the NMR signal and this chemical shift anisotropy (CSA) is good information of the phospholipids organization (see ^{31}P NMR and paper III, MS IV, MS V) and their associated dynamic.

Indeed, motional averaging can break the anisotropy due to tumbling and/or fast re-orientation of the molecule to isotropic chemical shift, as it appears in solution NMR.

The quadrupolar interaction

It applies for spin $I \geq 1$, which then posses an electric quadrupolar moment due to their charge distribution. The quadrupolar moment will interact with the local electric field gradient produced by the electronic environment. It dominates all other perturbations. This interaction causes the splitting of the resonances, and the so called quadrupolar splitting (in Hz) can be used to determine the *trans-gauche* isomerisation or the so called order parameter (see ^{2}H NMR and paper III).

Magic angle spinning (MAS)

Since the lipid or spin distribution in the cell mimicking MLVs systems conventionally used are often anisotropic, each orientation contributes to build a broad lineshape causing low resolution and sensitivity. By spinning the rotor fast enough, the angular dependence is scaled down to the second degree Legendre polynomial $\frac{1}{2}\left(3\cos^2\theta - 1\right)$. Therefore, at the so called magic angle, $\theta \approx 54.7°$, the angle between the rotor axis and the magnetic field, the anisotropic interactions are averaged out. However, in order to obtain only the isotropic contribution the spinning speed is critical and specific to each nucleus. For instance, for our partially averaged vesicle systems, MAS ^{31}P NMR required spinning at 6.5 kHz to average out completely the anisotropic contribution, and below, side bands spaced by multiple of the spinning frequency are observed. Of note, using side band analysis provides very interesting information of lipid populating different phases, for lipid segregation, etc.

- Investigation of the headgroup region: ^{31}P NMR and ^{14}N NMR

The phosphorous nucleus is a very interesting reporter for biomembranes. Indeed, all phospholipids obviously posses a phosphorous, located at their polar region or headgroup. It has a spin I = ½, and the dominant interaction is the chemical shift anisotropy. For peptide-membrane interaction studies, the usual membrane system used is the liposome, a lamellar phase. In this arrangement, phospholipids have a rapid axial rotation around their long axis and a uniform orientation distribution of phospholipids aggregates where the overlap of lineshapes from different orientations gives the typical uniaxial powder pattern lineshape. Indeed, the spherical organization provides more perpendicularly oriented lipids to the

magnetic field, $\sigma_{\perp}$, than parallel $\sigma_{//}$, the CSA is then determined as following $\Delta\sigma = \sigma_{//} - \sigma_{\perp}$. If the lipid organisation breaks down in small vesicle or micelle, the fast reorientation occurring will produce an isotropic resonance. Reduction of the CSA is then indication of fast headgroup motion. Therefore, ^{31}P NMR is a suitable technique to investigate the qualitative phase of membrane organization and the associated dynamic.

By using MAS technique, one can resolve in mixed membranes the lipids with different headgroups and determine for each lipid species how electrostatic and hydrophobic interactions can occur and can modulate their dynamics in a bilayer. The linewidth of the NMR resonances is governed by the T_2 relaxation, which monitor the slow motion of the membrane. The isotropic chemical shift frequencies are indicators of the electrostatic environment. If the nucleus is being de-shielded, e.g. by adding an electron withdrawing group like OH, it will cause a shift towards higher frequencies and higher ppm.

Another reporter of the average orientation and dynamic of a lipid is the nitrogen-14 nucleus, nearly to 100% abundant in phosphocholine lipids. It has a spin I = 1, and therefore a dominant quadrupolar interaction. The measured quadrupolar splitting, Δν, is dependent of the orientation and the motion of the headgroup. The reduction of Δν is associated with the average orientational order or more correctly the average spread of orientational order (« angular variance »), i.e. the order parameters as for the ^{2}H of the acyl chains. It is triggered by the modulation of the electrostatic surface and the molecular disorder of the choline segment. Of note, ^{14}N has a low magnetic ratio which leads to poor signal to noise ratio and the quality of the spectra are therefore limited [73].

- Investigation of the lipid hydrophobic core: ^{2}H NMR

Using synthetic deuterated acyl chains phospholipids, one can probe the hydrophobic core by detecting the ^{2}H signal. ^{2}H has a spin I=1 and will produce a quadrupolar splitting for each C-^2H_n of the acyl segment. Since the order parameter, or the rigidity, of each segment is different, the typical lineshape is a superposition of individual resonances centred at ω_0 [74]. Reduction in the value of Δν corresponds to a lower order parameter in the acyl chain. It is therefore a good indication of peptide penetration which can either promote disorder (MS IV) or can stabilize the acyl chains (paper III).

- Differential scanning calorimetry (DSC)

Based on the thermal behaviour of membrane, the DSC uses the heat absorption (or enthalpy) required for phase transitions. One measures the amount of energy which has to be provided to maintain zero temperature difference between the sample and the reference. The rate of energy absorption by the sample (e.g. millicalories/sec.), is proportional to the specific heat of the sample, the heat capacity, C_p. Any transition accompanied by a change in specific heat produces a discontinuity in the power signal, and exothermic or endothermic enthalpy changes give peaks whose areas are proportional to the total enthalpy change. Analysis of a DSC thermogram of a biomembrane enables the determination of two important parameters: the transition temperature peak (T_p) and the number of molefcules in a cooperative unit (cf. paper III)

c) Results & comments

BH4, from anti-apoptotic Bcl-2 protein, or Bax-α1, from pro-apoptotic Bax protein, are important regulative domains for the protein activity. Their close interactions with membranes have not been investigated at a molecular level so far. Therefore, in Paper III and MS IV, we concentrated on the molecular mechanism of peptide-phospholipid interactions.

While BH4 is the specific anti-apoptotic domain, its apoptosis preventing action is not understood yet. Previous studies showed its ability to trap some proteins involved in Bax activation, or its ability to close the VDAC opening, but no clear conclusion have been drawn so far [49; 57; 63]. Especially, one is missing. Indeed, since Bcl-2 is a membrane protein, BH4 is in close vicinity of the mitochondrial membrane and possible interactions could trigger membrane or peptide structure modifications that could play an important role. Paper III demonstrated the impact of BH4 on membrane dynamics. ^{2}H NMR and DSC displayed the striking stabilization of the lipids, forming rigid patch with BH4, when the latter is incorporated into the liposome. BH4 increased the order parameter of the membrane and diminished the number of lipid cooperative units, resembling the cholesterol effect [75; 76]. Furthermore, around body temperature, BH4 promoted peptide-bound and peptide-free phases, as seen in the overlapped ^{2}H NMR spectra but also in the static and MAS ^{31}P NMR spectrum where the lipids sensed the two different electrostatic environments. As determined with ATR technique, BH4 inserted into the membrane core at an averaged angle of $\theta = 42°$ which is characteristic for a planar and perpendicular mixed orientation, as confirmed by the hydrophobic and the headgroup regions perturbations. This strong effect on membrane dynamic was associated with BH4 aggregation at 30:1 lipid to peptide molar ratio which was

set to reproduce overexpression of the Bcl-2 protein in cancer disease. Therefore, the mechanism of BH4 interaction with the membrane is as follows: electrostatic interaction driving peptide accumulation at the membrane surface and then insertion of anti-parallel β-sheet by hydrophobic interactions, supported by the amphiphatic sequence of the peptide. These results make sense for the protective action on mitochondria permeabilization and raise the importance of considering a possible effect of Bcl-2 on mitochondrial membranes as a critical mechanism for anti-apoptotic activity.

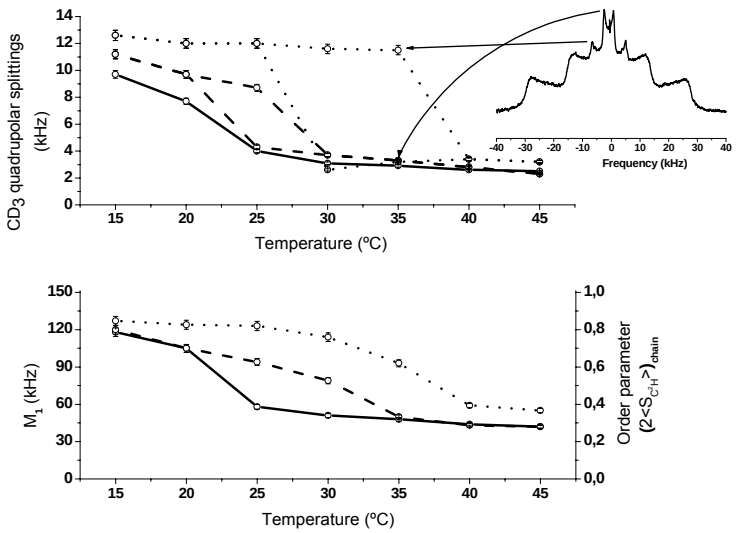

Figure 7 Temperature dependence change of the membrane order parameter upon interaction with BH4 (Diagram as in paper III)

The second case studied, presented in MS IV, was the addressing of the pro-apoptotic protein Bax. As already mentioned, the N-terminal helix, Bax-α1, is supposed to be the crucial part of the protein for recognition of the mitochondrial membranes. However, no information on which specific interaction drives this process has been obtained. MS IV describes how the preferential interaction with the mitochondrial phospholipids cardiolipin could be the key step for Bax addressing to mitochondria. Indeed, two membrane compositions were tested, the neutral outer membrane (OM) composed of the zwitterionic PC and PE lipids, and the contact site (CS) mimicking model containing 20%mol cardiolipin. Bax-α1 had complete by different interactions in the two models: while it did not interact much with OM membranes, which

triggered mainly a slight aggregation of the peptide, it showed a strong docking effect when in contact with CS membranes. The clear electrostatic interaction provided by cardiolipin promoted strong increases in α-helix secondary structure (+30%) as seen in CD spectra. The structure is not broken down by high salt concentration, which could have screened the vesicle surface. In MAS ^{31}P NMR spectra, cardiolipin appeared to be the preferential partner for Bax-membrane association by enriching the peptide-bound lipid population. This tight binding prevents any further insertion of the peptide even at high concentration, contrary to the case with OM membranes (see ^{2}H NMR and ATR spectra). Therefore, the important conclusion drawn by MS IV is that cardiolipin patches could act as a signalling domain for pro-apoptotic protein addressing. One can easily imagine that translocation of cardiolipin towards the OM is a key step for apoptosis regulation and might be used for disease therapy.

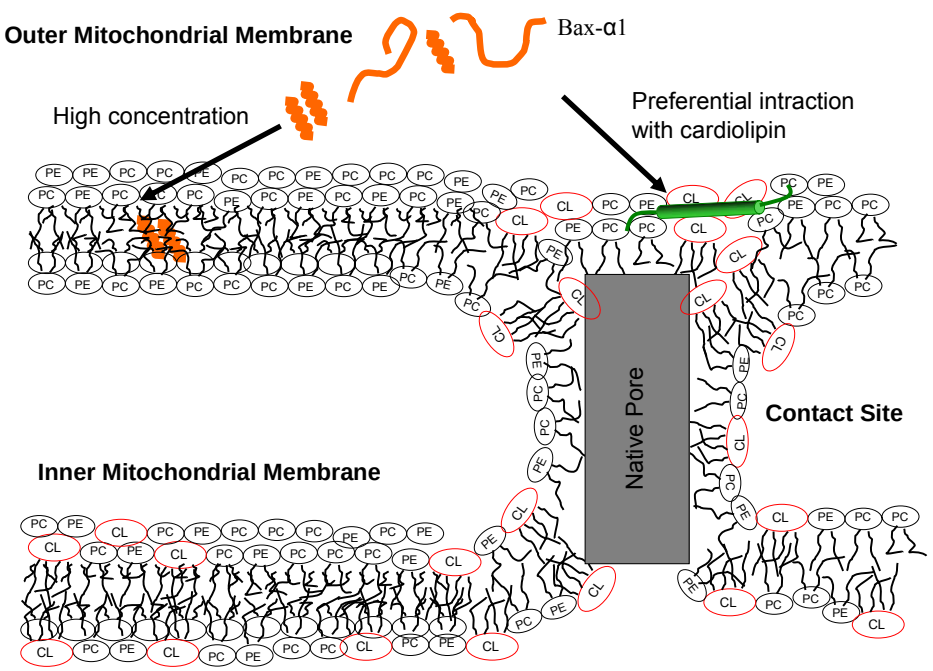

Figure 8 scheme of the molecular interaction between the addressing sequence Bax-a1 and two mitochondrial membrane compositions. (Diagram as in MS IV)

These studies allowed deciphering the role of regulative parts of two crucial proteins with membranes. Placed in the biological context and according to previous publications, these studies could improve the knowledge of apoptosis regulation even if biophysical studies are restrained to simple system as compared with *in vivo* studies. It allowed clarifying by which molecular mechanisms BH4 and Bax-α1 are linked to membranes with resolution and confidence. It also highlights the fact that mitochondrial membranes are not simple walls, but hold the keys for cytochrome C release. This hypothesis is emerging and favours the direct interaction between apoptotic proteins and mitochondrial membrane (instead with native pore), in which the two N-termini of Bax and Bcl-2 should be deeply involved.
However, it is always exciting to be able to understand the full mechanism as it occurs in real life. For this purpose, I decided to work onto isolated mitochondria to examine membrane behaviour during a potential apoptosis regulating event, as described in the next chapter.

IV Tracking lipid interactions in living mitochondria

a) Isolation of mitochondria

- "J'ai la patate"

Since apoptosis is a process occurring in mammals, working with mitochondria originating from potato tubers might initially sound inadequate, but several arguments justified this choice. Presently, vast amounts of material is needed for finding the correct conditions for living material in MAS NMR experiments. Therefore, a cheap system and a fast protocol have to be developed. Isolation of potato mitochondria is easy, and can be carried out in less than half a day at reasonable costs. Of course, since potatoes are purchased at the local market, the origin, growing conditions, etc., are undesired variations to carry out scientific work. However, these mitochondria are highly pure. No contaminant from other organelles or membrane systems is found in the isolated product, which is not the case for rat liver mitochondria where lysosomes are contaminants which are difficult to remove. Nevertheless, potato mitochondria have a high homology with mammalian mitochondria, with a quite similar composition of mitochondrial lipids and proteins. Finally, potato mitochondria have already been intensively studied with respect e. g. to the swelling phenomenon of mitochondrial membranes upon calcium stress, a common feature in apoptosis [77; 78], which was used to support our data.

The protocol used to obtain pure mitochondria was previously set up for extracting mitochondria originating from Arabidopsis leaves [79]. Briefly, Percoll gradients were used to separate mitochondria from all other cell constituents. After grinding sliced potatoes in sufficient buffer to prevent oxidation, the recovered juice was firstly slowly centrifuged to precipitate the starch and the heavy cellular fragments. The surpernatant was then centrifuged at intermediate speed to precipitate the mitochondria. The pellets were recovered and put on top of a *ca.* 28% Percoll gradient and further centrifuged at high speed. The pure mitochondria band was collected, and resuspended in a washing buffer used to remove the percoll beads by centrifugation at intermediate speed. The concentration of mitochondria recovered was quantified by light absorption based on the Lowry method, calibrated with bovine serum albumin (BSA) [80]. It is noteworthy that maintaining the temperature as low as possible during the entire procedure and measurements is crucial to keep the mitochondrial as "alive" as possible. From 2 kg of potato, approximately 400 µL of pure mitochondria were extracted at an averaged concentration of 150 $mg.mL^{-1}$ of proteins.

b) ^{31}P NMR ex vivo experiments

- Set up

The goal of this study (MS V) was to apply solid state, static and high resolution ^{31}P MAS NMR, as a non-invasive technique to monitor mitochondrial phospholipids in intact mitochondria and to investigate their response to calcium overload. The first part was to elaborate the NMR set up where mitochondria would not be degraded by the harsh condition of MAS, but also to see if the signal to noise ratio of the NMR signal could be enhanced. Since static and MAS NMR experiments had to be performed using the same sample, the time available for these two NMR experiments was highly restricted. Moreover, isolated mitochondria were heavily hydrated, meaning the spinning stability was reduced and high spinning speed conditions could not be applied. After several trials, 3 kHz spinning was chosen as good enough for an averaging of the CSA in the MAS NMR experiments, sufficient spinning stability and reduced mitochondria degradation. One hour of static NMR experiments followed by one hour under spinning conditions, sproved to be the best compromise between degradation and signal to noise ratio. First experiments were done with a 4 mm double resonance CP-MAS probe, where approximately 80 µL of pure mitochondria can be loaded which means the rotor contained about 2mg of lipids. Results were acceptable but in order to improve as much as possible the spectra resolution, a 5mm double resonance

CP-MAS probe was used, increasing the volume to 150 µL. However, spinning stability at 3 kHz was reduced because of a higher non homogenous volume, but remained in a ±5 Hz range. Finally, the mitochondrial integrity was checked by respiratory control measurements. These showed little degradation since the respiratory rates were only slightly reduced. This agreed with the static ^{31}P NMR spectra which also did not reveal any membrane degradation as no isotropic phase increase was observed after NMR measurements. Therefore, the method was validated as non-invasive with the potential to provide interesting information on mitochondrial phospholipid arrangements and association in an *ex vivo* context

The static ^{31}P NMR spectrum of isolated mitochondria showed the typical axially symmetric pattern of phospholipids organized in a lamellar liquid-crystalline phase, as previously seen in NMR spectra of much a lower resolution [81]. A small isotropic component was also visible, which accounted for less than 5% to the total spectrum and most probably reflected very small mitochondria fragments/compartments which underwent fast isotropic rotational diffusion. The individual phosphatidylcholine (PC) and phosphatidylethanolamine (PE) membrane constituents were easily detected with intensities of 49 ±5% and 41 ±5% of the total NMR spectrum. A third small broad component was visible and accounted for with roughly 10±5% to the total NMR spectrum. This small resonance might come from cardiolipin, the third major phospholipid of mitochondrial membranes, but with its strong association with proteins, as with the paramagnetic cytochrome C, relaxation and different in electronic environments spread over an extremely broadened NMR resonance. As a control, a ^{31}P MAS NMR spectrum was acquired using large multilamellar vesicles made of extracted phospholipids from isolated mitochondria. The NMR spectrum fully supported the presence of cardiolipin, as three well-resolved NMR components were observed with molar percentages of *ca.* 47 ±2% % PC, 37 ±2% PE and 16 ±2% cardiolipin, all values which are close to the reported ones for isolated mitochondria from rat liver (50 ±3%, 30 ±3% and 20 ±5%, respectively) or as found in isolated mitochondria from spinach (46 ±2%, 41 ±3% and 13 ±2%, respectively) [6; 82].

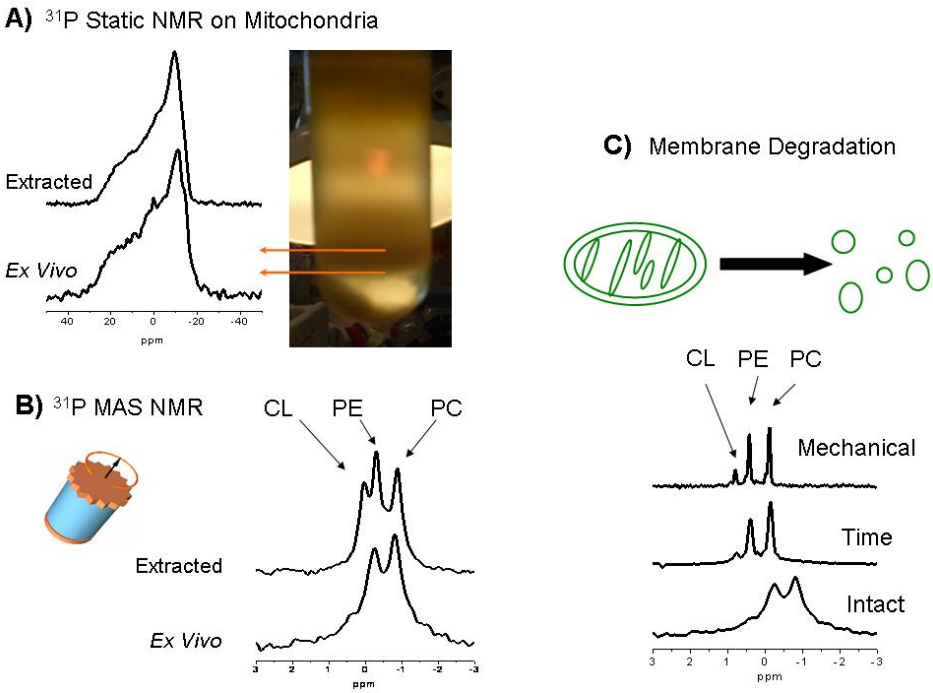

Figure 9 Ex vivo ^{31}P NMR of living mitochondria (as in MS V)

Deliberate degradation of mitochondria was also investigated with the aim of identifying degradation markers in the NMR spectra for use in quality controls. Time trials at higher temperature, and sonication treatment both promoted a strong disruption of the lamellar organization of the mitochondria into small vesicles (the CSAs of the various lipids were all severely reduced and produced a featureless broad isotropic-like NMR resonance line). The ^{31}P MAS NMR spectra displayed sharp resonances that all underwent a downfield NMR shift. The cardiolipin NMR signal was now much more clearly visible and well separated; both observations indicating therefore that the tight interaction of cardiolipin with proteins was severely disrupted. Therefore, this NMR tool could clearly be applied to monitor the fate of membrane integrity and individual phospholipids response upon stress, like calcium overload.

- Application: mitochondrial membrane response upon calcium stress

In the mitochondrial-dependant PCD pathway, the mitochondrial permeability transition (MPT) is often visualized as a process that induces the release of apoptotic factors such as

cytochrome C from the intermembrane space of mitochondria into the cytosol. The signalling substance calcium can promote the swelling of mitochondria and has been shown to be one of the main culprits which can induce MPT onto isolated mitochondria in the presence of inorganic phosphate (Pi) [78; 83; 84]. The effects of Ca^{2+} on mitochondrial membranes were investigated by our solid state ^{31}P NMR approach. The presence of calcium promoted partial membrane degradation for $[Ca^{2+}] \geq 1mM$; an observation confirmed by respiratory controls. However, the key lipid present in mitochondria, cardiolipin, could not be identified in the MAS NMR spectra, an observation which indicates still ongoing strong interactions between cardiolipin and mitochondrial proteins despite mitochondrial degradation. The degradation was also confirmed by respiratory measurements where isolated mitochondria were incubated with 1mM Ca^{2+} and 1mM Pi. However no complete inhibition occurred, indicating ongoing leakage of mitochondrial metabolites. Taken together with the absence of a cardiolipin signal in the relevant NMR spectra, cardiolipin is presumably still tightly bound to the inner mitochondrial membrane despite the fact that calcium-induced mitochondrial swelling has promoted partial disruption of the outer membrane and accelerated lipid dynamics.

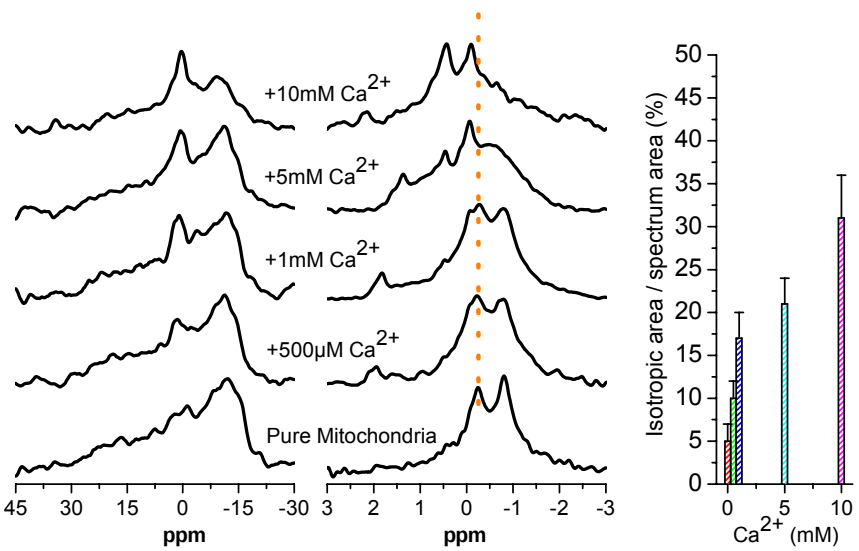

Figure 10 *Ex vivo* ^{31}P NMR of the isolated mitochondrial membrane response to calcium overload (As in MS V)

V Conclusions & Perspectives

The biophysical studies presented here were done in order to build a molecular picture of how mitochondrial membranes and apoptotic peptides could interact and modify each other. For this, the experimental designs required a range of interdisciplinary methods; starting from synthesis to spectroscopic techniques. What about the contribution to the apoptotic field? The two mains studies, paper III and MS IV, have shown how the regulative domains of proteins interact with membrane. This interplay must be crucial for the mitochondrial apoptotic pathway though extension to the *in vivo* mechanism if impossible. However, these studies enhanced the importance of considering lipids as important players, especially the mitochondrial specific cardiolipin. The membrane response to apoptotic stimuli cannot be neglected as the mitochondrial permeability is the key of the mitochondrial apoptotic pathway. Besides the fact that model membranes are different from the real biological membranes, these studies suffer also on the lipid/peptide ratio that was used. Indeed, in biological processes, the regulation often involves nanomolar concentration of proteins and a cell is an immense structure when considering the size of proteins. Therefore, signalling and addressing take all their importance, and specific interaction between proteins and lipid domains sustains a lot of answer for resolving molecular mechanisms. In apoptosis, the role of contact site, enriched in cardiolipin, is nowadays under intense investigation. The conclusion of this work should be used to verify if the BH4 domain change the mitochondrial membrane properties and if Bax-α1 requires cardiolipin at an *in vi*vo level. For this purpose, MS V shows promising results that investigating phospholipids in living system is possible, but requires a careful set up.

What next? MS V opened a new way to investigate apoptosis at a cellular level. It is still far from being enough for characterising what is happening during apoptosis and need to be further developed. Also, what I missed the most was to work with the full proteins (expression ongoing). Since I have not ended my formation yet, I would like to learn some biochemical engineering techniques to obtain the full panel required for a complete study, from protein expression to physiological interpretation. I have a long way to go…

Personal reflections

Good time and bad time: interplay

I experienced three phases during the last four years: the first is of course an overwhelming feeling of Nobel-hype, stimulating me like a baby opening its eyes to the aerobic world. One wants to grab every spin around itself, tasting each mixture one can make and publishing out the soonest results in a Nature-al Science-tific journal… Well, it lasts for one year and may be a half year more, before this extraordinary basic feeling let place to my second phase, the waste world (or time?). Yes, I am not talented enough to have spend four efficient, yielded, top ranking years spreading my name all over the community, except to some company listings of course, but I do not blame them, scientific or not, the world is a business where you have to FID-dle for your steaks. This eon where my scientific mojo decayed severely was probably indispensable since I have the feeling that one has to pass difficult time in life in order to learn harder, better, faster, stronger. What I have done during this extra one and a half (for this half I'm sure!) years was somehow a blank in my production, fortunately I am still a student so I was not fired for having throwing grant money (not the general but I heard he would have deserved it, even with Ulysses as first name…) out of the window (did someone took it?). After numerous discussions the conclusion was that, I acknowledge that you and my co-PhD mates (no reference but for review see supplement), experienced probably all approximately such difficulties, and the ones still standing out of the bulk have gained something through: toughness, thoughtfulness et al. And then today more or less, the final rush. You realize that in one year you have to acquire enough data to publish, according to the Umeå way of just do it, four articles, write a text book that will be printed in 100 copies but to be read by less then the square root, sort out your future and probably something I will forget to do… But you know what? A temporal failure must occur then because we all manage this Herculean (ok, not really but still it fits well I thought) task and we all then think, gosh if I would have worked like that during four years I probably would have done not a good PhD but just what Erick and Gerhard expected (always the best, thanks to you it cheers up). However, since I think I will achieve all of it on time with the requirements fulfilled; I hope my work was at the end of good quality.

Evolution of thoughts: from school to research

Remember few sentences above; I described my dynamic phase diagram but the different stages of critical thinking were somehow missing. I will take more of your time to talk about non-scientific (at least without equations, numbers, figures and so on) considerations. Indeed, or again, I had to build up my scientific vision of research since I lacked it from the beginning. I obtained my master degree in molecular chemistry of living system at the University of Bordeaux 1, where I assume, my skill for questioning and conception of biological molecular mechanism has been sharpened, well at least from a theoretical point of view. I started my PhD period straight afterwards at the Umeå University with a certain advantage, I have to admit. Namely, I had in my baggage already my master research training on Apoptosis (do not worry about the first appearance of this word, it will show up quite often in this thesis). Nevertheless, when I try to remember my way of designing experiments, interpreting the data, shaking when I was alone at the spectrometer, I can feel the famous (close enough) reverse sentence: “that’s a tiny step for mankind, but a giant leap for me”. I mean, I was not fit to do research, yet, and from my scholar way of thinking, I realized the non-ideal mixture of doing research. I guess that is why we have a supervisor, and I am glad I had two, totally unlikely, but so complementary, I have been very lucky. Yes, research is also about luck, because so many of us fall on a difficult subject, but I would say that is here that you have to put your effort in as well, by either doing a side project or tune up the main one in a better way. I somehow did the second one, not because my subject was going nowhere, but I had the feeling (that explains partially the phase transition towards the chaotic phase) that I was not improving anymore my - or contributing to the international - knowledge. Then I decided to take a step deeper in my investigation by working with living system, but this story, I will tell later. Finally, what has allowed me to upgrade my subject is the main objective of a PhD: you must become independent. For that I would thank again my two top ranking supervisors, from a student you helped to transform into a researcher.

PS: Even if I feel as an independent, better scientist, able to run my own research, I definitively know I am still on my way for that, and only hard work will make an acceptable researcher out of me.

Using available techniques/machines in the design of experiments: limiting?

The last point before the strong core of this thesis, and connected with the thoughts as mentioned above, is the field where you orient into it. What does it mean? No surprise, you conduct your investigations under the supervision of a solid researcher and then you learn his way of designing experiments, the techniques he is using and you shape your thinking with his experience. Therefore I will always remember that I am glad to have been under double supervisions, even if I stayed mostly in Umeå. I have been surrounding by a biophysical medium which, I suppose, makes me part of this family. You might feel it by reading this thesis but for the purists I would already apologize: first because I am not very good with theory and second because with time I slightly shift from a biophysicist to an indefinable metastable state by conjugating molecular biology (and I would like to add physiology in the future) with physicochemical studies. Also, as one of the last reflexions, I sometimes put forward contradictions so I will just enumerate the main technique I have been using in one word: multi… And it might be a problem because I have not really been deep in one technique; I am not a specialist in NMR (unfortunately) or calorimetry or *etc*, I just can handle each of them. In a couple of years I will see if it was a good choice. Finally, the point here is to explain why I have been using the techniques listed below: because they were used in the groups where I have been working in. I have not brought my own technique in these labs and therefore I feel like I have a missing string at my bow. However, I am glad to say I have applied high resolution solid-state NMR to a living system (isolated mitochondria) which has not been really done so far!

Acknowledgements

I first need to thank Gerhard, who has been like a father (not like an elder, no worries you still have good rest in table tennis) for me.
Erick thanks for your outstanding formation and beating me badly in our squash games.

The entire biophysical department, especially Tobias, you have been very kind to me, if you need a DJ or a brännball player do not hesitate!. Also a big THANKS to Anita, was not easy to take care of my case…
The IECB people I met, you were all ready to help me at any time, special mention to Axelle, merci.

Thanks to all my friends from Umea, it opened my eyes living with you.
What to say about the pianais… thanks for so many good tablée, good laughs and everything around.
Thanks Olivier, all our discussion of any kind at any hours helped me a lot. Also we should be glad that we saved so many monkeys…

Thanks to my family, supportive you have been during these long years far away from you.
Thanks to my parents, without you I would never manage to be a doctor, I hope you will be proud of yourself.

Thanks would not be enough for my sunshine; I have no words to say how happy I am with you and how I need you to be with me, it makes me strong and invincible. **Je t'aime** $+\infty$

References

1. Kerr, J. F., Wyllie, A. H. & Currie, A. R. (1972). Apoptosis: a basic biological phenomenon with wide-ranging implications in tissue kinetics. *British journal of cancer* **26**, 239-57.
2. Frey, T. G. & Mannella, C. A. (2000). The internal structure of mitochondria. *Trends Biochem Sci* **25**, 319-24.
3. Alberts, B., Johnson, A., Lewis, J., Raff, M., Roberts, K. & Walter, P. (2002). *Molecular biology of the Cell*, 4th, Garland Science, New-York.
4. Yaffe, M. P. (1999). The machinery of mitochondrial inheritance and behavior. *Science* **283**, 1493-7.
5. Mannella, C. A. (1982). Structure of the Outer Mitochondrial-Membrane - Ordered Arrays of Pore-Like Subunits in Outer-Membrane Fractions from Neurospora-Crassa Mitochondria. *Journal of Cell Biology* **94**, 680-687.
6. Ardail, D., Privat, J. P., Egret-Charlier, M., Levrat, C., Lerme, F. & Louisot, P. (1990). Mitochondrial contact sites. Lipid composition and dynamics. *J Biol Chem* **265**, 18797-802.
7. de Kroon, A. I., Dolis, D., Mayer, A., Lill, R. & de Kruijff, B. (1997). Phospholipid composition of highly purified mitochondrial outer membranes of rat liver and Neurospora crassa. Is cardiolipin present in the mitochondrial outer membrane? *Biochim Biophys Acta* **1325**, 108-16.
8. Hovius, R., Thijssen, J., van der Linden, P., Nicolay, K. & de Kruijff, B. (1993). Phospholipid asymmetry of the outer membrane of rat liver mitochondria. Evidence for the presence of cardiolipin on the outside of the outer membrane. *FEBS Lett* **330**, 71-6.
9. Ardail, D., Gasnier, F., Lerme, F., Simonot, C., Louisot, P. & Gateau-Roesch, O. (1993). Involvement of mitochondrial contact sites in the subcellular compartmentalization of phospholipid biosynthetic enzymes. *J Biol Chem* **268**, 25985-92.
10. Lutter, M., Fang, M., Luo, X., Nishijima, M., Xie, X. & Wang, X. (2000). Cardiolipin provides specificity for targeting of tBid to mitochondria. *Nat Cell Biol* **2**, 754-61.
11. Reichert, A. S. & Neupert, W. (2002). Contact sites between the outer and inner membrane of mitochondria-role in protein transport. *Biochim Biophys Acta* **1592**, 41-9.
12. Kuwana, T., Mackey, M. R., Perkins, G., Ellisman, M. H., Latterich, M., Schneiter, R., Green, D. R. & Newmeyer, D. D. (2002). Bid, Bax, and lipids cooperate to form supramolecular openings in the outer mitochondrial membrane. *Cell* **111**, 331-42.
13. Reed, J. C. (2002). Apoptosis-based therapies. *Nat Rev Drug Discov* **1**, 111-21.
14. Marchetti, P., Castedo, M., Susin, S. A., Zamzami, N., Hirsch, T., Macho, A., Haeffner, A., Hirsch, F., Geuskens, M. & Kroemer, G. (1996). Mitochondrial permeability transition is a central coordinating event of apoptosis. *J Exp Med* **184**, 1155-60.
15. Hajnoczky, G., Davies, E. & Madesh, M. (2003). Calcium signaling and apoptosis. *Biochem Biophys Res Commun* **304**, 445-54.
16. Roberts, D. L., Goping, I. S. & Bleackley, R. C. (2003). Mitochondria at the heart of the cytotoxic attack. *Biochem Biophys Res Commun* **304**, 513-8.
17. Macho, A., Castedo, M., Marchetti, P., Aguilar, J. J., Decaudin, D., Zamzami, N., Girard, P. M., Uriel, J. & Kroemer, G. (1995). Mitochondrial dysfunctions in

circulating T lymphocytes from human immunodeficiency virus-1 carriers. *Blood* **86**, 2481-7.
18. Herr, I. & Debatin, K. M. (2001). Cellular stress response and apoptosis in cancer therapy. *Blood* **98**, 2603-14.
19. Chomyn, A. & Attardi, G. (2003). MtDNA mutations in aging and apoptosis. *Biochem Biophys Res Commun* **304**, 519-29.
20. Schon, E. A. & Manfredi, G. (2003). Neuronal degeneration and mitochondrial dysfunction. *J Clin Invest* **111**, 303-12.
21. Debatin, K. M., Poncet, D. & Kroemer, G. (2002). Chemotherapy: targeting the mitochondrial cell death pathway. *Oncogene* **21**, 8786-803.
22. Zhu, S., Stavrovskaya, I. G., Drozda, M., Kim, B. Y., Ona, V., Li, M., Sarang, S., Liu, A. S., Hartley, D. M., Wu, D. C., Gullans, S., Ferrante, R. J., Przedborski, S., Kristal, B. S. & Friedlander, R. M. (2002). Minocycline inhibits cytochrome c release and delays progression of amyotrophic lateral sclerosis in mice. *Nature* **417**, 74-8.
23. Kluck, R. M., Esposti, M. D., Perkins, G., Renken, C., Kuwana, T., Bossy-Wetzel, E., Goldberg, M., Allen, T., Barber, M. J., Green, D. R. & Newmeyer, D. D. (1999). The pro-apoptotic proteins, Bid and Bax, cause a limited permeabilization of the mitochondrial outer membrane that is enhanced by cytosol. *J Cell Biol* **147**, 809-22.
24. Huser, J., Rechenmacher, C. E. & Blatter, L. A. (1998). Imaging the permeability pore transition in single mitochondria. *Biophys J* **74**, 2129-37.
25. Wolter, K. G., Hsu, Y. T., Smith, C. L., Nechushtan, A., Xi, X. G. & Youle, R. J. (1997). Movement of Bax from the cytosol to mitochondria during apoptosis. *J Cell Biol* **139**, 1281-92.
26. Chappell, J. B. & Crofts, A. R. (1965). Calcium Ion Accumulation and Volume Changes of Isolated Liver Mitochondria. Calcium Ion-Induced Swelling. *Biochem J* **95**, 378-86.
27. Kroemer, G., Galluzzi, L. & Brenner, C. (2007). Mitochondrial membrane permeabilization in cell death. *Physiol Rev* **87**, 99-163.
28. Adams, J. M. & Cory, S. (1998). The Bcl-2 protein family: arbiters of cell survival. *Science* **281**, 1322-6.
29. Cory, S. & Adams, J. M. (2002). The Bcl2 family: regulators of the cellular life-or-death switch. *Nat Rev Cancer* **2**, 647-56.
30. Mayer, B. & Oberbauer, R. (2003). Mitochondrial regulation of apoptosis. *News Physiol Sci* **18**, 89-94.
31. Vaux, D. L., Cory, S. & Adams, J. M. (1988). Bcl-2 gene promotes haemopoietic cell survival and cooperates with c-myc to immortalize pre-B cells. *Nature* **335**, 440-2.
32. Kelekar, A. & Thompson, C. B. (1998). Bcl-2-family proteins: the role of the BH3 domain in apoptosis. *Trends Cell Biol* **8**, 324-30.
33. Suzuki, M., Youle, R. J. & Tjandra, N. (2000). Structure of Bax: coregulation of dimer formation and intracellular localization. *Cell* **103**, 645-54.
34. Wei, M. C., Zong, W. X., Cheng, E. H., Lindsten, T., Panoutsakopoulou, V., Ross, A. J., Roth, K. A., MacGregor, G. R., Thompson, C. B. & Korsmeyer, S. J. (2001). Proapoptotic BAX and BAK: a requisite gateway to mitochondrial dysfunction and death. *Science* **292**, 727-30.
35. Janiak, F., Leber, B. & Andrews, D. W. (1994). Assembly of Bcl-2 into microsomal and outer mitochondrial membranes. *J Biol Chem* **269**, 9842-9.
36. McCullough, K. D., Martindale, J. L., Klotz, L. O., Aw, T. Y. & Holbrook, N. J. (2001). Gadd153 sensitizes cells to endoplasmic reticulum stress by down-regulating Bcl2 and perturbing the cellular redox state. *Mol Cell Biol* **21**, 1249-59.

37. Zong, W. X., Lindsten, T., Ross, A. J., MacGregor, G. R. & Thompson, C. B. (2001). BH3-only proteins that bind pro-survival Bcl-2 family members fail to induce apoptosis in the absence of Bax and Bak. *Genes Dev* **15**, 1481-6.
38. Petros, A. M., Medek, A., Nettesheim, D. G., Kim, D. H., Yoon, H. S., Swift, K., Matayoshi, E. D., Oltersdorf, T. & Fesik, S. W. (2001). Solution structure of the antiapoptotic protein bcl-2. *Proc Natl Acad Sci U S A* **98**, 3012-7.
39. Wang, Y., Cao, R., Liu, D., Chervin, A., Yuan, J., An, J. & Huang, Z. (2007). Oligomerization of BH4-truncated Bcl-x(L) in solution. *Biochem Biophys Res Commun* **361**, 1006-11.
40. Ayllon, V., Cayla, X., Garcia, A., Fleischer, A. & Rebollo, A. (2002). The anti-apoptotic molecules Bcl-xL and Bcl-w target protein phosphatase 1alpha to Bad. *Eur J Immunol* **32**, 1847-55.
41. Wang, H. G., Takayama, S., Rapp, U. R. & Reed, J. C. (1996). Bcl-2 interacting protein, BAG-1, binds to and activates the kinase Raf-1. *Proc Natl Acad Sci U S A* **93**, 7063-8.
42. Yin, X. M., Wang, K., Gross, A., Zhao, Y., Zinkel, S., Klocke, B., Roth, K. A. & Korsmeyer, S. J. (1999). Bid-deficient mice are resistant to Fas-induced hepatocellular apoptosis. *Nature* **400**, 886-91.
43. Bouillet, P., Purton, J. F., Godfrey, D. I., Zhang, L. C., Coultas, L., Puthalakath, H., Pellegrini, M., Cory, S., Adams, J. M. & Strasser, A. (2002). BH3-only Bcl-2 family member Bim is required for apoptosis of autoreactive thymocytes. *Nature* **415**, 922-6.
44. Putcha, G. V., Moulder, K. L., Golden, J. P., Bouillet, P., Adams, J. A., Strasser, A. & Johnson, E. M. (2001). Induction of BIM, a proapoptotic BH3-only BCL-2 family member, is critical for neuronal apoptosis. *Neuron* **29**, 615-28.
45. Letai, A., Bassik, M. C., Walensky, L. D., Sorcinelli, M. D., Weiler, S. & Korsmeyer, S. J. (2002). Distinct BH3 domains either sensitize or activate mitochondrial apoptosis, serving as prototype cancer therapeutics. *Cancer Cell* **2**, 183-92.
46. Zha, J., Harada, H., Yang, E., Jockel, J. & Korsmeyer, S. J. (1996). Serine phosphorylation of death agonist BAD in response to survival factor results in binding to 14-3-3 not BCL-X(L). *Cell* **87**, 619-28.
47. Li, H., Zhu, H., Xu, C. J. & Yuan, J. (1998). Cleavage of BID by caspase 8 mediates the mitochondrial damage in the Fas pathway of apoptosis. *Cell* **94**, 491-501.
48. Puthalakath, H., Huang, D. C., O'Reilly, L. A., King, S. M. & Strasser, A. (1999). The proapoptotic activity of the Bcl-2 family member Bim is regulated by interaction with the dynein motor complex. *Mol Cell* **3**, 287-96.
49. Shimizu, S., Konishi, A., Kodama, T. & Tsujimoto, Y. (2000). BH4 domain of antiapoptotic Bcl-2 family members closes voltage-dependent anion channel and inhibits apoptotic mitochondrial changes and cell death. *Proc Natl Acad Sci U S A* **97**, 3100-5.
50. Shimizu, S., Shinohara, Y. & Tsujimoto, Y. (2000). Bax and Bcl-xL independently regulate apoptotic changes of yeast mitochondria that require VDAC but not adenine nucleotide translocator. *Oncogene* **19**, 4309-18.
51. Brenner, C. & Grimm, S. (2006). The permeability transition pore complex in cancer cell death. *Oncogene* **25**, 4744-56.
52. Kanno, T., Sato, E. E., Muranaka, S., Fujita, H., Fujiwara, T., Utsumi, T., Inoue, M. & Utsumi, K. (2004). Oxidative stress underlies the mechanism for Ca(2+)-induced permeability transition of mitochondria. *Free Radic Res* **38**, 27-35.
53. Kagan, V. E., Tyurina, Y. Y., Bayir, H., Chu, C. T., Kapralov, A. A., Vlasova, II, Belikova, N. A., Tyurin, V. A., Amoscato, A., Epperly, M., Greenberger, J., Dekosky, S., Shvedova, A. A. & Jiang, J. (2006). The "pro-apoptotic genies" get out of

mitochondria: oxidative lipidomics and redox activity of cytochrome c/cardiolipin complexes. *Chem Biol Interact* **163**, 15-28.
54. Makin, G. W., Corfe, B. M., Griffiths, G. J., Thistlethwaite, A., Hickman, J. A. & Dive, C. (2001). Damage-induced Bax N-terminal change, translocation to mitochondria and formation of Bax dimers/complexes occur regardless of cell fate. *Embo J* **20**, 6306-15.
55. Lucken-Ardjomande, S., Montessuit, S. & Martinou, J. C. (2008). Contributions to Bax insertion and oligomerization of lipids of the mitochondrial outer membrane. *Cell Death Differ* **15**, 929-37.
56. Mikhailov, V., Mikhailova, M., Pulkrabek, D. J., Dong, Z., Venkatachalam, M. A. & Saikumar, P. (2001). Bcl-2 prevents Bax oligomerization in the mitochondrial outer membrane. *J Biol Chem* **276**, 18361-74.
57. Huang, D. C., Adams, J. M. & Cory, S. (1998). The conserved N-terminal BH4 domain of Bcl-2 homologues is essential for inhibition of apoptosis and interaction with CED-4. *Embo J* **17**, 1029-39.
58. Shimizu, S., Narita, M. & Tsujimoto, Y. (1999). Bcl-2 family proteins regulate the release of apoptogenic cytochrome c by the mitochondrial channel VDAC. *Nature* **399**, 483-7.
59. Pastorino, J. G., Tafani, M., Rothman, R. J., Marcinkeviciute, A., Hoek, J. B. & Farber, J. L. (1999). Functional consequences of the sustained or transient activation by Bax of the mitochondrial permeability transition pore. *J Biol Chem* **274**, 31734-9.
60. Degterev, A., Lugovskoy, A., Cardone, M., Mulley, B., Wagner, G., Mitchison, T. & Yuan, J. (2001). Identification of small-molecule inhibitors of interaction between the BH3 domain and Bcl-xL. *Nat Cell Biol* **3**, 173-82.
61. Hotchkiss, R. S., McConnell, K. W., Bullok, K., Davis, C. G., Chang, K. C., Schwulst, S. J., Dunne, J. C., Dietz, G. P., Bahr, M., McDunn, J. E., Karl, I. E., Wagner, T. H., Cobb, J. P., Coopersmith, C. M. & Piwnica-Worms, D. (2006). TAT-BH4 and TAT-Bcl-xL peptides protect against sepsis-induced lymphocyte apoptosis in vivo. *J Immunol* **176**, 5471-7.
62. McConnell, K. W., Muenzer, J. T., Chang, K. C., Davis, C. G., McDunn, J. E., Coopersmith, C. M., Hilliard, C. A., Hotchkiss, R. S., Grigsby, P. W. & Hunt, C. R. (2007). Anti-apoptotic peptides protect against radiation-induced cell death. *Biochem Biophys Res Commun* **355**, 501-7.
63. Sugioka, R., Shimizu, S., Funatsu, T., Tamagawa, H., Sawa, Y., Kawakami, T. & Tsujimoto, Y. (2003). BH4-domain peptide from Bcl-xL exerts anti-apoptotic activity in vivo. *Oncogene* **22**, 8432-40.
64. Merrifield, R. B. (1963). Solid Phase Peptide Synthesis .1. Synthesis of a Tetrapeptide. *Journal of the American Chemical Society* **85**, 2149-&.
65. Carpino, L. A. (1957). Oxidative Reactions of Hydrazines .2. Isophthalimides - New Protective Groups on Nitrogen. *Journal of the American Chemical Society* **79**, 98-101.
66. Ramachandran, G. N., Ramakrishnan, C. & Sasisekharan, V. (1963). Stereochemistry of polypeptide chain configurations. *J Mol Biol* **7**, 95-9.
67. Sreerama, N. & Woody, R. W. (1993). A self-consistent method for the analysis of protein secondary structure from circular dichroism. *Anal Biochem* **209**, 32-44.
68. Sreerama, N. & Woody, R. W. (2000). Estimation of protein secondary structure from circular dichroism spectra: comparison of CONTIN, SELCON, and CDSSTR methods with an expanded reference set. *Anal Biochem* **287**, 252-60.
69. Sreerama, N. & Woody, R. W. (2004). On the analysis of membrane protein circular dichroism spectra. *Protein Sci* **13**, 100-12.

70. Castano, S. & Desbat, B. (2005). Structure and orientation study of fusion peptide FP23 of gp41 from HIV-1 alone or inserted into various lipid membrane models (mono-, bi- and multibi-layers) by FT-IR spectroscopies and Brewster angle microscopy. *Biochim Biophys Acta* **1715**, 81-95.
71. Goormaghtigh, E., Raussens, V. & Ruysschaert, J. M. (1999). Attenuated total reflection infrared spectroscopy of proteins and lipids in biological membranes. *Biochimica Et Biophysica Acta-Reviews on Biomembranes* **1422**, 105-185.
72. Israelachvili, J. N. & Mitchell, D. J. (1975). A model for the packing of lipids in bilayer membranes. *Biochim Biophys Acta* **389**, 13-19.
73. Lindstrom, F., Williamson, P. T. & Grobner, G. (2005). Molecular insight into the electrostatic membrane surface potential by 14n/31p MAS NMR spectroscopy: nociceptin-lipid association. *J Am Chem Soc* **127**, 6610-6.
74. Dufourc, E. J. (2006). Solid state NMR in biomembranes. In *Chemical Biology* (Larijani, B., Woscholski, R., and Rosser, C. A., eds, ed.), pp. 113-131. J. Wiley & Sons, Ltd., London.
75. Dufourc, E. J. & Smith, I. C. (1986). A detailed analysis of the motions of cholesterol in biological membranes by 2H-NMR relaxation. *Chem Phys Lipids* **41**, 123-35.
76. Leonard, A. & Dufourc, E. J. (1991). Interactions of cholesterol with the membrane lipid matrix. A solid state NMR approach. *Biochimie* **73**, 1295-302.
77. Arpagaus, S., Rawyler, A. & Braendle, R. (2002). Occurrence and characteristics of the mitochondrial permeability transition in plants. *J Biol Chem* **277**, 1780-7.
78. Fortes, F., Castilho, R. F., Catisti, R., Carnieri, E. G. & Vercesi, A. E. (2001). Ca2+ induces a cyclosporin A-insensitive permeability transition pore in isolated potato tuber mitochondria mediated by reactive oxygen species. *J Bioenerg Biomembr* **33**, 43-51.
79. Keech, O., Dizengremel, P. & Gardestrom, P. (2005). Preparation of leaf mitochondria from Arabidopsis thaliana. *Physiologia Plantarum* **124**, 403-409.
80. Lowry, O. H., Rosebrough, N. J., Farr, A. L. & Randall, R. J. (1951). Protein measurement with the Folin phenol reagent. *J Biol Chem* **193**, 265-75.
81. De Kruijff, B., Nayar, R. & Cullis, P. R. (1982). 31P-NMR studies on phospholipid structure in membranes of intact, functionally-active, rat liver mitochondria. *Biochim Biophys Acta* **684**, 47-52.
82. Edman, K. & Ericson, I. (1987). Phospholipid and fatty acid composition in mitochondria from spinach (Spinacia oleracea) leaves and petioles. A comparative study. *Biochem J* **243**, 575-8.
83. Azzi, A. & Azzone, G. F. (1966). Swelling and shrinkage phenomena in liver mitochondria. III. Irreversible swelling induced by inorganic phosphate and Ca2+. *Biochim Biophys Acta* **113**, 438-44.
84. Tupper, J. T. & Tedeschi, H. (1967). Observations on low amplitude Ca2+-induced swelling in mitochondria. *Life Sci* **6**, 2021-8.

I

Journal of Peptide Science
J. Peptide Sci. 2006; **12**: 58–64
Published online 9 June 2005 in Wiley InterScience (www.interscience.wiley.com). DOI: 10.1002/psc.686

JOURNAL OF PEPTIDE SCIENCE

Synthesis and secondary structure in membranes of the Bcl-2 anti-apoptotic domain BH4

LUCIE KHEMTÉMOURIAN,[a,‡] MARC-ANTOINE SANI,[a,b,‡] KATELL BATHANY,[a] GERHARD GRÖBNER[b] and ERICK J. DUFOURC[a]*

[a] UMR 5144 MOBIOS, CNRS-Université Bordeaux 1, IECB, 33607 Pessac Cedex, France
[b] Department of Biophysical Chemistry, Umeå University, SE-901 87 Umeå, Sweden

Received 20 December 2004; Revised 19 February 2005; Accepted 2 March 2005

Abstract: Solid phase synthesis of BH4, the 26 amino-acid domain (^{6}RTGYDNREIVMKYIHYKLSQRGYEWD^{31}) of the anti-apoptotic Bcl-2 protein has been accomplished using Fmoc chemistry. The use of peculiar cleavage conditions provided high yields after purification such that tens to hundreds of mg could be obtained. A ^{15}N-labelled version of the peptide could also be synthesized for NMR studies in membranes. The peptide purity was not lower than 98% as controlled by UV and MALDI-TOF mass spectrometry. The secondary structure was determined in water, trifluoroethanol (TFE) and in lipid membrane using UV circular dichroism. The peptide shows dominant β-sheeted structures in water that convert progressively into α-helical features upon addition of TFE or membrane. The amphipathic character of the helix suggests that the peptide might have a structure akin to those of antimicrobial peptides upon interaction with membranes. Copyright © 2005 European Peptide Society and John Wiley & Sons, Ltd.

Keywords: solid phase synthesis; reverse-phase HPLC; MALDI-TOF mass spectrometry; circular dichroism; non-protected tryptophan; apoptotic peptides, ^{15}N-labelled amino acids

INTRODUCTION

Cell regulation via programmed cell death is an essential part of life in most organisms [1,2]. This apoptosis is highly regulated, enabling the body to control its cell population during developmental processes such as embryogenesis, tissue remodelling, maturing of immune and neuronal systems [1–3]. Apoptosis destroys normal cells at the end of their lifetime and ensures proper removal of pathogenic cells, such as cancer and auto-aggressive immune cells. If this tight regulation fails, pathological cells can escape their fate – the programmed cell death – thereby leading to diseases such as autoimmune disorders, neurodegeneration and cancer [2,3]. A common theme for all these diseases seems to be a serious distortion of the interplay between pro- and anti-apoptotic factors, an imbalance enabling, for instance, cancer cells to survive and to escape from the body protection system [1–3].

In apoptosis, protein–protein interactions tightly regulate two major pathways, the death-receptor pathway with caspases as the main executioners, and a mitochondrial pathway with the interplay of the Bcl proteins family. The latter contains three different groups of proteins: the first one exhibiting anti-apoptotic activity, while group II and III promote apoptosis [4,5]. In the mitochondrial pathway – a major execution track in mammalian cells – pro- and anti-apoptotic Bcl proteins meet on the mitochondrial membrane surface and tightly regulate the fate of a cell by controlling the release of the pro-apoptotic cytochrome c from mitochondria. Proteins of group I such as Bcl-2 or Bcl-x_L can interact with the pro-apoptotic members (Bax family) and may form hetero dimers in membranes [6]. However, it appears that proteins are located mainly outside the membrane and their insertion and complex formation is not well understood [7].

In cancer, a potential overexpression of anti-apoptotic Bcl-2 families or a reduced expression of apoptotic factors can presumably prevent the desired cell death. Sequence analysis of the antiapoptotic Bcl-2 proteins revealed four short conserved domains (BH1–BH4) and a hydrophobic *C*-terminal part that may anchor the anti-apoptotic proteins such as Bcl-2 in the outer mitochondrial membrane [2–7]. The group II of apoptotic proteins such as Bax and Bak, have a similar overall structure except for the BH4 domain (^{10}DNREIVMKYIHYKLSQRGYEW^{30}). This *N*-terminal extracellular amphiphatic BH4 domain thus appears as a key factor for the regulative anti-apoptotic activity of Bcl-2 proteins. This conserved BH4 domain could protect cells from death by interacting with the mitochondrial membranes, thereby blocking any action of the apoptotic family members, and preventing release of cytochrome c. However, the regulative mechanism of this domain is still unknown.

The synthesis and the purification of the BH4 domain have already been reported by Peherstorfer *et al.* [8]

*Correspondence to: E. J. Dufourc, UMR 5144 MOBIOS, CNRS-Université Bordeaux 1, IECB, 2 rue Robert Escarpit, 33607 Pessac, France; e-mail: e.dufourc@iecb.u-bordeaux.fr
‡ Authors who contributed equally to the publication.

and by Shimizu *et al.* [7]. Peherstorfer investigated the ability of synthetic peptides derived from proteins of the Bcl-2 family (defined by the sequence 10–30) to interfere with the apoptotic process in LLC-PK_1 cells. The BH4 was synthesized by Genemed Synthesis (South San Francisco, CA) but no information about the synthesis and the purification was provided. The synthesis was checked by means of mass spectrometry and a purity of ca. 95% was reported. Shimizu performed the synthesis of the human Bcl-2 BH4 (amino acids 7–30) with a model 396 multiple peptide synthesizer (Advanced ChemTech) by using diisopropylcarbodiimide/1-hydroxybenzotriazole-activated, fluorenylmethoxycarbonyl-protected amino acids. The purity of this peptide was determined to be 95% by MALDI-TOF spectrometry. Again no information on the synthesis, purification and yield were given, no HPLC or MALDI-TOF spectra were shown. Moreover, Lee and co-workers [9] performed the synthesis of three BH4 (^{2}AHAGRSGYDNREIVMKYIHYKLSQRGYEWD^{31}, ^{6}RSGYDNREIVMKYIHYKLSQR^{26} and ^{10}DNREIVMKYIHYKLSQR^{26}) using standard 1-fluorenylmethoxycarbonyl chemistry and the purification using a preparative reverse-phase high performance liquid chromatography. The purities of the peptides were confirmed by analytical reverse-phase chromatography and mass spectral analysis. No further information about the synthesis and the purification were given. They studied by circular dichroism the secondary structure of those three peptides and they estimated from analysis of band intensities that the proportion of α-helix content was ca. 27%, when embedded in detergent (SDS) micelles. No structure was found in aqueous solution.

In order to elucidate its interaction with membranes on a molecular level the BH4 (6–30) domain of the Bcl-2 protein (^{6}RTGYDNREIVMKYIHYKLSQRGYEW^{30}) and BH4 (6–31) (^{6}RTGYDNREIVMKYIHYKLSQRGYEWD^{31}) were synthesized. This was done with the goal of higher yield and purity than those reported. The complete synthesis protocol was revisited and refined. Because SDS micelles poorly mimic the membrane medium, the secondary structure was investigated by dichroism circular in negatively charged lipid vesicles that best represent the mitochondrial membrane. Proper deconvolution of CD traces was performed using robust software. This is the first step towards a comprehension of the interaction between Bcl-2 protein and a model membrane. As will be shown below, the peptide is mainly β-sheeted in water and converts into α-helix upon addition of membranes or TFE.

MATERIALS AND METHODS

Chemicals

Fmoc-Asp(OtBu)-Novasyn TGA and Fmoc-Trp-Novasun resin, 2-(1H-benzotriazole-1-yl)-1,1,3,3-tetramethyl-uronium hexafluorophosphate (HBTU), *N*-hydroxybenzotriazole (HOBt) and *N*-α-Fmoc-amino acids were purchased from VWR-NovaBiochem (Läufelfingen, Switzerland). Amino acids were protected as follows: t-butyl (tBu) for threonine, aspartic acid, glutamic acids, serine; t-butoxycarbonyl (Boc) for lysines, tryptophan; trityl (trt) for histidine, asparagine, glutamine; 2,2,4,6,7-pentamethyl-dihydrobenzofuran-5-sulfonyl (pbf) for arginines. ^{15}N-labelled amino acids (valine and leucine) were obtained from Euriso-top, groupe CEA (Gif-sur-Yvette, France).

N-Methylpyrrolidone (NMP), piperidine, dichloromethane (DCM), dimethylformamide (DMF), diisopropylethylamine (DIEA) and anhydride acetic acid were purchased from SDS (Peypin, France); trifluoroacetic acid (TFA) was obtained from Applied Biosystems (Courtaboeuf, France); triisopropylsilane (TIS) from ACROS Organics (Geel, Belgium) and 1,2-ethanedithiol (EDT) from Aldrich (Saint Quentin Fallavier, France). 1,2-Dimyristoyl-sn-glycero-3-phosphocholine (DMPC) and 1,2-dimyristoyl-sn-glycero-3-phosphocholine (DMPG) were obtained from Sigma (UK).

Peptide Synthesis

The syntheses were performed on an Applied Biosystems 433A Peptide Synthesizer (PE Biosystem, Courtaboeuf, France) using Fmoc strategy [10] both for the 25- and 26-residue peptides. The polyethylene glycol-polystyrene (PEG-PS) resin was preloaded with an unprotected tryptophan substituted at 0.18 mmol g^{-1} and a protected aspartic acid substituted at 0.22 mmol g^{-1}. Fastmoc chemistry was carried out in four major steps per cycle: (i) deprotection of Fmoc groups by piperidine, (ii) activation of added amino acid with HBTU/HOBt (37.9 g/13.6 g) in 200 ml of DMF, (iii) coupling by amide link formation with a solution of 35% DIEA in NMP and (iv) capping to prevent truncated peptide elongation with acetic anhydride/DIEA/HOBt (19 ml/9 ml/0.8 g) in 400 ml of NMP. Each deprotection step was monitored by conductivity.

Cleavage from the Resin

The final peptide mixture was cleaved from its resin and deprotected in 94% TFA including the following scavengers: 2.5% EDT, 2.5% milli-Q water, 1% TIS. The solution was prepared at 4 °C and typically 10 ml was mixed to 0.4 g of peptide containing resin. Total deprotection and cleavage were achieved after 120 min in a covered Erlenmeyer. The peptide solution was then filtered under vacuum. The crude peptide was precipitated by adding 100 ml of cold diethyl ether and the cloudy aqueous phase was collected and centrifuged in a benchtop machine at 8000 rpm for 10 min. After removal of the supernatant, 5 ml of water was added and the sample was lyophilized.

Purification and Analysis

The crude peptide was dissolved in distilled water with 0.1% TFA, bath sonicated for 15 min at 50 °C and purified by reverse-phase HPLC (Waters Alliance 2695 with photodiode array detector) using a milli-Q water/acetonitrile gradient. Both aqueous (A) and acetonitrile (B) solutions included 0.1% TFA. A semi-preparative Vydac (Hesperia, USA) C4 column

(300 Å, 5 µm, 250 × 10 mn) was equilibrated in 100% of A at a flow rate of 3 ml/min. Absorption was monitored at 225 and 280 nm, the best wavelengths being determined by the UV photodiode detector. 8–16 mg of crude peptide was dissolved in 1.8 ml of solvent A and the sample was loaded into a 2 ml loop, injected immediately onto the column at room temperature and eluted over 38 min going from 100% to 68% of solvent A. All peptides were collected using ~70% of A.

MALDI TOF Mass Spectrometry

Matrix assisted laser desorption and ionization time of flight (MALDI-TOF) mass spectrometry was performed on a Bruker REFLEX III in the reflectron mode with a 20 kV acceleration voltage and a 23 kV reflector voltage. α-Cyano-4-hydroxycinnamic acid (Sigma) was used as a matrix, prepared as a saturated solution of 50% acetonitrile/0.1% TFA in water. Peptide was mixed in a ratio 1 : 1 (v/v) with the matrix solution. Samples were prepared with the dried droplet method on a stainless steel target with 26 spots. External mass calibration was achieved with a mixture of eight peptides having masses ranging from 961 Da (fragment 4–10 of adrenocorticotropic hormone) to 3495 Da (β-chain of oxidized bovine insulin).

Circular Dichroism (CD)

CD-spectra (Jasco J-720 spectropolarimeter, USA) were recorded at 1 nm intervals over the 190–250 nm wavelength range using a 1 mm pathlength quartz cell (Hellma, Germany). Eight scans were performed. The experiments were run at 50 nm/min and the temperature was fixed at 298 K. The peptide secondary structure was determined in water, TFE and lipid membranes that mimic the mitochondrial negatively charged external membrane in the same concentration of 50 µM. To prepare lipid vesicles DMPC/DMPG(2 : 1) were co-dissolved in $CHCl_3/CH_3OH$ (3 : 1 v/v) that was evaporated under vacuum. The lipid film was then hydrated in distilled water and freeze-dried. The fluffy powder was re-suspended with buffer A: TKEB (10 mM Tris, 10 mM KCl, 0.5 mM EDTA, pH 7.4) to obtain large multilamellar vesicles. The solution was subjected to three freeze-thaw cycles followed by pulsed sonication for 5 min at power 7 using a probe-type sonicator Soniprep 150 (MSE, USA) under cooling to obtain small unilamellar vesicles (SUV) to reduce light scattering. Metal particles possibly coming from the sonicating tip were removed by centrifugation.

To estimate the peptide secondary structure content, an analysis of the relevant CD-spectra was carried out using the CDPro software (http://lamar.colstate.edu/~ssreeram/CDPro) developed by R. W. Woody and coworkers [11]. Measured CD traces, CD_{meas}, were converted to mean residue ellipticity $[\Theta](\mathrm{deg\,cm^2dmol^{-1}})$ using the relationship $[\Theta] = CD_{meas}(\mathrm{degree})/(C(\mathrm{mol\,l^{-1}})1(\mathrm{cm})NR.10)$, where NR is the number of residues per peptide, l the cell length and C the concentration. The basis set 4 of the CDPro software was used [12]. Analysis was performed using three methods, CONTIN, CONTIN/LL and SELCON 3 [13]. In general, CONTIN/LL, a self-consistent method with an incorporated variable selection procedure, produced the most reliable results.

RESULTS

Peptide Synthesis and Purification

Three different synthesis pathways were tested with the aim of providing sufficient amounts of pure BH4 peptide for biophysical studies. The solid phase synthesis was carried out using the FastMoc strategy in a simple coupling mode, with 1 mmol of resin and a ten-fold excess of amino acids for the synthesis of BH4 (6–30) and BH4 (6–31). As the structural studies require large amounts of ^{15}N-labelled peptides, the synthesis of the BH4 (6–31) ^{15}N-labelled was carried out on a medium range scale: 2.5 mmol of resin and with a four-fold excess of amino acids.

The first synthesis was carried out with 555 mg of resin that was preloaded with unprotected Trp. From 555 mg resin only 135 mg of crude peptide was obtained after cleavage (yield of 54%). The peptide was

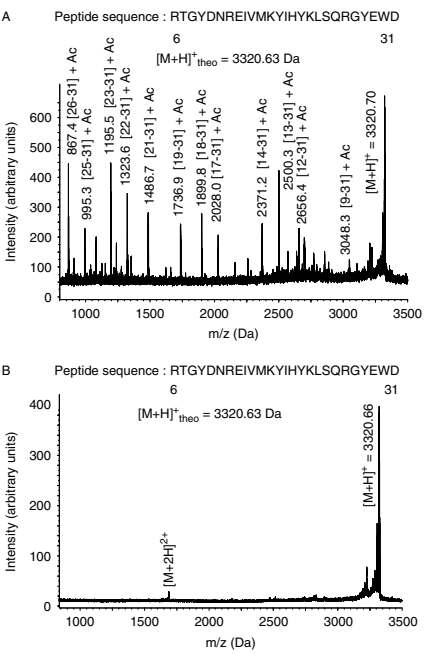

Figure 1 MALDI-TOF spectrum of (A) the crude reaction mixture containing the 26 amino acid long BH4 (6–31) domain of the Bcl-2 protein. The numbering in brackets [x-31] corresponds to truncated peptide segments. (B) BH4 (6–31) after purification by reverse phase HPLC. The second ionization product is observed at (M + nH)/(n), with a m/z of 1661 Da. The group of lines before the main peak comes from degradation by the MALDI laser.

characterized by MALDI-TOF (data not shown). Its main peak indicates a molecular mass of 3205.3 g.mol^{-1}, in agreement with the theoretical molecular weight of the 25 amino acids peptide of 3205.6 g mol^{-1}. In addition, there were several peaks, with one at m/z 3261 Da corresponding to the peptide with a tBu group (+56), one at m/z 3261 Da indicative of the peptide plus the resin linker (+164), and one at 3457 Da indicative of an attached pbf group (+252). The best purification by semi-preparative HPLC was achieved using a linear gradient with the following time intervals: eluent A varied in a 6 min linear gradient from 0% to 12%, then a 15 min linear gradient from 12% to 29% was applied and finally a 9 min linear gradient from 29% to 32% was used. BH4 (6–30) was eluted from the C4 reverse-phase HPLC column at a low percentage of acetonitrile (30%). The retention time was approximately 26 min. Absorption was monitored at 280 nm, the best wavelengths being determined by the UV photodiode detector. The BH4 (6–30) sequence contains five aromatic amino acids that have a high molar extinction coefficient and a high absorption peak at 280 nm. Only 1 mg of pure peptide (characterized by MALDI-TOF) was obtained.

In the second synthesis it was decided to make a 26 amino acid peptide, i.e. BH4 (6–31) extended to the next residue, aspartic acid (^{6}RTGYDNREIVMKYIHYKLSQRG-YEWD^{31}). From 455 mg resin preloaded with aspartic acid, 188 mg of crude peptide was obtained after cleavage (74% yield). Figure 1 shows that the end capping segments are clearly seen, and the highest peak reflects BH4 (6–31), assuming that the full peptide was the principal product and no corresponding adducts were detected. The purification was carried out as before providing highly pure peptide. A typical elution profile is shown in Figure 2 with a major peak indicating pure BH4 (6–31) peptide. The high purity degree of BH4 (6–31) (around 99%), as required for structural analysis, was checked by HPLC (the chromatogram shows one peak integrated to obtain a degree of purity of 98%) and MALDI-TOF (Figure 1), no by-adducts are detected after purification. 67 mg of peptide was recovered giving a purification yield of ca 36%.

The final synthesis was performed with the aim of incorporating ^{15}N-labelled amino acids (valine and leucine) for NMR studies. The synthesis was carried out on a medium range scale (2.5 mmol of resin and with a four-fold excess of amino acids), using 1.136 g of an aspartic acid preloaded resin, from which 615 mg of crude peptide was recovered. Purification and characterization were carried out as before. A total 250 mg of pure peptide was obtained after purification that provided a yield of 41%. The final purity was 98% as checked by HPLC and MALDI-TOF.

Secondary Structure Analysis by Circular Dichroism of BH4 (6–31)

Circular dichroism was used to assess the secondary structure of the synthetic peptide under aqueous solution, TFE and upon interaction with small unilamellar vesicles (SUV). The peptide conformation was determined in water at pH 5, in TFE at pH 6 and upon interaction with SUV at pH 7.4. All experiments were performed at 25 °C.

The solid line in Figure 3 shows the CD spectrum in water and exhibits a minimum at 198 nm and a weak maximum at 230 nm. The weakness of the

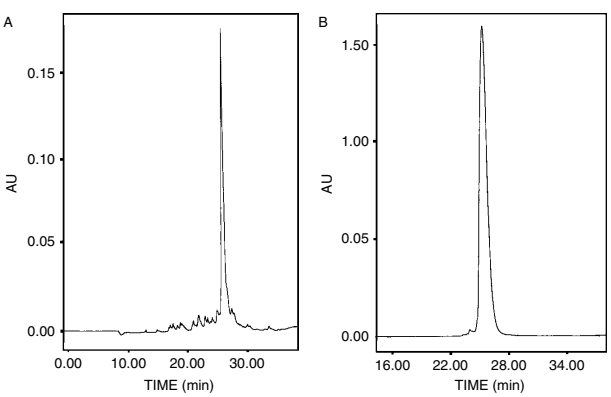

Figure 2 Photodiode UV chromatograms at 280 nm of (A) the crude peptide after cleavage from the resin, (B) the purified peptide. Both used reverse phase chromatography on a semi-preparative C4 column at a flow rate of 3 ml/min. The small peaks in (A) originate from truncated peptide segments. The major fraction was eluted after 26 min treatment with 30% of eluent B (see text).

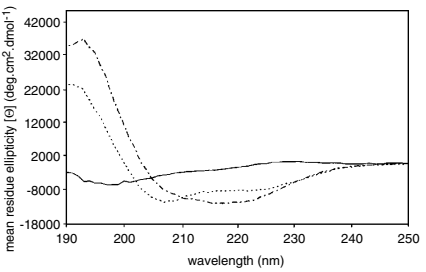

Figure 3 Circular dichroism spectra of BH4 (6–31) obtained in water (full line), in pure TFE (dash) and upon interaction with SUV of DMPC/DMPG 2 : 1 in a L/P molar ratio of 80/1 (dash-dot). The pH was 4.5 in pure water, 6 in pure TFE and 7.4 in the membrane buffer solution. Eight scans were accumulated at 25 °C. Scan speed was set at 50 nm/min.

signal is presumably due to the presence of a positive band at 225 nm arising from the four tyrosine residues that might interfere with a negative ellipticity band at 220 nm [14]. The tryptophan residue also has an irregular (depending of its environment) but high tendency to absorb in the entire spectral range (190–250 nm) [15]. It is well known that TFE promotes the α-helix conformation by strengthening the peptide H-bonds and may interrupt the hydrophobic interaction and then the ternary structure formation [16]. The dashed line represents the spectrum in TFE and displays minima at 208 and 222 nm and a maximum at 192 nm. No temperature-dependence is noticed in CD measurements indicated by no significant structural changes between 25 °C and 65 °C (data not shown). The dash-dot line in Figure 3 denotes the peptide spectrum in DMPC/DMPG vesicles. When small unilamellar vesicles are added in a ratio of 80/1 (L/P) a very broad minimum around 216 nm is detected and a maximum is reached at 193 nm, suggesting a mixture of α-helix and β-sheet conformations.

Deconvolution of CD traces was performed as described in the materials and methods to obtain accurate values of secondary structure elements using CDPro software [10] and an appropriate protein basis. The results reported in Table 1 show a higher peptide structure in membrane, with only 18% of random coil compared with ca 30% in solution (water and TFE). The secondary structure is mostly in β-sheet conformation (43%) in aqueous solution and turns into α-helix (38%) upon titration of SUV. As expected, TFE promotes highest contents of α-helix with 45%. Turns remain constant in the three media around 20%.

Table 1 Percentage of Secondary Structure Elements for the BH4 (6–31) Peptide in Water, TFE and upon Addition of DMPC/DMPG (2 : 1) SUV

Secondary structure	Water	SUV	TFE
α-Helix	5%	38%	45%
β-Sheet	43%	22%	10%
Turns	22%	22%	17%
Random coil	30%	18%	28%

Deconvolution of CD spectra was accomplished using basis 4 from the CDPro software and the CONTIN/LL algorithm (see text). Accuracy is estimated to be of ca 5%.

DISCUSSION

In this work, two main results appear: (i) an improvement in the synthesis and purification of the peptide BH4 in an effective way with a reproducible protocol and (ii) changes in the secondary structure from water to phospholipid model membranes. These different points will be discussed below.

High Yield and High Peptide Purity

The synthesis yield of the peptide BH4 (6–30) is 54%, whereas that of peptides BH4 (6–31) is 74%. Because the theoretical yield can be calculated to 77%, considering a 99% yield per step [17], it is seen that the BH4 (6–31) synthesis worked much better than that of BH4 (6–30). This first synthesis (6–30) was not very successful presumably because the resin was preloaded with unprotected tryptophan. Only 54% of peptide was cleaved from the resin. As suggested in the literature it is supposed that this low yield is not related to incomplete ester bond cleavage but merely to re-addition of the intermediate benzyl cation to the indole nucleus [18]. No further peptide was released from the resin after repeated treatment with trifluoroacetic acid. The *C*-terminal position of the tryptophan residue could favour the intramolecular process as this has already been suggested by Atherton and co-workers [18]. During the second synthesis a resin preloaded with aspartic acid was used to eliminate the risk of any side linkage to tryptophan. This residue was Boc protected to avoid any trouble [19]. The sequence contains some residues with delicate behaviour during the cleavage due to the presence of various nucleophilic functional groups in Trp, Met, Tyr, Arg. They are extremely susceptible to alkylation by cations produced during the cleavage process. Reaction of tryptophan, methionine with t-butyl cations results in modification of the product peptide. With the addition of scavengers such as EDT these side reactions can be suppressed. During the synthesis, the presence of thiols in the cleavage solution was necessary because it eliminated problems arising from cationic groups and reduced the number of adducts in the crude peptide. In general, the high yields of peptide obtained in the second and third synthesis trials are related to the dominant

hydrophilic character of the peptide sequence and the advanced methods recently developed in solid phase synthesis, such as the use of HBTU/HOBt activators and that of advanced solution cleavage procedures [17, 19–20]. Another crucial parameter involved in high yield is the cleavage time. During a long cleavage period protected groups such as pbf, are well removed, but the probability of a new complex between the linker and the indole ring of the tryptophan increases [21]. A period of 2 h was used here, providing the best compromise for the BH4 (6–31) peptide.

Structural Changes upon Binding to Vesicles

In contact with a model membrane that mimics the mitochondrial membrane, the β-sheet conformation of BH4(6–31) in water is converted into an α-helical structure. An α-helix was also reported by Lee and co-workers [9] upon addition of SDS micelles, whereas no structure was reported in water contrary to our results. The variance of the results in water is presumably due to the fact that deconvolution was not used to assess their conclusion. Although the results go in the same direction for structure in SDS and membranes, it must be noted that they worked on a longer peptide, BH4 (1–31), and estimated the helical content (27%) by comparison of 208 nm and 222 nm intensities, while our calculation showed 38% using solid deconvolution software. It must also be remarked that SDS micelles are less suitable for mimicking the mitochondrial membrane as they induce higher constraints by curvature and expose a smaller surface to the peptide. As the peptide is basic it can be proposed that the change in secondary structure going from water to a negatively charged surface is driven by electrostatic interactions, the flat membrane surface ensuring an additional structuring effect as opposed to small spherical micelles. TFE induced a higher α-helical structure than in SUVs; this is not surprising due to the well known role of this solvent in favouring hydrogen bonds and breaking aggregates. The helical character of BH4 upon binding to membrane gives an amphipathic character to the peptide where the distribution of hydrophobic and hydrophilic/charged residues may be located on different sides of the helix barrel. Interestingly this secondary amphipathicity is reminiscent of antibacterial peptides that are known to strongly interact with negatively charged membrane surfaces [22]. Further studies are being conducted in the laboratory to follow the possible perturbation effect of BH4 on membranes by solid state NMR.

The BH4 domain is thought to be the regulative part of anti-apoptotic Bcl-2 proteins. By looking thoroughly at the solution structure determined by solution NMR of the entire Bcl-2 protein in Tris and DTT buffer at pH 7.8 [23], the secondary structure of BH4 (6–31) in the protein is helical in majority (11–24) conferring to the peptide ca 50% of α-helix content. This is very close to the content found for the isolated peptide when interacting with membranes. It appears therefore that the BH4 part of Bcl-2 has an appropriate structure to interact favourably with negatively charged membranes. Because Bcl-2 proteins are presumably anchored to the membrane by their trans-membrane BH1 and BH2 domains, the contact of this amphipathic helix could ensure additional binding through electrostatic/amphipathic interactions that could in some cases lead to mitochondrial membrane instability or to compete for binding with pro-apoptotic proteins. However, additional experimental evidence are needed to assess this hypothesis.

CONCLUSION

Reproducible methods to prepare in large amounts and with very high purity the peptide corresponding to the BH4 domain of the anti-apoptotic human Bcl-2 have been developed herein. It must been remarked that starting the synthesis from a tryptophan residue presents some difficulties due to side-reactions on the indole ring and should be avoided whenever possible.

It must also been noticed that secondary structure changes upon membrane addition are better detected when proper lipidic membranes and deconvolution algorithms are used.

Acknowledgements

We thank gratefully Professor Jean-Marie Schmitter (IECB-MOBIOS, UMR 5144, MoBIOS, Pessac, France), for assistance and help in mass spectroscopy analyses. This work was supported by Knut and Alice Wallenberg Foundation, Swedish Research Council (621-2001-3185), Umeå University Biotechnology Fund and by the Association pour la Recherche contre le Cancer, France (ARC-4261). We also thank A. Söderlind and G. Lindblom for their support.

REFERENCES

1. Kerr JF, Wyllie AH, Currie AR. Apoptosis: a basic biological phenomenon with wide-ranging implications in tissue kinetics. *Br. J. Cancer* 1972; **26**: 239–257.
2. Hengartner MO. The biochemistry of apoptosis. *Nature* 2000; **407**: 770–776.
3. Thompson CB. Apoptosis in the pathogenesis and treatment of disease. *Science* 1995; **267**: 1456–1462.
4. Thornberry NA, Labzenick Y. Caspases: enemies within. *Science* 1998; **281**: 1312–1316.
5. Enari M, Sakahira H, Yokoyama H, Okawa K, Iwamatsu A, Nagata S. A caspase-activated DNase that degrades DNA during apoptosis, and its inhibitor ICAD. *Nature* 1998; **391**: 43–50.
6. Yin XM, Oltvai ZN, Veis-Novack J, Linette GP, Korsmeyer SJ. BH1 and BH2 domains of Bcl-2 are required for inhibition of apoptosis and heterodimerization with Bax. *Nature* 1994; **369**: 321–323.

7. Shimizu S, Konishi A, Kodama T, Tsujimoto Y. BH4 domain of antiapoptotic Bcl-2 family members closes voltage-dependent anion channel and inhibits apoptotic mitochondrial changes and cell death. *PNAS* 2000; **97**: 3100–3105.
8. Peherstorfer E, Mayer B, Boehm S, Lukas A, Hauser P, Mayer G, Oberbauer R. Effects of microinjection of synthetic Bcl-2 domain peptides on apoptosis of renal tubular epithelial cells. *Am. J. Physiol. Renal. Physiol.* 2002; **283**: F190–F196.
9. Lee LC, Hunter JJ, Mujeeb A, Turck C, Parslow TG. Evidence for α-helical conformation of an essential *N*-terminal region in the human Bcl2 protein. *J. Biol. Chem.* 1996; **271**: 23 284–23 288.
10. Simon C, Pianet I, Dufourc EJ. The synthesis and circular dichroism study of the human, salivary proline-rich protein IB7. *J. Pept. Sci.* 2003; **9**: 125–131.
11. Sreerama N, Woody RW. A self-consistent method for the analysis of protein secondary structure from circular dichroism. *Anal. Biochem.* 1993; **209**: 32–44.
12. Sreerama N, Venyaminov SY, Woody RW. Estimation of peptide secondary structure from circular dichroism spectra: Inclusion of denatured peptides with native peptides in the analysis. *Anal. Biochem.* 2000; **287**: 243–251.
13. Sreerama N, Woody RW. Estimation of peptide secondary structure from circular dichroism spectra: Comparison of CONTIN, SELCON, and CDSSTR methods with an expanded reference set. *Anal. Biochem.* 2000; **287**: 252–260.
14. Bradley EK, Thomason JF, Cohen FE, Kosen PA, Kuntz ID. Studies of synthetic helical peptides using circular dichroism and nuclear magnetic resonance. *J. Mol. Biol.* 1990; **215**: 607–622.
15. Andersson D, Carlsson U, Freskgård PO. Contribution of tryptophan residues to the CD spectrum of the extracellular domain of human tissue factor. *Eur. J. Biochem.* 2001; **268**: 1118–1128.
16. Luo P, Baldwin RL. Mechanism of helix induction by trifluoroethanol: a framework for extrapolating the helix-forming properties of peptides from trifluoroethanol/water mixtures back to water. *Biochemistry* 1997; **36**: 8413–8421.
17. Fields GB, Noble RL. Solid-phase peptide synthesis utilizing 9-fluorenylmethyloxycarbonyl amino acids. *Int. J. Pept. Protein Res.* 1990; **35**: 161–214.
18. Atherton E, Cameron LR, Sheppard RC. Peptide synthesis: Part 10. Use of pentafluorophenyl esters of fluorenylmethoxycarbonylamino acids in solid phase peptide synthesis. *Tetrahedron* 1988; **44**: 843–857.
19. Chang CD, Meienhofer J. Solid-phase peptide synthesis using mild base cleavage of N alpha-fluorenylmethyloxycarbonyl amino acids. *Int. J. Pept. Protein Res.* 1978; **11**: 246–249.
20. Nilsson MR, Nguyen LL, Raleigh DP. Synthesis and purification of amyloidogenic peptides. *Anal. Biochem.* 2001; **288**: 76–82.
21. Giraud M, Cavelier F, Martinez J. A side-reaction in the SPPS of Trp-containing peptides. *J. Pept. Sci.* 1999; **5**: 457–461.
22. Shai Y. Mechanism of the binding, insertion and destabilization of phospholipid bilayer membranes by alpha-helical antimicrobial and cell non-selective membrane-lytic peptides. *Biochim. Biophys. Acta* 1999; **1462**: 55–70.
23. Petros AM, Medek A, Nettesheim DG, Kim DH, Yoon HS, Swift K, Matayoshi ED, Oltersdorf T, Fesik SW. Solution structure of the antiapoptotic protein Bcl2. *PNAS* 2001; **98**: 3012–3017.

II

Journal of Peptide Science
J. Pept. Sci. 2007; **13**: 100–106
Published online 15 November 2006 in Wiley InterScience (www.interscience.wiley.com). DOI: 10.1002/psc.803

JOURNAL OF PEPTIDE SCIENCE

Pro-apoptotic bax-α1 synthesis and evidence for β-sheet to α-helix conformational change as triggered by negatively charged lipid membranes

MARC-ANTOINE SANI,[a,b] CÉCILE LOUDET,[a] GERHARD GRÖBNER[b]* and ERICK J. DUFOURC[a]*

[a] UMR 5144 MOBIOS, CNRS-Université Bordeaux 1, IECB, 33607 Pessac Cedex, France
[b] Department of Biophysical Chemistry, Umeå University, SE-901 87 Umeå, Sweden

Received 11 August 2006; Accepted 3 September 2006

Abstract: Solid phase synthesis of Bax-α1, the 25 amino acids domain (^{14}TSSEQIMKTGALLLQGFIQDRAGRM^{38}) of the pro-apoptotic Bax protein has been accomplished using Fmoc chemistry. A new fast and harmless protocol is described for complete TFA removal from the purified peptide powder leading to a final purity greater than 98% as controlled by ^{19}F-NMR, UV and MALDI-TOF mass spectrometry. Secondary structure was determined in various solution and membrane media using UV Circular Dichroism. In water solution, Bax-α1 is present as a mixture of β-sheet and unstructured (random coil) conformations. A marked change from β-sheet to α-helix secondary structures is observed upon interaction with negatively charged phospholipids vesicles whereas neutral lipid membranes have no significant effect on the aqueous peptide conformation. Results are discussed in terms of Bax binding to mitochondrial membranes. Copyright © 2006 European Peptide Society and John Wiley & Sons, Ltd.

Keywords: solid phase synthesis; TFA removal; ^{19}F NMR; UV circular dichroism; electrostatic interaction; apoptotic peptides

INTRODUCTION

Understanding the regulation of the programmed cell death -apoptosis- is a challenge that can promote valuable information to treat diseases including autoimmune disorders, neuro-degeneration and cancer [1–4]. In general, pro- and anti-apoptotic members of the Bcl-family meet at the mitochondrial membrane, and arbitrate a life or death decision for the cell [2,5–7]. Once this internal pathway is activated the outer mitochondrial membrane gets permeabilized, thereby inducing the lethal and irreversible release of cytochrome C [8,9]. Normally, the anti-apoptotic Bcl-2 protein and its homologues prevent this process by keeping the pro-apoptotic proteins such as Bax and its homologues under control, thereby maintaining the integrity of the mitochondrial membrane [9–12]. Nevertheless, the process of such interplay is still poorly understood, but clearly the ability of Bax to bind at the mitochondrion outer membrane is a key step to induce apoptosis. Membrane proteins, such Bax, Bcl-XL or Bcl-2, possess helical anchor segments to promote insertion into the hydrophobic core of the mitochondrion membrane; they are usually located at the protein *C*-Termina part (CT). Substitution of the Bcl-XL CT by the Bax CT inhibits the insertion capability of Bcl-XL protein while the opposite leads to massive binding to the mitochondrion [13,14]. On the other hand, deletion of the protein *N*-terminal part (NT) impairs the binding of Bax to mitochondria, whereas a fusion of the NT terminus of Bax with a cytosolic protein results in the binding of the chimeric proteins to mitochondria, both in a cell-free assay and *in vitro* [15].

To elucidate both the conformation and the membrane insertion capability of this 'anchor' peptide, we decided to use an optimized solid phase peptide synthesis method [16] to produce reasonable amounts of highly pure Bax NT segment. During the purification process we faced the problem of elevated amounts of TFA contaminating the purified peptide, which was removed by implementing a special procedure. A circular dichroism (CD) study was thus undertaken in different media, including negatively charged phospholipid vesicles that mimic the mitochondrion outer membrane, to follow the Bax-α1 peptide structural modifications.

MATERIALS AND METHODS

Chemicals

Fmoc-Asp(OtBu)-Novasyn TGA resin, 2-(1H-benzotriazole-1-yl)-1,1,3,3-tetramethyl-uronium hexafluorophosphate (HBTU), *N*-hydroxybenzotriazole (HOBt) and *N*-α-Fmoc-amino acids were purchased from VWR-NovaBiochem (Läufelfingen, Switzerland). Amino acids were protected as follows: t-butyl (tBu) for threonine, aspartic acid, glutamic acids, serine; t-butoxycarbonyl (Boc) for lysines, tryptophan; trityl (trt) for histidine, asparagine, glutamine; 2,2,4,6,7-pentamethyl-dihydrobenzofuran-5-sulfonyl (pbf) for arginines. ^{15}N-labeled amino acids (valine and leucine) as required for NMR structural

*Correspondence to: E. J. Dufourc, UMR5144 MOBIOS CNRS-Université Bordeaux 1, IECB, 2 rue Robert Escarpit, 33607 Pessac, France; e-mail: e.dufourc@iecb.u-bordeaux.fr

studies were obtained from Euriso-top, groupe CEA (Gif-sur-Yvette, France). *N*-methylpyrrolidone (NMP), piperidine, dichloromethane (DCM), dimethylformamide (DMF), diisopropylethylamine (DIEA) and anhydride acetic acid were purchased from SDS (Peypin, France); Trifluoroacetic acid (TFA) was obtained from Applied Biosystems (Courtaboeuf, France); triisopropylsilane (TIS) from ACROS organics (Geel, Belgium) and 1,2-ethanedithiol (EDT) from Aldrich (Saint Quentin Fallavier, France).

Peptide Synthesis

The synthesis was performed on an Applied Biosystems 433A Peptide Synthesizer (PE Biosystem, Courtaboeuf, France) using the Fmoc strategy. The polyethylene glycol-polystyrene (PEG-PS) resin was preloaded with an unprotected methionine substituted at 0.23 mmol g^{-1}. Fastmoc chemistry was carried out according to reported procedures [16] in four major steps per cycle: (i) deprotection of Fmoc groups by piperidine, (ii) activation of added amino acid with HBTU/HOBt (37.9 g/13.6 g) in 200 ml of DMF, (iii) coupling by amide link formation with a solution of 35% DIEA in NMP and (iv) capping to prevent truncated peptide elongation with acetic anhydride/DIEA/HOBt (19 ml/9 ml/0,8 g) in 400 ml of NMP. Each deprotection step was monitored by conductivity measurements.

Cleavage from the Resin

The final peptide mixture was cleaved from its resin and deprotected in 94% TFA including the following scavengers: 2.5% EDT, 2.5% milli-Q water, 1% TIS. The solution was prepared at 4 °C and typically 10 ml was added to 0.5 g of peptide-containing resin. Total deprotection and cleavage were achieved after 120 min in a covered Erlenmeyer. The peptide solution was then filtered under vacuum. Adding 100 ml of cold diethyl ether precipitated the crude peptide and the cloudy aqueous phase was collected and centrifuged in a bench-top apparatus at 8000 rpm for 10 min. After removal of the supernatant, 10 ml of water/acetonitrile in a 60 : 40 v/v ratio was added and the solution was lyophilized.

Purification and Analysis

The crude peptide was dissolved in distilled water with 0.1% TFA and purified by reverse phase-high performance chromatography (RP-HPLC) (Waters Alliance 2695 with photodiode array detector) using a milli-Q water/acetonitrile gradient. Both aqueous (A) and acetonitrile (B) solutions included 0.1% TFA. A semi-preparative Vydac (Hesperia, USA) C4 column (300 Å, 5 µm, 250 × 10 nm) was equilibrated in 100% of A at flow rate of 3 ml min^{-1}. Absorption was monitored at 225 nm. 5 mg ml^{-1} of crude peptide was dissolved in solvent A and the sample was loaded into a 2-ml loop, injected immediately onto the column at room temperature and eluted over 31 min going from 100% to 45% of solvent A. All peptides were collected using ~60% of A.

MALDI-TOF Mass Spectrometry

Matrix assisted laser desorption and ionization time of flight (MALDI-TOF) mass spectrometry was performed on a Bruker REFLEX III in the reflectron mode with a 20-kV acceleration voltage and a 23-kV reflector voltage. α-cyano-4-hydroxycinnamic acid (Sigma) was used as a matrix, prepared as a saturated solution of 50% acetonitrile/0.1% TFA in water. Peptide was mixed in the ratio 1 : 1 (v/v) with the matrix solution. Samples were prepared with the dried droplet method on a stainless steel target with 26 spots. External mass calibration was achieved with a mixture of eight peptides having masses ranging from 961 Da (fragment 4–10 of adrenocorticotropic hormone) to 3495 Da (β-chain of oxidized bovine insulin).

^{19}F Nuclear Magnetic Resonance

NMR experiments were carried out at room temperature on a Bruker Avance DPX 400 NB spectrometer. ^{19}F NMR spectra were acquired at 376.5 MHz, using a single pulse sequence. Typical acquisition parameters were as follows: spectral window of 8.8 kHz, $\pi/2$ pulse width of 13 µs. A recycle delay of 10 s was used and 45 scans were recorded with deuterium (D_2O) lock. Quadrature detection was used and a line broadening of 2 Hz was applied prior to Fourier transformation.

Model Membrane Preparation

Stock solutions of 10 mM dimyristoylphosphatidylcholine/dimyristoylphosphatidylglycerol (DMPC/DMPG) with different molar ratios were prepared by co-dissolving the desired amount of phospholipids in $CHCl_3/CH_3OH$ (3 : 1 v/v), which was evaporated under vacuum. The lipid film was hydrated with distilled water and lyophilized. The fluffy lipid powder was re-suspended in Tris buffer (10 mM Tris, 10 mM KCl, 0.5 mM EDTA, pH 7.4) to obtain large multilamellar vesicles (MLVs). The solution was subjected to 10 freeze-thaw cycles to homogenize the size of the vesicles. Large unilamellar vesicles (LUV) were then produced by size extrusion method, where the solutions were passed subsequently through 100 nm pore size polycarbonate filters under nitrogen pressure.

Circular Dichroism (CD)

CD-spectra (Jasco J-810 spectropolarimeter, USA) of peptide solutions upon titration with large unilamellar vesicles (LUVs, 100 nm diameter) of DMPC containing different amounts of DMPG were recorded between 190–250 nm, using a 1-mm path-length quartz cell (Hellma, Germany). Samples were allowed to equilibrate 15 min between each addition of LUVs. In order to estimate the peptide secondary structure content, an analysis of the relevant CD-spectra was carried out using the CDPro program [17–19]. The analysis was performed using the self-consistent method Contin-LL and the basis 10 that contains 56 reference proteins.

RESULTS

Peptide Synthesis and Evaluation

The synthesis of Bax-α1 (^{14}TSSEQIM KTGALLLQGF IQDRAGRM^{38}) was carried out on a medium range scale (0.25 mmol of resin and with a fourfold excess of amino

DOI: 10.1002/psc

acids), using 1.1 g of methionine preloaded resin. A mass of 1.9 g of dried peptide/resin was recovered. If the coupling efficiency were 100%, 0.25 mmol of peptide with protected groups (MW 6908.1 g mol^{-1}) would have yielded a crude protected peptide mass of 1.7 g. Here, 0.9 g of crude protected peptide was synthesized (i.e. ~0.13 mmol). Consequently, the coupling efficiency of the synthesizer corresponds to 97% per amino acid. After 2 h of cleavage in the appropriate solution of TFA and scavengers (*cf* methods), and precipitation in cold ether, 320 mg of crude peptide was obtained, which was close to the expected mass of 360 mg (0.13 mmol at 2752 g mol^{-1}). As it will be discussed below, residual TFA is still present as a counter ion for basic residues and seriously alters the crude peptide mass, which turned out to be only 250 mg. The crude peptide was characterized by MALDI-TOF spectroscopy (Figure 1(A)). The main peak indicates a molecular mass of 2751.3 g mol^{-1}, in agreement with the theoretical molecular weight of the 25 amino acids peptide of 2752 g mol^{-1}. In addition, there were several peaks, corresponding to truncated peptides stopped by the acetic acid capping during the synthesis. HPLC purification by semi-preparative C4 reverse-phase column was achieved using a linear gradient with the following time intervals applied: eluent B varying in a 15-min linear gradient from 0 to 32%, a 6-min linear gradient from 32% to 40%, a 2-min plateau at 40%, a 2-min linear gradient form 40% to 55% and finally a 2-min plateau at 0% was used to wash and equilibrate the columns for the next injection. 1.8 ml of crude peptide at 5 mg ml^{-1} in solvent A was injected per run at a flow rate of 3 ml min^{-1}. Bax-α1 was eluted from the column at 40% acetonitrile after 24 min. A typical elution profile is shown in Figure 2 with a major peak indicating pure Bax-α1 peptide. The high degree of purity of Bax-α1 (around 98%), as it is required for structural analysis, was checked using pure peptide by HPLC and MALDI-TOF (Figure 1(B), Figure 2 dashed line). Injection was done with the same gradient but using an analytic C4 reverse-phase column in order to improve the separation and detect any by-adduct. 0.5 ml at 5 mg ml^{-1} in solvent A was injected per run at a flow rate of 1 ml min^{-1}. No by-adducts have been noticed after purification. Total mass after purification was 85 mg giving a total synthesis yield of *ca* 12%.

TFA Removal by Counter Ion Exchange

During the cleavage step, TFA interacts strongly with the peptide: as the sequence of Bax-1 includes three basic amino acids (one Lys and two Arg), it is an ideal counter ion to equilibrate these charges. Remarkably, the interaction is so strong that TFA cannot be removed after solvent evaporation and large errors in mass determination can thus be made. To elucidate this behavior in a systematic way, solution state ^{19}F NMR

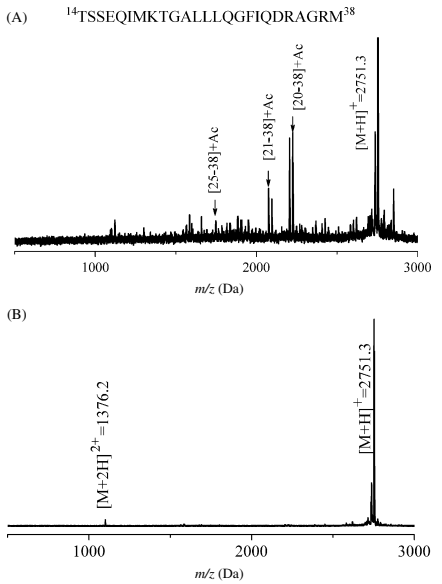

Figure 1 MALDI-TOF spectrum of (A) the crude reaction mixture containing the 25 amino acid long Bax-α1 peptide. The numbering in brackets [x-38] corresponds to truncated peptide segments. (B) Bax-α1 after purification by reverse phase HPLC. The second ionization product is observed at (M + nH)/(n), with a m/z of 1376 Da. The massif before the main peak comes from degradation by the MALDI laser.

was performed to accurately measure the amount of TFA and then calculate the ratio of counter ions per basic amino acids. 65 µl of TFE reference solution in $H_2O/D_2O/CH_3CN$ (40 : 35 : 25) at 10 mM in a capillary was thus inserted in 5 mm diameter NMR tube filled with a 600 µl solution of Bax-α1 (1 mM) in the same solvent mixture. In Figure 3, the top spectrum monitors out the TFA presence with a typical single resonance at 77 ppm while the reference TFE triplet resonances (due to J^{HF} couplings) appear at 75.7 ppm. Nevertheless, areas of the two peaks are directly comparable as TFE and TFA both contain the same amount of fluorine, i.e., three per molecule. Therefore, the area ratio provides a measure of the TFA concentration in Bax-α1 solution. A TFE/TFA ratio of 1 : 5 was calculated from the NMR spectrum (Figure 3), corresponding to a mass of 0.37 mg of TFA (*ca* 23% of the initial mass). Because 1.62 mg of powder from the synthesis/purification was weighed for the experiment, only 1.25 mg represents that of the pure peptide. Hence, the TFA/peptide molar ratio is 7 : 1 corresponding approximately to two counter ions per basic amino acid. As the TFA counter ions induce dramatic mass error and could be harmful for

DOI: 10.1002/psc

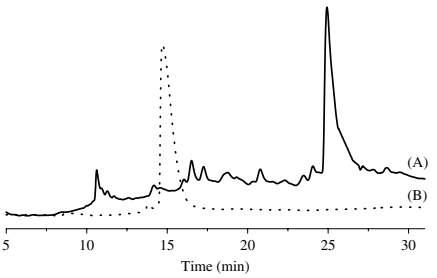

Figure 2 Photodiode UV chromatograms at 225 nm of the crude peptide (A) after cleavage from the resin (solid line) using a reverse phase chromatography on a semi-preparative C4 column at a flow rate of 3 ml min^{-1}. Photodiode UV chromatograms at 225 nm of the purified peptide (B) (dashed line) using a reverse phase chromatography on an analytic C4 column at a flow rate of 1 ml min^{-1}. See text for gradient settings. Please note that the Y-scale is not directly comparable between the two chromatograms due to the different injection volumes and flow rates.

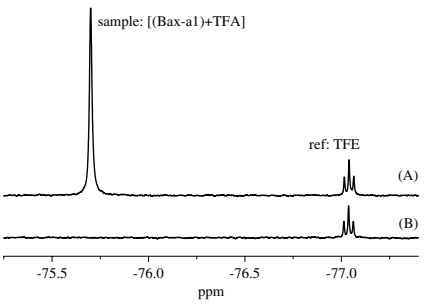

Figure 3 Solution ^{19}F NMR spectrum of Bax-α1 peptide in 600 µl H_2O/D_2O/ACN (40 : 35 : 25) at 1 mM within internal reference of TFE solution (65 µl in H_2O/D_2O/ACN (40 : 35 : 25) at 10 mM in a capillary) before treatment with HCl (A, top spectrum), after treatment (B, bottom spectrum). Triplet resonances arise from the J^{HF} couplings of the three fluorines in TFE and single resonance from the three fluorines in the TFA counter ions of Bax-α1. The sample/reference area ratio is 1 : 5. Experiment was done at room temperature on a 400 MHz Bruker spectrometer.

study in delicate media or in spectroscopic experiments (e.g. Infra-Red), it has to be replaced by a softer counter ion. Threefold molar excess of HCl per TFA was used in Bax-α1 solution under ice cooling during 20 min. Treatment with HCl acid, which has a pKa value (−7) lower than that of TFA (0.5), induces re-protonation of the TFA anions to form the free acid, which can easily be removed by freeze-drying. From 10 mg of peptide/TFA weighed, 7.8 mg of product was recovered after treatment, which indeed corresponds to the expected mass of the pure peptide released from TFA counter ions. Finally, mass spectroscopy (not shown) demonstrated that there was no peptide degradation induced by the procedure and ^{19}F NMR (Figure 3, bottom spectrum) reported the absence of residual TFA.

Secondary Structure Analysis by Circular Dichroism

The membrane-mediated conformational behavior of Bax-α1 was characterized by CD. The results for the peptide before and upon titration with LUV of varying surface charge are shown in Figure 4. In phosphate buffer, the membrane-free peptide exhibits a broad minimum between 222 nm and 208 nm with a weak maximum at 190 nm, indicating a mixture of secondary structure elements. Deconvolution using protein basis 10 and the self-consistent method contin-LL [17–19] lead to 13% of α-helix, 22% of β-turn, 31% of β-sheet and 33% of random coil structures (Table 1). Titration with zwitterioninc, pure DMPC LUV ranging from 10 to 100 lipid to peptide (L/P) molar ratio, induces no significant changes in the peptide secondary structure on comparing with the membrane-free state, (Figure 4, top panel). To evaluate any effect on Bax-α1 conformation induced by electrostatically driven association with membranes, DMPC LUVs containing increasing amounts of the negatively charged DMPG lipid were used. Adding LUVs composed of DMPC/DMPG at a 9 : 1 molar ratio, to Bax-α1 in phosphate buffer induces significant changes in the CD spectrum (Figure 4, middle panel), clearly depending on the L/P ratio. The titration with LUVs induces an isodichroic point at 206 nm and the presence of two marked negative dichroic bands at 208 and 222 nm, typical for helical structures. Nevertheless, the intensities remain low in comparison to those obtained for pure α-helix or β-sheet structure. The deconvolution results of these CD patterns as a function of the L/P ratios are shown in Table 1. Most remarkably, the α-helix fraction in the peptide structure increased on increasing the L/P ratio to reach up to 28% for L/P = 100. The importance of electrostatic interactions in binding is even more pronounced when increasing the DMPG contents in the LUVs up to 33 mol%. In Figure 4, bottom panel, the α-helical features dramatically increase, as visible in the strong increase of the typical dichroic band intensities. Deconvolution (Table 1) reveals a major α-helix population (60%) at a L/P ratio of 100 that had already almost reached at L/P = 30.

DISCUSSION

Besides the success in synthesizing the Bax-α1 peptide, the major outcome from this study is the clear evidence of a conformational change from a β-sheet secondary

DOI: 10.1002/psc

Table 1 Secondary structure of the Bax-α1 peptide[a] upon titration by DMPC LUV[b] containing increasing amount of DMPG

	L/P	α Helix[c]	β Sheet[c]	β Turn[c]	Random coil[c]
Phosphate buffer pH 7	—	13	31	23	33
DMPC	10	13	31	22	34
	30	13	31	22	34
	50	13	33	22	32
	100	12	36	21	31
DMPC/DMPG 9 : 1	10	14	30	23	33
	30	18	27	22	33
	50	19	28	22	31
	100	28	21	21	30
DMPC/DMPG 2 : 1	10	27	30	19	24
	30	54	16	11	19
	50	56	15	10	19
	100	60	15	8	17

[a] Concentration varying from 50 μM (L/P = 0) to 37 μM (L/P = 100).
[b] LUV of 100 nm diameter.
[c] Deconvolution of CD spectra was accomplished using basis 10 from the CDPro software and the CONTIN/LL algorithm [17–19]. Accuracy is estimated to be few percents.

structure to an α-helix in one of the peptides, upon interaction with model membranes that mimic the mitochondrial outer membrane. Also, a minor but nonetheless important result, is the new protocol to completely remove TFA ions from the synthesized peptide. These results will be discussed sequentially.

Electrostatically Driven Membrane Binding Induces Bax-α1 Helix Formation

While Bax-α1 peptide population is mainly partitioned between β-structures and unstructured conformations in buffer or uncharged vesicles, electrostatic interactions induce a pronounced transition from β-sheet to α-helical structures. Clearly, helix formation requires binding of the peptide to anionic phospholipids. Because no structural change happened in the presence of neutral lipid vesicles, no insertion by hydrophobic forces seems to occur, which too could have driven helical formation [20,21]. Here, not only the presence of the anionic PG lipid seems to be important, but also the absolute fraction of DMPG in the membrane. Correlating the helical fractions obtained in the presence of various DMPC/DMPG ratios with corresponding L/P ratios (Table 1), one remarks that ten negative charges per peptide (9 : 1 PC/PG and L/P = 100) lead to a helix content of *ca* 30% whereas 60% α-helix is obtained with 33 negative charges per peptide (2 : 1 PC/PG and L/P = 100). Of course the

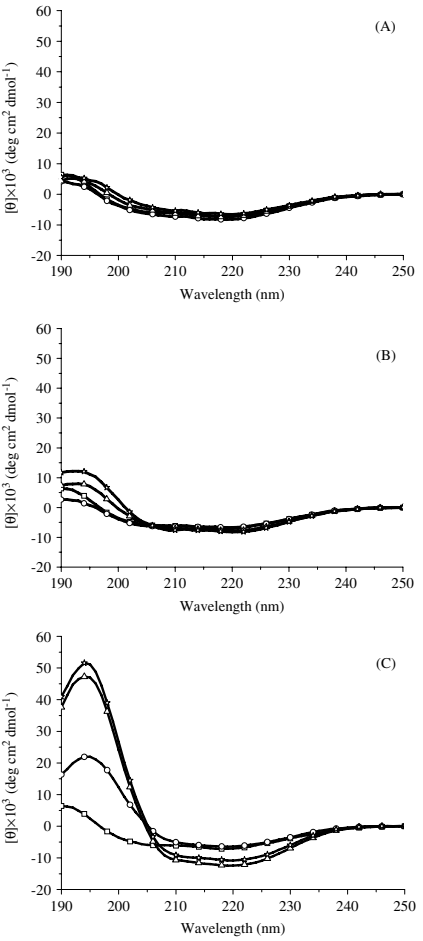

Figure 4 CD spectra of Bax-α1 peptide upon titration by DMPC LUV containing increasing amount of DMPG. Top panel (A) corresponds to LUV of pure DMPC, middle panel (B) to LUV of DMPC/DMPG in molar ratio in ratio 9 : 1 and bottom panel (C) to LUV of DMPC/DMPG in molar ratio 2 : 1. The lipid to peptide molar ratios (L/P) depicted in the three panels are 100 (star), 50 (triangle), 10 (circle) and pure peptide in phosphate buffer at pH 7 (square). 4 scans accumulated at 25 °C between 190 nm and 250 nm.

increase in helicity is not linear with the surface charge density (in principle, only half of the charges are available for the interaction, the others being in the inner vesicle monolayer) but this suggests that membrane patches of negative charges will clearly be in favor of

DOI: 10.1002/psc

a strong interaction with helix stabilization for Bax-α1. This suggests that two major factors govern this process: (i) the absolute concentration of anionic lipids, and (ii) the size of the available membrane surface for optimal association between peptide and negatively charged lipids.

At this level of the discussion it is interesting to consider the solution structure determined by solution NMR for the entire Bax human protein in Tris and DTT buffer [22]. At pH 6 the secondary structure of Bax-α1 (residues 14–38) within the whole protein is helical at 76% (residues 17–36). Because this segment alone exhibits mostly random coil or β-state in buffer (*vide supra*), it must therefore require stabilization either by hydrophobic or electrostatic interactions with other segments of the whole protein. Our data show no real interaction with uncharged liposomes whereas anionic lipids stabilize the helix. If the ability of Bax to bind the mitochondrion is mostly provided by its NT part [13,15], the helical conformation must play an important role and so do anionic lipids at the outer mitochondrion membrane. Recent results [23], on the interaction of Bax with negatively charged membranes showed the following results (i) in the presence of lipids the percentage of secondary structure elements as found from CD is essentially unchanged (67% α-helices, 23% β-structures and 10% random), (ii) the membrane prevents Bax from thermal denaturation and (iii) the *N* terminus is still available for apoptosis activity as probed by antibody binding capability. For the latter result, which is questioned by the authors, it is reported that activity is surprisingly obtained both with neutral or negatively charged membranes. Replacing our results in this context would suggest that the entire Bax protein would loosely bind to neutral membranes by preserving most of its solution structure by offering, nonetheless, its *N* terminus for activity whereas with negatively charged membranes, as in the outer mitochondrial membrane, strong electrostatic interaction with the Bax-a1 would happen, resulting in a larger exposure of the *N* terminus helix for greater activity as it could be guessed from the immunoprecipitation gel pictures reported by Andrews and coworkers [23]; the overall secondary structure is nonetheless preserved, although the topology of the helices could be changed upon membrane interaction. A structural study, at atomic resolution and upon interaction with membranes, is clearly required to understand further the mode of action.

A New Protocol to Efficiently Remove TFA During the Purification

It has been reported that TFA is considered a contaminant for various reasons. Firstly, we point out the dramatic error in mass weighing. Indeed, depending on the number of basic amino acids number in the peptide sequence, a nonnegligible amount of TFA, for instance, 23% in mass in our case, leads to serious inaccuracy as in molar concentration calculation, peptide/lipid ratio, etc... Moreover, light spectroscopy as IR is sensitive to TFA molecules since this salt leads to serious signal distortions and misinterpretation in spectra deconvolutions [24,25]. Also of importance in the course of membrane interactions is the fact that a peptide capped with TFA counter ions will not interact in the same manner with negatively charged membrane. The reverse situation could be obtained. Replacement of TFA counter ions by HCl has already been used for years [25], but was never addressed precisely. Here, we describe a simple fast and accurate method that uses 19F-NMR to ascertain that TFA is completely removed.

CONCLUSION

The peptide corresponding to the first helix of the pro-apoptotic human Bax protein has been synthesized with very high purity. TFA salt has been drastically removed in order to avoid any problem for further studies. UV CD in the presence of membranes of different nature has been efficiently used to monitor Bax-α1 secondary structure changes from a mostly β-sheet in water to a mainly α-helix upon association to negatively charged biological model membrane systems. The propensity to stabilize a helical structure for the *N* terminus may be an important parameter when Bax interacts with the mitochondrial membrane during apoptosis.

Acknowledgements

We thank Axelle Grelard (UMR 5144, MoBIOS, Pessac, France), for assistance and help in NMR spectroscopy and Katell Bathany (UMR 5144, MoBIOS, Pessac, France), for mass spectrometry measurements. This work was supported by the Knut and Alice Wallenberg Foundation, Swedish Research Council, the University Bordeaux 1 and the Centre National de la Recherche Scientifique (CNRS). The Aquitaine region is also thanked for equipment funding.

REFERENCES

1. Costantini P, Jacotot E, Decaudin D, Kroemer G. Mitochondrion as a novel target of anticancer chemotherapy. *J. Natl. Cancer Inst.* 2000; **92**: 1042–1053.
2. Hengartner MO. The biochemistry of apoptosis. *Nature* 2000; **407**: 770–776.
3. Okada H, Mak TW. Pathways of apoptotic and non-apoptotic death in tumour cells. *Nat. Rev. Cancer* 2004; **4**: 592–603.
4. Thompson CB. Apoptosis in the Pathogenesis and Treatment of Disease. *Science* 1995; **267**: 1456–1462.
5. Kerr JF, Wyllie AH, Currie AR. Apoptosis: a basic biological phenomenon with wide-ranging implications in tissue kinetics. *Br. J. Cancer* 1972; **26**: 239–257.
6. Cory S, Adams JM. The BCL2 family: regulators of the cellular life-or-death switch. *Nat. Rev. Cancer* 2002; **2**: 647–656.

7. Loeffler M, Kroemer G. The mitochondrion in cell death control: certainties and incognita. *Exp. Cell Res.* 2000; **256**: 19–26.
8. Li H, Kolluri SK, Gu J, Dawson MI, Cao X, Hobbs PD, Lin B, Chen G, Lu J, Lin F, Xie Z, Fontana JA, Reed JC, Zhang X. Cytochrome c release and apoptosis induced by mitochondrial targeting of nuclear orphan receptor TR3. *Science* 2000; **289**: 1159–1164.
9. Shimizu S, Narita M, Tsujimoto Y. Bcl-2 family proteins regulate the release of apoptogenic cytochrome c by the mitochondrial channel VDAC. *Nature* 1999; **399**: 483–487.
10. Kowaltowski AJ, Vercesi AE, Fiskum G. Bcl-2 prevents mitochondrial permeability transition and cytochrome c release via maintenance of reduced pyridine nucleotides. *Cell Death Differ.* 2000; **7**: 903–910.
11. Shimizu S, Konishi A, Kodama T, Tsujimoto Y. BH4 domain of antiapoptotic Bcl-2 family members closes voltage-dependent anion channel and inhibits apoptotic mitochondrial changes and cell death. *Proc. Natl. Acad. Sci. U.S.A.* 2000; **97**: 3100–3105.
12. Armstrong JS, Steinauer KK, French J, Killoran PL, Walleczek J, Kochanski J, Knox SJ. Bcl-2 inhibits apoptosis induced by mitochondrial uncoupling but does not prevent mitochondrial transmembrane depolarization. *Exp. Cell Res.* 2001; **262**: 170–179.
13. Arokium H, Camougrand N, Vallette FM, Manon S. Studies of the interaction of substituted mutants of BAX with yeast mitochondria reveal that the C-terminal hydrophobic alpha-helix is a second ART sequence and plays a role in the interaction with anti-apoptotic BCL-x(L). *J. Biol. Chem.* 2004; **279**: 52566–52573.
14. Oliver L, Priault M, Tremblais K, LeCabellec MT, Meflah K, Manon S, Vallette FM. The substitution of the C-terminus of bax by that of bcl-xL does not affect its subcellular localization but abrogates its pro-apoptotic properties. *FEBS Lett.* 2000; **487**: 161–165.
15. Cartron PF, Priault M, Oliver L, Meflah K, Manon S, Vallette FM. The N-terminal end of Bax contains a mitochondrial-targeting signal. *J. Biol. Chem.* 2003; **278**: 11633–11641.
16. Khemtemourian L, Sani MA, Bathany K, Grobner G, Dufourc EJ. Synthesis and secondary structure in membranes of the Bcl-2 anti-apoptotic domain BH4. *J. Pept. Sci.* 2006; **12**: 58–64.
17. Sreerama N, Woody RW. Estimation of protein secondary structure from circular dichroism spectra: comparison of CONTIN, SELCON, and CDSSTR methods with an expanded reference set. *Anal. Biochem.* 2000; **287**: 252–260.
18. Sreerama N, Woody RW. Analysis of protein CD spectra: Comparison of CONTIN, SELCON3, and CDSSTR methods in CDPro software. *Biophys. J.* 2000; **78**: 334A.
19. Sreerama N, Woody RW. On the analysis of membrane protein circular dichroism spectra. *Protein Sci.* 2004; **13**: 100–112.
20. He K, Ludtke SJ, Heller WT, Huang HW. Mechanism of alamethicin insertion into lipid bilayers. *Biophys. J.* 1996; **71**: 2669–2679.
21. Ludtke SJ, He K, Heller WT, Harroun TA, Yang L, Huang HW. Membrane pores induced by magainin. *Biochemistry* 1996; **35**: 13723–13728.
22. Suzuki M, Youle RJ, Tjandra N. Structure of Bax: coregulation of dimer formation and intracellular localization. *Cell* 2000; **103**: 645–654.
23. Yethon JA, Epand RF, Leber B, Epand RM, Andrews DW. Interaction with a membrane surface triggers a reversible conformational change in Bax normally associated with induction of apoptosis. *J. Biol. Chem.* 2003; **278**: 48935–48941.
24. Ahmad A, Madhusudanan KP, Bhakuni V. Trichloroacetic acid and trifluoroacetic acid-induced unfolding of cytochrome c: stabilization of a native-like folded intermediate(1). *Biochim. Biophys. Acta.* 2000; **1480**: 201–210.
25. Gaussier H, Morency H, Lavoie MC, Subirade M. Replacement of trifluoroacetic acid with HCl in the hydrophobic purification steps of pediocin PA-1: a structural effect. *Appl. Environ. Microbiol.* 2002; **68**: 4803–4808.

III

the FEBS Journal

Restriction of lipid motion in membranes triggered by β-sheet aggregation of the anti-apoptotic BH4 domain

Marc-Antoine Sani[1,2], Sabine Castano[1], Erick J. Dufourc[1] and Gerhard Gröbner[2]

1 UMR 5248 CBMN, CNRS-Université Bordeaux 1-ENITAB, Pessac, France
2 Department of Chemistry, Umeå University, Sweden

Keywords
apoptosis; BH4 domain; membrane; protein–lipid interactions; solid state NMR

Correspondence
G. Gröbner, Department of Chemistry, Umeå University, 901 87 Umeå, Sweden
Fax: +46 907 86 7655
Tel: +46 907 86 6346
E-mail: gerhard.grobner@chem.umu.se
E. J. Dufourc, UMR 5248 CBMN CNRS-Université Bordeaux 1-ENITAB, IECB 2 rue Robert Escarpit, 33607 Pessac, France
Fax: +33 5 4000 2218
Tel: +33 5 4000 2218
E-mail: e.dufourc@iecb.u-bordeaux.fr

(Received 21 October 2007, revised 28 November 2007, accepted 5 December 2007)

doi:10.1111/j.1742-4658.2007.06222.x

The regulative BH4 domain of human Bcl-2 protein exerts its anti-apoptic activity via the mitochondrion. In the present study, we investigated the molecular interactions of this domain with negatively charged liposomes mimicking the outer mitochondrial membrane. To model the overproduction of Bcl-2 found in cancer processes, we studied the impact of elevated concentrations of its regulative BH4 segment on these mitochondrial membranes from the peptide and lipid perspective. Combined solid state ^{2}H-NMR and differential scanning calorimetry revealed the coexistence of small sized fluid and rigid membrane domains over a large temperature range, which is confirmed by ^{31}P-NMR at 30 °C. The latter are stabilized, in a cholesterol-like manner, by the presence of a BH4 peptide. In the same time scale, the reduction of the headgroup order is seen in the static ^{14}N and ^{31}P-NMR spectra when BH4 inserts into the bilayers. Indeed, attenuated total reflection spectroscopy indicated a dominant aggregated β-sheet secondary structure of BH4 with a 42° tilt relative to the membrane surface. These results are discussed in terms of membrane stabilization versus apoptotic mechanisms at the outer mitochondrial membrane location.

Understanding the regulation of the programmed cell death (i.e. apoptosis) is a challenge that can provide valuable information for treating diseases, including autoimmune disorders, neurodegeneration and cancer [1–5]. In the mitochondrial pathway, pro- and anti-apoptotic members of the Bcl family meet at the mitochondrial membrane, and arbitrate a life or death decision for the cell [2,6–8]. Once this internal pathway is activated, the outer mitochondrial membrane is permeabilized, thereby inducing the lethal and irreversible release of cytochrome *c* [9–11]. Normally, anti-apoptotic proteins such as Bcl-2 prevent this process, thereby maintaining the integrity of the mitochondrial membrane [11–13]. Sequence analysis of the anti-apoptotic Bcl-2 proteins reveals four short conserved domains (BH1 to BH4) whereas, for pro-apoptotic proteins such as Bax and Bak, a similar overall primary structure is found except for the BH4 domain (^{10}DNREIVMKYIHYKLSQRGYEW^{30}) [2,7]. This N-terminus domain thus appears as a key factor for the regulative anti-apoptotic activity of Bcl-2 proteins. Several studies have shown that the BH4 fragment alone is functional when delivered *in vivo* coupled with the penetrating TAT sequence (TAT only required for translocation into the cell). Indeed, the TAT-BH4 peptide inhibits apoptosis in various tissues (islets,

Abbreviations
ATR, attenuated total reflection; CSA, chemical shift anisotropy; DMPC, 1,2-dimyristoyl-*sn*-glycero-3-phosphocholine; DMPG, 1,2-dimyristoyl-*sn*-glycero-3-phosphoglycerol; DSC, differential scanning calorimetry; MAS, magic angle spinning; MLV, multilamellar vesicle; PC, phosphocholine; PG, phosphoglycerol.

intestine cells, heart cells, etc.) [5,14–16]. Moreover, 'BH4-only' was used on isolated mitochondria to stop membrane potential loss after apoptosis triggering, where it is believed to block the action of the natural voltage-dependent anion channel [17]. Nevertheless, a recent study performed by Baines *et al.* [18] disagreed with respect to the need for the voltage-dependent anion channel to induce apoptosis. Another possibility is blocking of the lipid pore mediated by Bax [13,19,20], meaning that the mechanism is complex and possibly multifaceted but involves the membrane lipids.

How does BH4 reach the mitochondrial membrane and how does it exert its inhibiting effect on the various members of the apoptotic machinery [1,2,21–24]? Most likely, it will first bind to the mitochondrial membrane surface followed by insertion and diffusion to the required location. To our knowledge, there is no information on membrane perturbations due to such binding, especially when BH4, as part of the Bcl-2 protein, is overproduced, protecting cancer cells against apoptosis. To understand the initial steps of this complex process at the molecular level, we studied the organization of assemblies formed by the regulatory BH4 peptide segment of the Bcl-2 human protein with mitochondrial model membranes. Using a high lipid-to-peptide ratio, we mimicked Bcl-2 overproduction. To further understand the role of BH4 when Bcl-2 translocates to the mitochondria, followed by its insertion into the mitochondrial membranes, we studied the effect of external addition versus intimate incorporation into these membranes. The conformational changes of BH4 were monitored by polarized attenuated total reflection (ATR) spectroscopy. The impact of the BH4 domain on membrane integrity and organization was then studied in detail by a combination of differential scanning calorimetry (DSC) [25–27], solid state ^{2}H-NMR using 1,2-dimyristoyl-*sn*-glycero-3-phosphocholine (DMPC) lipids labeled by chain deuteration [28–30] for the hydrophobic core of the membrane, and solid state ^{31}P-[31–33] and ^{14}N-NMR [34,35] of the phospholipid headgroup.

Results

BH4 orientation and structure: polarized ATR spectroscopy

To investigate the behavior of the BH4 peptide in lipid multibilayers, polarized ATR experiments were performed using the BH4 peptide either added onto or co-solubilized into membranes composed of DMPC/1,2-dimyristoyl-*sn*-glycero-3-phosphoglycerol (DMPG) (2 : 1 molar ratio) at a 30 : 1 L/P molar ratio. The ATR spectra presented in the 1800–1550 cm^{-1} domain (Fig. 1) show the ν (C=O) ester band of the lipid around 1735 cm^{-1} and the amide I region characteristic of the BH4 between 1600–1700 cm^{-1}. When BH4 is directly co-solubilized into lipids (Fig. 1A), a main amide I component around 1615 cm^{-1} is characteristic of β-sheets and, more precisely, such a low value indicates characteristic antiparallel arrangements [36,37]. Decomposition of the amide I region allows the estimation of 55% antiparallel β-sheets, 22% random structure, 11% α-helix and 10% β-turns. When BH4 is added onto lipids

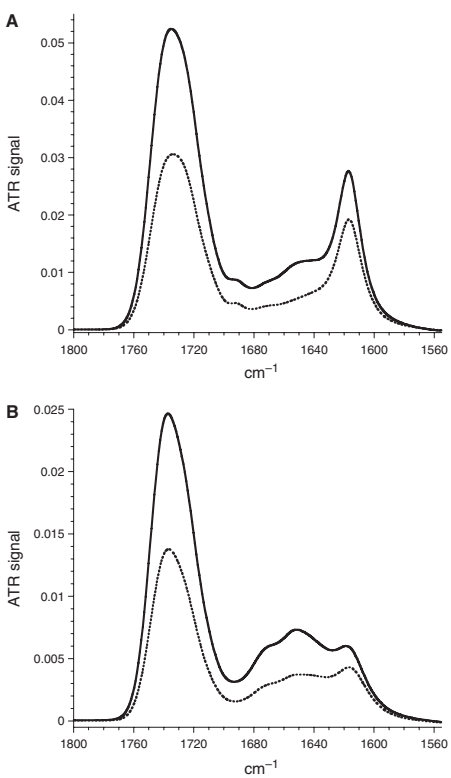

Fig. 1. Polarized ATR spectra of mixed BH4/lipid multibilayers: *p* polarization (solid line), *s* polarization (dotted line). (A) BH4 peptide co-solubilized at a 30 : 1 L/P molar ratio. (B) BH4 peptide added at 30 : 1 L/P molar ratio. Experiments were performed at 25 °C (1000 scans accumulated).

(Fig. 1B), the amide I region is more complex. Decomposition of this region allows the estimation of 31% random structure, 29% antiparallel β-sheets, 21% β-turns and 16% α-helix.

It is worth noting in Fig. 1A that, due to the two-dimensional symmetry and the selection rule of an antiparallel β-sheet, the amide I vibration is split [38]: two bands are detected at 1615 cm^{-1} and 1695 cm^{-1}, corresponding to the amide I vibration oriented along the interchain hydrogen bonds and the amide I′ vibration along the β-sheet axis, respectively. Because polarized-ATR spectroscopy is sensitive to the orientation of the structures [36,39,40], it can be used to estimate the orientation of the antiparallel β-sheet fraction in the oriented bilayers using evaluation of the dichroic ratio of the amide I (R_I) and I′ (R_I') bands [41]. Ratios calculated from decomposition of the spectrum in Fig. 1A (R_I of 1.3 and R_I' of 2.1) correspond to a 30° tilt angle around the β-sheet axis and 35° around the interchain hydrogen bonds, respectively. This specifies the β-sheet plane to be tilted by approximately 42° relative to the membrane plane. A similar analysis was performed on the added peptide system after decomposition. The orientation of this antiparallel β-sheet fraction essentially leads to the same results but with a greater inaccuracy with respect to the 1695 cm^{-1} dichroic ratio.

Lipid cooperativity: DSC

DSC measurements were performed with BH4 either externally added onto or co-solubilized into multilamellar membrane vesicles as used above. Fig. 2 shows the main phase transition, from the gel to a lamellar liquid-crystalline phase (L_α) of the peptide-free lipid mixture, which is split into two sharp peaks, occurring upon heating at 22.5 °C and 23 °C (solid line). A pre-transition occurs at 13.6 °C corresponding to the transition from the planar gel to the rippled gel phase [42]. An enthalpy of transition (ΔH_{cal}) of approximately 4.2 kcal·mol^{-1} was calculated by integrating the area under the C_p curve over the temperature range 19–27 °C. According to Eqn (1), the van't Hoff enthalpy ΔH_{vH} can be obtained from the C_p curve and thus an approximate number of 160 lipid molecules per cooperative unit was deduced.

Addition of BH4 to charged lipid vesicles induces serious changes in their thermotropic behavior (Fig. 2, dashed–dotted line). The pre-transition is dramatically reduced and the main transition shows a broad pattern with peptide-free peaks emerging at lower temperatures (22 °C and 22.5 °C). The strikingly broad transition occurs in the temperature range 18–33 °C and induces

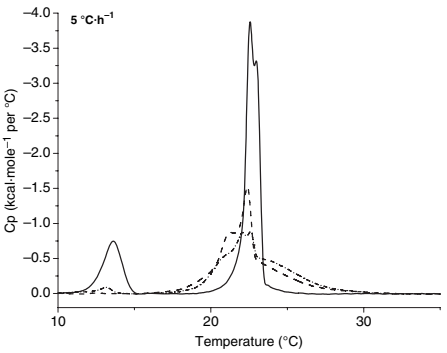

Fig. 2. Thermograms showing the excess heat capacity of MLVs (0.62 mM, pH 7.4) (solid line), of MLVs (0.62 mM, pH 7.4) with BH4 added at a 30 : 1 L/P molar ratio (0.62 mM, pH 7.4) (dashed–dotted line) and of MLVs (0.62 mM, pH 7.4) with BH4 co-solubilized at a 30 : 1 L/P molar ratio (0.62 mM, pH 7.4) (dashed line). The scan rate was 5 °C/h from 5–45 °C.

a slightly smaller enthalpy of approximately 3.7 kcal·mol^{-1} and an approximate number of 25. When BH4 is co-solubilized into multilamellar vesicles (MLVs), the pre-transition is totally abolished and the main phase transition occurs across a slightly wider temperature range of 15–33 °C (Fig. 2, dashed line). The enthalpy of 4.1 kcal·mol^{-1} is comparable to that of the free system and the approximate number is 30 (i.e. comparable to that of the added peptide system).

Lipid chain perturbation: solid state ^{2}H-NMR

Representative temperature dependent ^{2}H-NMR spectra for multilamellar vesicles composed of DMPC-$^2H_{54}$/DMPG lipids (2 : 1 molar ratio) are shown in the absence (Fig. 3A) and presence of either added (Fig. 3B) or co-solubilized (Fig. 3C) BH4 peptide. At 10 °C, the NMR spectrum of the peptide-free system vesicles exhibits typical features of membranes in their gel phase (L_β'). This broad NMR powder pattern is characteristic of lipids undergoing slow motions, with their fatty acid chains being highly ordered and tilted with respect to the membrane normal [28,43,44]. The only axially symmetric motional process visible is that of the chain methyl group (C^2H_3) around its C3 axis, giving a quadrupolar splitting of 9.5 kHz. The small visible isotropic line arises either due to a small fraction of small unilamellar vesicles or to the natural abundance of deuterium in the buffer and can be neglected for first moment calcula-

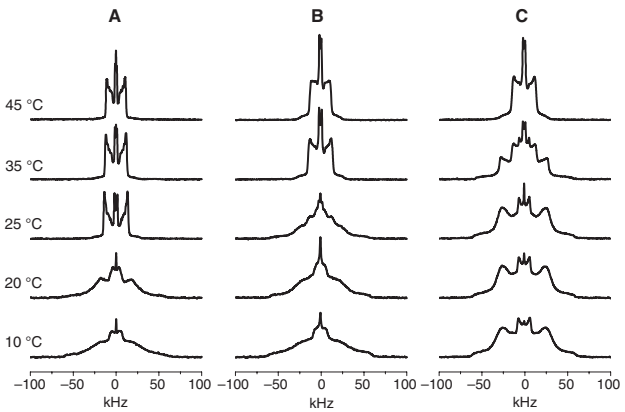

Fig. 3. Thermal variation of ^{2}H-NMR powder spectra of pure MLVs of acyl chain perdeuterated DMPC mixed with DMPG at a ratio of 2 : 1, respectively (A), with the BH4 peptide externally added at a 30 : 1 L/P molar ratio (B) and co-solubilized at the same L/P ratio (C). Samples were allowed to equilibrate for 45 min at a given temperature prior to NMR acquisition.

tions. The first moment, M_{1O}, is around 124 kHz. At 30 °C, the membrane is entirely in its L_α fluid state and exhibits fast intra- and intermolecular axially symmetric motions [44,45]: this leads to a well resolved doublet for the C^2H_2 groups in the 'plateau' region (C_2–C_8) with a quadrupolar splitting of approximately 25 kHz, a reduction of the C^2H_3 splitting to 3.1 kHz, and a first moment of 51 kHz (M_{1F}). The main phase transition occurs in the temperature range 20–25 °C, where the fraction of lipids in the L_α phase increases from 0.25 to 0.89, as calculated using Eqn (3). The fluid phase fraction is not zero below the main phase transition due to the existence of an intermediate rippled $P_{\beta'}$ phase for bilayers containing phosphocholine (PC) [44,46–48].

Addition of BH4 to the lipid bilayers at a 30 : 1 L/P molar ratio induces a pronounced perturbation of thermotropism and dynamics of the membrane matrix (Fig. 3B). Low temperature NMR spectra reflect a gel phase-like membrane with a superposition of a small negligible isotropic line. In addition, broadened spectra are now visible up to 25 °C. A pure liquid-crystalline phase appears first at 35 °C, with a C^2H_2 'plateau' splitting of 25 kHz and 3.2 kHz for the C^2H_3 group, and a first moment of 50 kHz (M_{1F}). The main phase transition occurs in the temperature range 20–30 °C, with the fraction of lipids in the fluid phase increasing from 0.22 to 0.85. Clearly, the spectrum at 25 °C exhibits a superposition of two NMR subspectra of DMPC being present in both, the ordered and fluid L_α phases, with 40% of the lipids populating the fluid L_α-phase.

Incorporation of BH4 into identical lipid bilayers, at the same 30 : 1 L/P molar ratio, leads to significant changes in the corresponding ^{2}H-NMR spectra (Fig. 3C). At low temperatures, the spectral shape changes considerably compared to the pure system. Axially symmetric spectra are now detected indicating the presence of C3 symmetry due to the occurrence of fast axial motions. Quadrupolar splittings of approximately 50 kHz and 14 kHz are respectively measured for the C^2H_2 'plateau' and -C^2H_3 groups, together with a first moment of 132 kHz (M_{1O}). The fluid phase is solely dominating at 45 °C, with a C^2H_2 'plateau' splitting of 24 kHz, a C^2H_3 splitting of 3.4 kHz and a first moment of 55 kHz (M_{1F}). The phase transition region occurs between 25 °C and 40 °C, with the fraction of lipids in the fluid phase varying from 0.13 to 0.88. NMR spectra at 35 °C clearly exhibit a superposition of two NMR spectra, as is also the case for peptides added onto the membrane at 25 °C.

The NMR quadrupolar splittings observed for the fatty acid methyl groups in the DMPC lipid molecules and the respective first moments are displayed in Fig. 4. Quadrupolar splittings are plotted versus temperature to visualize variations in membrane matrix properties as a function of BH4 association and incorporation. In the low temperature region, quadrupolar splitting values increase significantly in the presence of BH4, where added BH4 induces intermediate values that are between the peptide free and the peptide co-solubilized system. The gel-to-fluid transition, where values decrease dramatically, is shifted to higher temperatures. Between 20 °C and 30 °C (BH4 added) and 25 °C and 45 °C (BH4 co-solubilized), two splittings are observed for the terminal methyl groups (Fig. 4, inset). One of the splittings reflects the value of a BH4-free system, whereas the other shows BH4

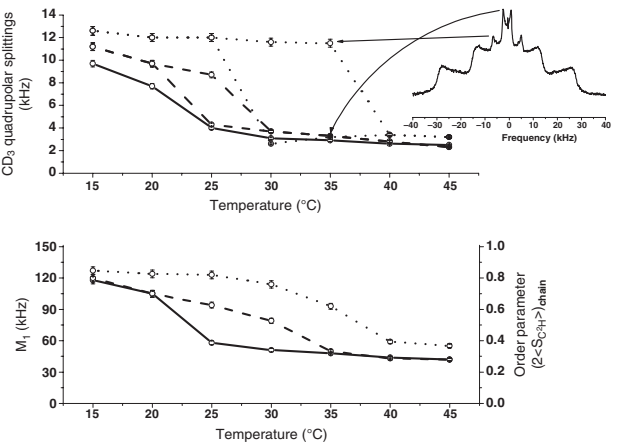

Fig. 4. Temperature variation of the methyl group quadrupolar splitting (top panel) and of the first spectral moment (bottom panel) of pure MLVs of acyl chain perdeuterated DMPC mixed with DMPG at a 2 : 1 molar ratio (solid line), upon addition of BH4 at a 30 : 1 L/P molar ratio (dashed line) and BH4 peptide co-solubilized at a 30 : 1 L/P molar ratio (dotted line). The accuracy of calculation is approximately 5%. For the *y*-axis on the right, the C-^{2}H order parameter is calculated from Eqn (3). Insert: superposition of quadrupolar splitting arising from fluid and ordered overlapped spectra.

inducing an ordered phase. For elevated temperatures, only one splitting is observed. The measured quadrupolar splittings correspond to that of a peptide-free membrane only in the case of surface added BH4 at very high temperatures.

The temperature dependent first moments can be converted into an average chain order parameter using Eqn (2) and plotted in Fig. 4. Although the addition of BH4 to membranes barely modifies the ordering of the lipid gel phase, the incorporation of BH4 leads to higher ordering values, in the range 0.8–0.9. Both peptide–membrane systems show a more gradual gel-to-fluid transition with the membrane remaining in a more ordered state over a broad temperature range. Upon the addition of BH4 to the membrane, but only at elevated temperatures, a similar state of membrane ordering can be reached as in the peptide-free case.

Headgroup perturbation: solid state ^{31}P- and ^{14}N-NMR

To monitor the impact of the BH4 peptide on the lipid organization and polar headgroup region, ^{31}P and ^{14}N-NMR were performed on the either added or co-solubilized BH4/lipid assemblies. In Fig. 5A, the ^{31}P static spectrum of MLV vesicles composed of DMPC/DMPG at a 2 : 1 molar ratio exhibits a typical pattern of lipid bilayers in a liquid crystalline phase at 30 °C. It is dominated by the chemical shift anisotropy (CSA) of the phosphate groups from both PC and phosphoglycerol (PG), partially averaged by fast axial rotation [33,45]. Superimposed spectra arising from PG and PC can be resolved at the high field edge ($\sigma_{\perp}$) with two maxima at −12 and −14 p.p.m. but, because their low field ($\sigma_{//}$) shoulder is unresolved, an

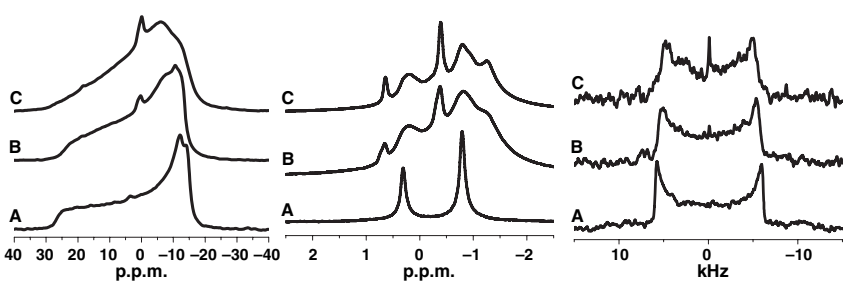

Fig. 5. ^{31}P and ^{14}N-NMR spectra at 400 MHz proton frequency. Left panel: static ^{31}P-NMR spectra; middle panel: MAS ^{31}P-NMR spectra at 3 kHz; right panel: static ^{14}N-NMR spectra. (A) MLVs composed of DMPC/DMPG at a 2 : 1 molar ratio. (B) BH4 peptide added at a 30 : 1 L/P molar ratio. (C) BH4 peptide co-solubilized at a 30 : 1 L/P molar ratio. Experiments were conducted at 30 °C.

averaged value of the CSA ($\Delta\sigma = \sigma_{//} - \sigma_{\perp}$) of 37 ± 1 is estimated, in agreement with previous studies [34,49]. For BH4 added to MLVs at a 30 : 1 L/P molar ratio (Fig. 5B), the liquid crystalline pattern of the bilayers is conserved with a loss of the high field edge resolution and a downfield component at −7 p.p.m. appears. A superposition of two powder patterns is seen indicating that at least two lipid phases are present simultaneously and are in slow exchange with each other on the NMR time scale [50]. Because one phase has a CSA value approximately identical to the free-peptide spectrum ($\Delta\sigma = 35 \pm 2$ p.p.m.), it can be concluded that partitioning of the peptide has taken place. When BH4 is co-solubilized within the lipid matrix, the spectrum (Fig. 5C) still reflects a liquid crystalline phase, but with a proportion of peptide-bound phase more pronounced, with a very broad high field edge emerging at −6 p.p.m. Furthermore, the downfield edge resolution is diminished leading to high inaccuracy of the CSA value. Small isotropic peaks can be observed but they account for less than 2% of the spectrum and can be neglected.

Using magic angle spinning (MAS) provides a useful tool for monitoring the impact of BH4 on each lipid independently. It allows both the PC and PG phosphate isotropic chemical shifts to be resolved by averaging partially the CSA into isotropic resonances and spinning side bands spaced by a multiple of the MAS frequency (off scale in Fig. 5). The spectrum in Fig. 5A (middle panel) shows the two components with typical chemical shifts of 0.31 and −0.78 p.p.m., corresponding to DMPG and DMPG respectively, in agreement with previous work [51]. Addition (Fig. 5B, middle panel) or co-solubilization (Fig. 5C, middle panel) spectra are mostly similar together but differ strongly compared to the spectrum of the peptide-free MLVs. Indeed, the spectra are no longer composed of two sharp lines but, instead, a multitude of peaks are present and the side bands are considerably reduced (not shown). Once again, this reveals different electrostatic environments where DMPC and DMPG sense, or not, the BH4 peptide. The broad component at −0.80 p.p.m. is assigned to free-DMPC whereas the broad peak at 0.23 p.p.m. could be assigned to lightly perturbed DMPG. Two sharp resonances at 0.6 and −0.4 p.p.m. (broader for BH4 added) could arise from DMPG and DMPC, respectively, interacting with BH4. The last broad peak shifted upfield at −1.1 p.p.m. might arise from pure DMPC, meaning that DMPG is segregated by BH4. Unfortunately, the resolution of the side bands is not sufficient to quantify the proportion of peptide-free and peptide-bounded phases, especially for quantifying the amount of DMPG and DMPC in each phase.

In Fig. 5A (right panel), the ^{14}N-NMR spectrum of free-peptide MLVs is characteristic of the choline response to orientation-dependent interaction between the electric field gradient and the electric quadrupole moment of the nitrogen (spin I = 1). Therefore, only DMPC lipids can contribute to the typical lineshape drawn by the quadrupolar splitting averaged to 11.7 ± 0.3 kHz by the fast axial rotation of the whole lipids plus the fast rotation of the choline bond [51,52]. BH4 added to MLVs reduced the splitting to 10.7 ± 0.5 kHz whereas co-solubilization of BH4 to lipid matrix reduced the splitting to 10 ± 0.5 kHz. The reduction of the quadrupolar splitting is a combination of modulation in the surface electrostatic and molecular order-disorder of the choline segment, as described previously for melittin-membrane interactions [53]. Therefore, it is not surprising to obtain only one splitting, and not several as for a previously described DMPC population [50]. Nevertheless, the reduction of the quadrupolar splitting is in agreement with the reduction of the CSA in ^{31}P-NMR spectra. Disorder is clearly made in the headgroup where BH4 peptides exchange rapidly between different phases, allowing more space for the headgroup and thus higher amplitude of re-orientation. Moreover, the lower splitting induced by co-solubilization is probably due to the higher amount of β-sheet peptides inserted leading to re-orientation of the headgroup region, whereas BH4 added to MLVs leads to a greater proportion of peptide remaining in solution (random coil).

Discussion

Two major outcomes of the present study can be summarized. First, the regulative BH4 domain of the anti-apoptotic Bcl-2 protein family adopts an substantial fraction of tilted aggregated β-sheet structures upon close contact with lipid bilayers. Second, BH4 has a severe impact on the dynamic organization of the membrane matrix without breaking membrane cohesion. These aspects are discussed below, together with implications for the potential regulative role of the BH4 domain in the mitochondrial apoptotic pathway.

High confinement of BH4 at negatively charged membrane surface induces aggregated β-sheet structures

The BH4 domain adopts different secondary structures according to the environment where it localizes: it is mostly helical inside the soluble form of the Bcl-2

human protein [54], whereas our previous study showed a partitioning between random coil and β-sheet structures in aqueous medium whereas, in tetrafluoroethylene, a low dielectric constant medium favoring the hydrogen bonding, dominant helical structures was found [55]. Moreover, in a highly dilute system comprising small unilamellar vesicles containing acidic lipids, we found that the BH4 domain interacts strongly with the membrane to adopt a major helical structure above a 80 : 1 L/P molar ratio.

In the lipid–peptide systems used in the present study to mimic an overproduction of anti-apoptotic proteins of the Bcl family occurring at the mitochondrial membranes, a dominant β-sheet population at a 30 : 1 L/P molar ratio was observed, as observed in the ATR experiments. Remarkably, the BH4 domain rearranges itself in pronounced antiparallel structures. Such a predominant aggregated state could be due to an electrostatically-driven high peptide concentration at the charged membrane surface and to hydrophobic peptide–peptide interactions induced by this surface crowding effect as previously reported for amyloidogenic peptides [56,57]. The difference between surface addition and membrane incorporation can be explained by the addition of BH4 peptides onto MLV limiting the fraction of BH4–lipid association, with more peptides remaining in solution (random coil, β-turn). By contrast, intimate incorporation, where BH4 interacts with all parts of the bilayers, reduces the amount of random coil and β-turn.

Size reduction of cooperative units and ordered domain formation

To mimic the outer mitochondrial membrane, mixed lipid bilayer systems with a negative surface potential were used. These experienced severe changes upon interaction with the regulative BH4 unit. Independent of the type of peptide–lipid assembly (association–insertion), the main phase transition of the lipid systems was broadened, as indicated in the thermograms (Fig. 3). The appearance of a broad phase transition indicates a loss of lipid cooperativity reflected in a reduction (approximately six-fold) in the average number of lipids per cooperative unit [26]. This corresponds to the coexistence of small peptide-free and lipid–peptide domains with high interfacial energy, which melt independently, hence slowing down the transition towards an entirely fluid phase [58,59]. Moreover, a similar transition enthalpy indicates that the peptide does not perturb the membrane cohesion by changing the size of the vesicles as occurs with membrane fusion, micelle formation or breaking down the membrane [60,61], which is confirmed by the conserved lamellar lineshape of the static ^{31}P spectra.

This effect of BH4 on membranes is confirmed by the ^{2}H-NMR spectra obtained within the temperature region of the broad phase transition. Here, fractions of highly ordered and less ordered lipids coexist on the NMR time scale [28,29,62]. At temperatures well above the transition, the molecules exchange rapidly and only an averaged peptide–lipid environment is now detected by NMR. At 30 °C, ^{31}P-NMR spectra confirmed a co-existence between peptide-free lipids and peptide-associated lipid phases. According to the ^{2}H-NMR at the same temperature, a higher peptide-bound proportion should be found for the peptide co-solubilized than for the added system. This is in agreement with the results presented in Fig. 5.

Surprisingly, BH4 co-solubilized into membranes induces an effect similar to that promoted by the presence of cholesterol in membranes (i.e. the abolishment of a clear gel phase in the membrane matrix and the promotion of very ordered lipids at elevated temperatures). The effect observed is less pronounced at high temperatures, probably due to the lower amount of peptide (approximately 3 mol%) in membranes compared to cholesterol (10–50 mol%) and a different location into the hydrophobic core. Indeed, cholesterol is deeply inserted into the hydrophobic membrane core [30,43,63], whereas the orientation of BH4 determined for its β-sheet form (approximately half of the peptide secondary structure) by the ATR technique indicates a shallow insertion (not transmembraneous). Once again, the difference between co-solubilization and addition may reside in the amount of peptide interacting with the bilayers because, in the later case, a higher proportion of peptides remains in solution, diminishing the mol% ratio in membrane.

Nevertheless, because BH4 converts its aggregate structures upon interaction with membranes, perturbations of the lipid dynamics remain strong. Although the hydrophobic core is more ordered, the headgroup region is disordered by the BH4 domain, as demonstrated by the reduction of the CSA and the quadrupolar splittings reductions (Fig. 5), which are agreement with a shallow insertion and a fast exchange of the peptide into the membrane. Because BH4 possesses five basic and four acidic residues at pH 7.4, leading to a cationic +1 global charge, a preferred interaction with the anionic lipid is probable, with the MAS ^{31}P spectra revealing more perturbed DMPG resonances than DMPC. Furthermore, the reduction of the ^{14}N quadrupolar splitting from bilayers composed of DMPC with 50 mol% DMPG included to pure DMPC bilayers was previously described as a reorientation of the choline groups [34]

by a change of the electrostatic surface potential, supporting the insertion of the peptide and a possible segregation of the DMPG lipids by the BH4 domain from DMPC lipids. These points are of possible interest in the regulative process of the Bcl-2 protein to which the BH4 domain belongs.

Biological implications

In cancer, the regulation of the apoptotic pathway associated with mitochondria is characterized by an overproduction of the anti-apoptotic Bcl proteins such as Bcl-2 [1,3,4,7]. Due to those proteins being natively anchored into the mitochondria, their regulative BH4 unit can potentially be in contact with mitochondrial membranes. In this case, the results obtained in the present study indicate that BH4 interacts with negatively charged vesicles where it even converts into aggregated structures and increases the order of the membranes and therefore their stiffness. Such modifications could play a role in the regulation of apoptosis, thereby interfering with the anchoring of the pro-apoptotic Bax protein into the outer mitochondrial membrane system. This suggests that the anti-apoptotic specificity of the entire Bcl-2 protein could arise from strong interactions with the mitochondrial membrane: a process which would act as a 'protective' mechanism against pore forming pro-apoptotic proteins.

Experimental procedures

Reagents

DMPC and DMPG were obtained from Sigma (Poole, UK); chain deuterated DMPC-$^2H_{54}$ was purchased from Avanti Polar Lipids (Alabaster, AL, USA). The BH4 peptide (^{4}RTGYDNREIVMKYIHYKLSQRGYEWD^{31}) from the Bcl-2 human protein was synthesized by solid phase methods on an Applied Biosystems 433A Peptide Synthesizer (PE Biosystem, Courtaboeuf, France) [55]. The peptide purity was greater than 98% as determined by UV and MALDI-TOF MS.

Procedure for sample preparation

Trifluroacetic acid salt was removed from the peptide powder and the purity was checked by ^{19}F-NMR and MS [55,64]. A stock solution of DMPC/DMPG with a 2 : 1 molar ratio was prepared by co-dissolving the desired amount of phospholipids in $CHCl_3/CH_3OH$ (3 : 1, v/v), which was evaporated under a vacuum. The lipid film was hydrated and lyophilized. The fluffy lipid powder was resuspended in a TKEB buffer (10 mM Tris, 10 mM KCl, 0.5 mM EDTA, pH 7.4) containing the desired amount of peptide to obtain large MLV at a 30 : 1 L/P molar ratio. The solution was subjected to three freeze–thaw cycles to homogenize the vesicle size. For intimate incorporation of the BH4 domain into MLV, the peptide was co-dissolved with lipids in a $CHCl_3/CH_3OH$/tetrafluoroethylene (2 : 1 : 3, v/v) mixture. The organic solvents were removed under high vacuum; the film was resuspended in the same Tris buffer and subjected to the same treatment. This procedure was adapted by adjusting the hydration ratio depending on the technique used. Briefly, NMR and ATR samples were rehydrated at approximately 80% (w/w) to reach a lipid concentration of approximately 0.3 M, whereas DSC samples where prepared in the same way but then diluted by around a factor of 600 (at a concentration of approximately 0.5 mM).

ATR spectroscopy

ATR spectra were recorded on a Nicolet Magna 550 spectrometer (Ramsey, MN, USA), equipped with a MCT detector cooled to 77 °K, where the sample was sheared at the diamond ATR crystal surface (Golden Gate, Eurolabo, Paris, France). To estimate the secondary structure content of BH4, ATR spectra were analyzed using GRAMS 32 software (Thermo Electron Corp., Madison, WI, USA). Because ATR spectroscopy is sensitive to the orientation of structures [36,39,40], spectra were recorded with a parallel (*p*) and perpendicular (*s*) polarization of the incident light with respect to the ATR plate. Generally, 1000 scans were accumulated at a resolution of 8 cm^{-1} and a two-level zero filling was performed. All the orientational information is then contained in the dichroic ratio $R_{ATR} = A_p/A_s$, where A_i represents the absorbance of the considered band for the *p* or *s* polarization of the incident light, respectively.

DSC

DSC was performed on a VP-DSC calorimeter (MicroCal, Inc., Northampton, MA, USA) using a 0.6 mM lipid suspension in a cell volume of 0.5 mL. All experiments were preceded by a heating and a cooling cycle. The temperature range was 5–45 °C with a final heating rate of 5 °C·h^{-1}. The data were analyzed using ORIGINE 5.0 software (Microcal, Inc.) and the calorimetric enthalpy of transition (ΔH_{cal}) was calculated by integration of the area under the normalized, baseline corrected thermogram. The van't Hoff enthalpy was determined by:

$$\Delta H_{vH} = \frac{4RT^2\Delta C_{p,max}}{\Delta H_{cal}} \quad (1)$$

where $\Delta C_{p,max}$ is the maximum excess heat capacity [27,58]. The ratio $\Delta H_{vH}/\Delta H_{cal}$ is a measure of the average number of lipids per cooperative unit [65,66]. This measure is

considered to be an approximate estimation because thermograms are rather broad and asymmetric for peptide–lipid systems.

Solid state NMR spectroscopy

^{2}H-NMR experiments were performed at 76.77 MHz on a Bruker Avance DSX 500 (Bruker, Wissembeurg, France). A quadrupole echo pulse sequence ($\pi/2$-τ-$\pi/2$-τ-acquisition) [67] was used with an interpulse delay τ of 30 μs. The 90° pulse length was 5.6 μs and the repetition time 1.5 s. 2k–4k acquisitions were typically recorded and a Lorentzian line broadening of 100 Hz was used prior to Fourier transformation. Variable temperature spectra were acquired between 10 °C and 45 °C with a 5 °C interval; the temperature was regulated to ± 1 °C. Samples were allowed to equilibrate for 45 min between each temperature interval before the NMR signal was acquired. Additionally, one cycle (up and down) of temperature scans was performed to ensure reproducible and consistent measurements. First moments of NMR spectra were calculated by standard procedures [28]. To avoid zero values for the symmetrical spectra relative to the origin, a sign reversal was used for negative frequencies. When spectra are axially symmetric, M_1 may be used to directly estimate the chain average carbon-deuterium bond order parameter, S_{C^2H} by [68]:

$$\langle S_{C^2H}\rangle_{chain} = \frac{\sqrt{3}}{\pi A_Q} M_1 \qquad (2)$$

Because myristic fatty acyl chains are perdeuterated in DMPC, angular brackets represent the average over all labelled positions. A_Q is the static quadrupolar coupling constant (167 kHz) [69]. The relationship defined by Jarrell [46], was also used to characterize phase fractions during the order-disorder transition:

$$M_1 = fM_{1F} + (1-f)M_{1O} \qquad (3)$$

where f is the fraction of lipids in the fluid-disordered phase, and M_{1O} and M_{1F} are the first moments measured in the ordered phase prior to and in the fluid phase after the transition, respectively.

^{14}N and ^{31}P measurements were carried out on an 400 MHz Infinity spectrometer (Chemagnetics, Fort Collins, CO, USA) with a 4 mm double resonance MAS probe. ^{14}N-NMR spectra were acquired using a quadrupole echo sequence with a 200 μs interpulse delay and a $\pi/2$ pulse duration of 7.3 μs and a repetition rate of 300 ms. The isotropic shift of DMPC vesicles was used as an external reference (0.0 p.p.m.). The number of scans collected for static ^{14}N-NMR did not exceed 250 000.

^{31}P MAS NMR experiments were acquired under proton decoupling (40 kHz) using a single $\pi/2$-pulse with a duration of 6.5 μs. A Hahn echo sequence was applied for ^{31}P static measurements with an interpulse delay of 50 μs. All ^{31}P spectra were referenced externally to –0.9 p.p.m., using DMPC vesicles at 308 °K. Between 100 to 15000 transients were studied with a repetition time of 3 s. Calculation of the chemical shift anisotropy (CSA) was performed according to the formula $\Delta\sigma = \sigma_{//} - \sigma_{\perp}$.

Acknowledgements

We are grateful to Axelle Grelard for assistance and help with NMR and Bernard Desbat for discussions with respect to ATR (Université Bordeaux 1-ENITAB, France). Göran Lindblom, Lennart Johansson and Eric Rosenbaum are thanked for all their support (Umeå University). This work was supported by Knut and Alice Wallenberg Foundation, Swedish Research Council, Umeå University Biotechnology Fund and the Centre National de la Recherche Scientifique (CNRS). The Aquitaine region is acknowledged for providing funding for equipment. The Universities of Bordeaux 1 and Umeå are acknowledged for setting up a co-tutoring PhD program.

References

1 Costantini P, Jacotot E, Decaudin D & Kroemer G (2000) Mitochondrion as a novel target of anticancer chemotherapy. *J Natl Cancer Inst* **92**, 1042–1053.
2 Hengartner MO (2000) The biochemistry of apoptosis. *Nature* **407**, 770–776.
3 Okada H & Mak TW (2004) Pathways of apoptotic and non-apoptotic death in tumour cells. *Nat Rev Cancer* **4**, 592–603.
4 Thompson CB (1995) Apoptosis in the pathogenesis and treatment of disease. *Science* **267**, 1456–1462.
5 Ono M, Sawa Y, Ryugo M, Alechine AN, Shimizu S, Sugioka R, Tsujimoto Y & Matsuda H (2005) BH4 peptide derivative from Bcl-xL attenuates ischemia/reperfusion injury thorough anti-apoptotic mechanism in rat hearts. *Eur J Cardiothorac Surg* **27**, 117–121.
6 Kerr JF, Wyllie AH & Currie AR (1972) Apoptosis: a basic biological phenomenon with wide-ranging implications in tissue kinetics. *Br J Vancer* **26**, 239–257.
7 Cory S & Adams JM (2002) The BCL2 family: regulators of the cellular life-or-death switch. *Nat Rev Cancer* **2**, 647–656.
8 Jacotot E, Ravagnan L, Loeffler M, Ferri KF, Vieira HL, Zamzami N, Costantini P, Druillennec S, Hoebeke J, Briand JP *et al.* (2000) The HIV-1 viral protein R induces apoptosis via a direct effect on the mitochondrial permeability transition pore. *J Exp Med* **191**, 33–46.
9 Finucane DM, Bossy-Wetzel E, Waterhouse NJ, Cotter TG & Green DR (1999) Bax-induced caspase activation and apoptosis via cytochrome c release from

mitochondria is inhibitable by Bcl-xL. *J Biol Chem* **274**, 2225–2233.
10 Li H, Kolluri SK, Gu J, Dawson MI, Cao X, Hobbs PD, Lin B, Chen G, Lu J, Lin F *et al.* (2000) Cytochrome c release and apoptosis induced by mitochondrial targeting of nuclear orphan receptor TR3. *Science* **289**, 1159–1164.
11 Shimizu S, Narita M & Tsujimoto Y (1999) Bcl-2 family proteins regulate the release of apoptogenic cytochrome c by the mitochondrial channel VDAC. *Nature* **399**, 483–487.
12 Hanada M, Aime-Sempe C, Sato T & Reed JC (1995) Structure-function analysis of Bcl-2 protein. Identification of conserved domains important for homodimerization with Bcl-2 and heterodimerization with Bax. *J Biol Chem* **270**, 11962–11969.
13 Mikhailov V, Mikhailova M, Pulkrabek DJ, Dong Z, Venkatachalam MA & Saikumar P (2001) Bcl-2 prevents Bax oligomerization in the mitochondrial outer membrane. *J Biol Chem* **276**, 18361–18374.
14 Hotchkiss RS, McConnell KW, Bullok K, Davis CG, Chang KC, Schwulst SJ, Dunne JC, Dietz GP, Bahr M, McDunn JE *et al.* (2006) TAT-BH4 and TAT-Bcl-xL peptides protect against sepsis-induced lymphocyte apoptosis *in vivo*. *J Immunol* **176**, 5471–5477.
15 Klein D, Ribeiro MM, Mendoza V, Jayaraman S, Kenyon NS, Pileggi A, Molano RD, Inverardi L, Ricordi C & Pastori RL (2004) Delivery of Bcl-XL or its BH4 domain by protein transduction inhibits apoptosis in human islets. *Biochem Biophys Res Commun* **323**, 473–478.
16 Sugioka R, Shimizu S, Funatsu T, Tamagawa H, Sawa Y, Kawakami T & Tsujimoto Y (2003) BH4-domain peptide from Bcl-xL exerts anti-apoptotic activity *in vivo*. *Oncogene* **22**, 8432–8440.
17 Shimizu S, Konishi A, Kodama T & Tsujimoto Y (2000) BH4 domain of antiapoptotic Bcl-2 family members closes voltage-dependent anion channel and inhibits apoptotic mitochondrial changes and cell death. *Proc Natl Acad Sci USA* **97**, 3100–3105.
18 Baines CP, Kaiser RA, Sheiko T, Craigen WJ & Molkentin JD (2007) Voltage-dependent anion channels are dispensable for mitochondrial-dependent cell death. *Nat Cell Biol* **9**, 550–555.
19 Jurgensmeier JM, Xie Z, Deveraux Q, Ellerby L, Bredesen D & Reed JC (1998) Bax directly induces release of cytochrome c from isolated mitochondria. *Proc Natl Acad Sci USA* **95**, 4997–5002.
20 Yethon JA, Epand RF, Leber B, Epand RM & Andrews DW (2003) Interaction with a membrane surface triggers a reversible conformational change in Bax normally associated with induction of apoptosis. *J Biol Chem* **278**, 48935–48941.
21 Green DR & Reed JC (1998) Mitochondria and apoptosis. *Science* **281**, 1309–1312.
22 Loeffler M & Kroemer G (2000) The mitochondrion in cell death control: certainties and incognita. *Exp Cell Res* **256**, 19–26.
23 Kroemer G & Reed JC (2000) Mitochondrial control of cell death. *Nat Med* **6**, 513–519.
24 Zamzami N & Kroemer G (2001) The mitochondrion in apoptosis: how Pandora's box opens. *Nat Rev Mol Cell Biol* **2**, 67–71.
25 Mabrey S & Sturtevant JM (1976) Investigation of phase transitions of lipids and lipid mixtures by high sensitivity differential scanning calorimetry. *Proc Natl Acad Sci USA* **73**, 3862–3866.
26 Ivanova VP, Makarov IM, Schaffer TE & Heimburg T (2003) Analyzing heat capacity profiles of peptide-containing membranes: cluster formation of gramicidin A. *Biophys J* **84**, 2427–2439.
27 Sturtevant JM (1982) A scanning calorimetric study of small molecule-lipid bilayer mixtures. *Proc Natl Acad Sci USA* **79**, 3963–3967.
28 Davis JH (1983) The description of membrane lipid conformation, order and dynamics by H-2-Nmr. *Biochim Biophys Acta* **737**, 117–171.
29 Seelig J & Macdonald PM (1987) Phospholipids and proteins in biological membranes. Deuterium NMR as a method to study structure, dynamics, and interactions. *Acc Chem Res* **20**, 221–228.
30 Dufourc EJ, Parish EJ, Chitrakorn S & Smith ICP (1984) Structural and dynamical details of cholesterol-lipid interaction as revealed by deuterium NMR. *Biochemistry* **23**, 6062–6071.
31 Dufourc EJ, Maillet JC, Pott T & Leonard A (1993) P-31 NMR methods for investigating phospholipid-based molecular-structure and dynamics. *Phosphorus Sulfur and Silicon* **77**, 673–676.
32 Dufourc EJ, Mayer C, Stohrer J & Kothe G (1992) P-31 and H-1-NMR pulse sequences to measure lineshapes, T1z and T2e relaxation-times in biological-membranes. *J Chim Phys Pcb* **89**, 243–252.
33 Seelig J (1978) 31P nuclear magnetic resonance and the head group structure of phospholipids in membranes. *Biochim Biophys Acta* **515**, 105–140.
34 Lindstrom F, Williamson PT & Grobner G (2005) Molecular insight into the electrostatic membrane surface potential by 14n/31p MAS NMR spectroscopy: nociceptin-lipid association. *J Am Chem Soc* **127**, 6610–6616.
35 Rothgeb TM & Oldfield E (1981) Nitrogen-14 nuclear magnetic resonance spectroscopy as a probe of lipid bilayer headgroup structure. *J Biol Chem* **256**, 6004–6009.
36 Goormaghtigh E, Cabiaux V & Ruysschaert JM (1994) Determination of soluble and membrane protein structure by Fourier transform infrared spectroscopy. III. Secondary structures. *Subcell Biochem* **23**, 329–450.
37 Surewicz WK, Mantsch HH & Chapman D (1993) Determination of protein secondary structure by

Fourier transform infrared spectroscopy: a critical assessment. *Biochemistry* **32**, 389–394.
38 Moore WH & Krimm S (1976) Vibrational analysis of peptides, polypeptides, and proteins. II. beta-poly(L-alanine) and beta-poly(L-anaylglycine). *Biopolymers* **15**, 2465–2483.
39 Goormaghtigh E, Cabiaux V & Ruysschaert JM (1990) Secondary structure and dosage of soluble and membrane-proteins by attenuated total reflection Fourier-transform infrared-spectroscopy on hydrated films. *Eur J Biochem* **193**, 409–420.
40 Goormaghtigh E, Raussens V & Ruysschaert JM (1999) Attenuated total reflection infrared spectroscopy of proteins and lipids in biological membranes. *Biochim Biophys Acta* **1422**, 105–185.
41 Castano S & Desbat B (2005) Structure and orientation study of fusion peptide FP23 of gp41 from HIV-1 alone or inserted into various lipid membrane models (mono-, bi- and multibi-layers) by FT-IR spectroscopies and Brewster angle microscopy. *Biochim Biophys Acta* **1715**, 81–95.
42 Heimburg T (2000) A model for the lipid pretransition: coupling of ripple formation with the chain-melting transition. *Biophys J* **78**, 1154–1165.
43 Leonard A, Escrive C, Laguerre M, Pebay-Peyroula E, Neri W, Pott T, Katsaras J & Dufourc EJ (2001) Location of cholesterol in DMPC membranes. A comparative study by neutron diffraction and molecular mechanics simulation. *Langmuir* **17**, 2019–2030.
44 Weisz K, Grobner G, Mayer C, Stohrer J & Kothe G (1992) Deuteron nuclear-magnetic-resonance study of the dynamic organization of phospholipid cholesterol bilayer-membranes – molecular-properties and viscoelastic behavior. *Biochemistry* **31**, 1100–1112.
45 Dufourc EJ, Mayer C, Stohrer J, Althoff G & Kothe G (1992) Dynamics of phosphate head groups in biomembranes – comprehensive analysis using P-31 nuclear-magnetic-resonance lineshape and relaxation-time measurements. *Biophys J* **61**, 42–57.
46 Jarrell HC, Byrd RA & Smith IC (1981) Analysis of the composition of mixed lipid phases by the moments of 2H NMR spectra. *Biophys J* **34**, 451–463.
47 Lewis RN, Mak N & McElhaney RN (1987) A differential scanning calorimetric study of the thermotropic phase behavior of model membranes composed of phosphatidylcholines containing linear saturated fatty acyl chains. *Biochemistry* **26**, 6118–6126.
48 Mason JT (1998) Investigation of phase transitions in bilayer membranes. *Methods Enzymol* **295**, 468–494.
49 Pukala TL, Boland MP, Gehman JD, Kuhn-Nentwig L, Separovic F & Bowie JH (2007) Solution structure and interaction of cupiennin 1a, a spider venom peptide, with phospholipid bilayers. *Biochemistry* **46**, 3576–3585.
50 Carbone MA & Macdonald PM (1996) Cardiotoxin II segregates phosphatidylglycerol from mixtures with phosphatidylcholine: P-31 and H-2 NMR spectroscopic evidence. *Biochemistry* **35**, 3368–3378.
51 Lindstrom F, Bokvist M, Sparrman T & Grobner G (2002) Association of amyloid-beta peptide with membrane surfaces monitored by solid state NMR. *Phys Chem Chem Phys* **4**, 5524–5530.
52 Semchyschyn DJ & Macdonald PM (2004) Conformational response of the phosphatidylcholine headgroup to bilayer surface charge: torsion angle constraints from dipolar and quadrupolar couplings in bicelles. *Magn Reson Chem* **42**, 89–104.
53 Smith R, Separovic F, Bennett FC & Cornell BA (1992) Melittin-induced changes in lipid multilayers. A solid-state NMR study. *Biophys J* **63**, 469–474.
54 Petros AM, Medek A, Nettesheim DG, Kim DH, Yoon HS, Swift K, Matayoshi ED, Oltersdorf T & Fesik SW (2001) Solution structure of the antiapoptotic protein bcl-2. *Proc Natl Acad Sci USA* **98**, 3012–3017.
55 Khemtemourian L, Sani MA, Bathany K, Grobner G & Dufourc EJ (2006) Synthesis and secondary structure in membranes of the Bcl-2 anti-apoptotic domain BH4. *J Pept Sci* **12**, 58–64.
56 Terzi E, Holzemann G & Seelig J (1995) Self-association of beta-amyloid peptide (1-40) in solution and binding to lipid membranes. *J Mol Biol* **252**, 633–642.
57 Terzi E, Holzemann G & Seelig J (1997) Interaction of Alzheimer beta-amyloid peptide(1-40) with lipid membranes. *Biochemistry* **36**, 14845–14852.
58 Constantinides PP, Inouchi N, Tritton TR, Sartorelli AC & Sturtevant JM (1986) A scanning calorimetric study of the interaction of anthracyclines with neutral and acidic phospholipids alone and in binary mixtures. *J Biol Chem* **261**, 10196–10203.
59 Halstenberg S, Heimburg T, Hianik T, Kaatze U & Krivanek R (1998) Cholesterol-induced variations in the volume and enthalpy fluctuations of lipid bilayers. *Biophys J* **75**, 264–271.
60 Heimburg T & Biltonen RL (1996) A Monte Carlo simulation study of protein-induced heat capacity changes and lipid-induced protein clustering. *Biophys J* **70**, 84–96.
61 Ivanova VP & Heimburg T (2001) Histogram method to obtain heat capacities in lipid monolayers, curved bilayers, and membranes containing peptides. *Phys Rev E* **63**, 1914–1926.
62 Huster D, Scheidt HA, Arnold K, Herrmann A & Muller P (2005) Desmosterol may replace cholesterol in lipid membranes. *Biophys J* **88**, 1838–1844.
63 Marsan MP, Muller I, Ramos C, Rodriguez F, Dufourc EJ, Czaplicki J & Milon A (1999) Cholesterol orientation and dynamics in dimyristoylphosphatidylcholine bilayers: a solid state deuterium NMR analysis. *Biophys J* **76**, 351–359.
64 Sani MA, Loudet C, Grobner G & Dufourc EJ (2006) Pro-apoptotic bax-alpha1 synthesis and evidence for

beta-sheet to alpha-helix conformational change as triggered by negatively charged lipid membranes. *J Pept Sci* **13**, 100–106.

65 Epand RM & Sturtevant JM (1981) A calorimetric study of peptide-phospholipid interactions: the glucagon-dimyristoylphosphatidylcholine complex. *Biochemistry* **20**, 4603–4606.

66 Schuster B, Prassl R, Nigon F, Chapman MJ & Laggner P (1995) Core lipid structure is a major determinant of the oxidative resistance of low density lipoprotein. *Proc Natl Acad Sci USA* **92**, 2509–2513.

67 Davis JH (1979) Deuterium magnetic resonance study of the gel and liquid crystalline phases of dipalmitoyl phosphatidylcholine. *Biophys J* **27**, 339–358.

68 Beck JG, Mathieu D, Loudet C, Buchoux S & Dufourc EJ (2007) Plant sterols in 'rafts': a better way to regulate thermal shock to membranes. *FASEB J* **21**, 1714–1723.

69 Burnett LJ & Müller BH (1971) Deuteron quadrupolar coupling constants in three solid deuterated paraffin hydrocarbons: C_2D_6, C_4D_{10}, C_6D_{14}. *J Chem Phys* **55**, 5829–5831.

IV

How does the Bax-α1 targeting sequence interact with mitochondrial membranes: The role of cardiolipin

***Marc-Antoine Sani*[§, †], *Erick J. Dufourc** [§] *and Gerhard Gröbner** [†]

Running title: Bax-α1 affinity for cardiolipin

[§] **UMR 5248 CBMN, CNRS - Université Bordeaux 1 - ENITAB, IECB, 33607 Pessac Cedex, France**

[†] **Department of Chemistry, Umeå University, 90187 Umeå, Sweden**

*Corresponding authors:

- Gerhard Gröbner, Department of Chemistry, Umeå University, 901 87 Umeå, Sweden tel/fax: +46 907866346/7779; e-mail: gerhard.grobner@chem.umu.se
- Erick J. Dufourc, UMR 5248 CBMN CNRS - Université Bordeaux 1 - ENITAB, IECB 2 rue Robert Escarpit, 33607 Pessac, France, tel/fax +33 5 4000 2218, email: e.dufourc@iecb.u-bordeaux.fr

Key words: Apoptosis, Bax N-terminus, Cardiolipin, Solid-State NMR

Abstract

A key event in programmed cell death is the translocation of the apoptotic Bax protein from the cytosol towards mitochondria. The first helix localized at the N-terminus of Bax (Bax-α1) can act here as an addressing sequence, which directs activated Bax towards the mitochondrial surface. Solid state NMR (nuclear magnetic resonance), CD (circular dichroism) and ATR (attenuated total reflection) spectroscopy were used to elucidate this recognition process of a mitochondrial membrane system by Bax-α1. Two potential target membranes were studied, with the outer mitochondrial membrane (OM) mimicked by neutral phospholipids, while mitochondrial contact sites (CS) contained additional anionic cardiolipin. ^{1}H and ^{31}P magic angle spinning (MAS) NMR revealed Bax-α1 induced pronounced perturbations in the lipid headgroup region only upon cardiolipin presence. Bax-α1 could not insert into CS membranes but at elevated concentrations it inserted into the hydrophobic core of cardiolipin-free OM vesicles, thereby adopting β-sheet-like features, as confirmed by ATR. CD studies revealed, that the cardiolipin mediated electrostatic locking of Bax-α1 at the CS membrane surface promotes conformational change into an α-helical state; a process which seems to be necessary to induce further conformational transition events in activated Bax which finally cause irreversible membrane permeabilization during the mitochondrial apoptosis.

Programmed cell death is essential for the regulation of cell homeostasis in complex organisms. Failures in this physiological regulation trigger severe pathological diseases including autoimmune disorders, neuro-degeneration and cancer [1-3]. Induction of apoptosis via the mitochondrial pathway is mainly controlled by the Bcl-2 protein family which is made up of three different groups of proteins: the anti-apoptotic proteins including Bcl-2, all with four Bcl-2 homology domains (BH1-4); the pro-apoptotic proteins such as Bax with three Bcl-2 homology domains (BH1-3); and the BH3-only

proteins like Bid or Bad, which can activate pro-apoptotic proteins or inhibit anti-apoptotic proteins activities [4-6]. The interplay between these different protein fractions regulates the permeability of the mitochondrial membrane system, and in particular any release of apoptotic activator factors such as cytochrome c, which reside between the outer (OM) and the inner (IM) membranes of the mitochondrion [7-9].

While anti-apoptotic proteins are originally anchored at the outer mitochondrial membrane, the main pro-apoptotic protein, Bax, is located in the cytosol in an inactive form [10-12]. However, binding of an external apoptotic stimulus - often BH3 only proteins - to Bax protein will induce a conformational change into its active conformation. This process will expose Bax targeting/anchoring domains, thereby forcing its translocation to the mitochondria membrane, where it can exert its apoptotic role [10, 12-14]. It has been proposed that the first helix localized at the N-terminus (Nterm) of the Bax protein is an effective addressing sequence because its deletion prevents Bax localization into mitochondria while the very first amino acids are an inhibitory sequence [14, 15]. However, debates exists on which of the N-terminus or the C-terminus, or both of them, are required for the protein localization at OM membrane [16, 17]. Furthermore, the mechanism by which Bax induces the release of apoptotic factors is controversial, involving different locations of Bax activity and therefore an important role of the mitochondrial membrane composition. Especially, the role of cardiolipin, a mitochondrion specific phospholipid, for Bax functioning is hardly discussed but a recent study showed its importance for Bax targeting towards and functioning at mitochondrial membrane surface [18]. The Bax specific recognition prior activation of the mitochondrial membrane is still not understood and in order to address this question one clearly has to know how and where the activated Bax protein does target the complex mitochondrial membrane system.

Using several biophysical techniques, Solid state NMR (nuclear magnetic resonance), CD (circular dichroism) and ATR (attenuated total reflection) spectroscopy, we investigated the interactions between the supposed addressing sequence, the first helix of Bax (Bax-α1), (^{14}TSSEQIMKTGALLLQGFIQDRAGRM^{38}), with two potential target models – outer membrane

(OM) *versus* contact site (CS) mimicking vesicles. The OM membrane is mainly composed of neutral phosphatidylcholine and phosphatidylethanolamine lipids [19]. However, contact sites which reside between the inner and the outer membranes, are known to be highly enriched in the anionic phospholipid cardiolipin [20]. Depending on the target membrane, we observed two different interaction mechanisms (electrostatically driven *versus* hydrophobically driven) and membrane specific structural changes in the Bax-α1 peptide; information that is useful to elucidate the potential role of cardiolipin in the Bax addressing process.

Experimental Procedures

Materials

1-Palmitoyl-2-Oleoyl-*sn*-Glycero-3-Phosphocholine (POPC), 1-Palmitoyl-2-Oleoyl-*sn*-Glycero-3-Phosphoethanolamine (POPE), heart cardiolipin and chain deuterated 1-Palmitoyl ($^2H_{31}$)-2-Oleoyl-sn-Glycero-3-Phosphocholine ($^2H_{31}$-POPC) were purchased from Avanti Polar Lipids (Alabama, USA). The Bax-α1 peptide (^{14}TSSEQIMKTGALLLQGFIQDRAGRM^{38}) from the Bax human protein was synthesized by solid phase methods on an Applied Biosystems 433A Peptide Synthesizer (PE Biosystem, Courtaboeuf, France) [21]. The peptide purity was greater than 98% as controlled by UV and MALDI-TOF mass spectrometry.

Circular Dichroism (CD)

The lipids were dissolved in $CHCl_3$/CH_3OH (3:1 v/v) at the desired molar ratio and the solvent removed under vacuum. The lipid films were then re-suspended in water, followed by a lyophilization step. The fluffy lipid powders were finally re-suspended in a 20mM HEPES buffer containing 150 mM NaCl salt to reach a concentration of 3mM. Small unilamellar vesicles (SUV) were prepared by sonication using a tip sonicator (soniprep 150, MSE, Tokyo, Japan). CD-spectra (Jasco J-810 spectropolarimeter, USA) of peptide solutions were recorded between 190-250 nm using a 1 mm path-length quartz cell (Hellma, Germany). Samples were allowed to equilibrate 15 min at 35°C prior to

accumulation of 8 scans. The lipid background was subtracted. To estimate the peptide secondary structure content, an analysis of the relevant CD-spectra was carried out using the CDPro software (http://lamar.colstate.edu/~ssreeram/CDPro) developed by R. W. Woody and coworkers [22]. CD values were converted to mean residue ellipticity (MRE). The basis set 10 of the CDPro software was used [23]. Analysis was performed using three methods, CONTIN, CONTIN/LL, and SELCON 3 [24, 25]. In general, CONTIN/LL, a self-consistent method with an incorporated variable selection procedure, produced the most reliable results.

Polarized Attenuated Total Reflecxion spectroscopy (ATR)

ATR spectra were recorded on a Nicolet Magna 550 spectrometer (Ramsey, Minnesota, USA), equipped with a MCT detector cooled to 77 K, where the sample was sheared at the diamond ATR crystal surface (golden gate, Eurolabo, France). Deconvolution of the ATR spectra was done using Grams 32 software (Thermo electron). Because ATR spectroscopy is sensitive to the orientation of structures, spectra were recorded with a parallel (p) and perpendicular (s) polarization of the incident light with respect to the ATR plate [26, 27]. All the orientational information is then contained in the dichroic ratio $R_{ATR}= A_p/A_s$, where A_i represents the absorbance of the considered band for the p or s polarization of the incident light, respectively [28, 29]. Generally 1000 scans were accumulated at a resolution of 8 cm^{-1} and a two-level zero filling was performed.

Solid State Nuclear Magnetic Resonance Spectroscopy (NMR)

As described before, fluffy lipid powder mixtures were resuspended in identical HEPES buffer containing the desired amount of peptide to obtain 20:1 or 50:1 lipid-to-protein (L/P) molar ratios, and freeze-dried overnight. For ^{1}H NMR and ^{31}P NMR experiments, each sample (*ca.* 15mg of lipids) was re-suspended in 45 µL of $^{2}H_2O$ (75% hydration) followed by three freeze-thaw cycles to homogenize the multilamellar vesicle sample. For ^{2}H NMR, 1mg of $^{2}H_{31}$-POPC was added to each previous sample, followed by five freeze-thaw cycles and freeze-drying overnight. Each sample was finally re-suspended in 45µL deuterium-depleted water and homogenized.

^{1}H NMR and ^{31}P NMR measurements were carried out on a 400 MHz Infinity spectrometer (Chemagnetics, USA) with a 4 mm double resonance CP-MAS probe. ^{1}H NMR experiments were acquired by using a single π/2-pulse with 6 μs duration and a repetition delay of 3s at a magic angle spinning speed of 6 kHz. Spectra were referenced by setting the water signal to 4.7 ppm. ^{31}P MAS NMR experiments were acquired under proton decoupling (40 kHz) using a single π/2-pulse with 7 μs duration at spinning speed of 6 kHz [30]. A Hahn-echo pulse sequence was applied for static ^{31}P NMR measurements with an interpulse delay of 50 μs and a Lorentzian line broadening of 100 Hz was used prior to Fourier transformation. All ^{31}P NMR spectra were referenced externally to -0.9 ppm, using DMPC vesicles at 35°C. 100 to 15000 transients were co-added with a repetition time of 3 s.

^{2}H NMR experiments were performed at 76.77 MHz on a Bruker Avance DSX 500. A quadrupole echo pulse sequence (π/2-τ-π/2-τ-acquisition) [31] was used with an interpulse delay τ of 30 μs. The 90° pulse length was 3μs and the repetition time 1.5 s. 8k acquisitions were typically recorded and a Lorentzian line broadening of 200 Hz was used prior to Fourier transformation. Spectra were acquired at 35ºC and 25ºC; the temperature was regulated to ±1ºC. Samples were allowed to equilibrate for 30 min between each temperature before the NMR signal was acquired.

Results

CD and ATR spectroscopies were used to monitor conformational changes in the Bax-α1 domain upon its association to outer membrane (OM) and contact site (CS) membrane mimicking systems. The ion strength was varied to elucidate the contribution of electrostatics to the membrane affinity of the Bax-α1 peptide. ^{1}H MAS NMR was applied to follow changes across the whole lipid bilayer whereas wideline and MAS ^{31}P NMR provided a picture of peptide-induced structural and dynamical perturbations in the lipid headgroup region. Finally changes in the hydrophobic core of the membrane were monitored by using deuterium-labeled POPC and ^{2}H NMR.

Secondary structure of Bax-α1 upon titration with OM or CS mimicking lipid vesicles.

Membrane-mediated conformational behavior of Bax-α1 was characterized by circular dichroism (CD). For this purpose peptide in buffer solution was titrated with small unilamellar vesicles (SUV) composed either of POPC/POPE (65:35, molar ratio) mimicking the outer membrane (OM) or POPC/POPE/CL (43:36:21, molar ratio) mimicking the contact sites (CS) of mitochondria. Two different salt concentrations were used, 1mM or 50mM, in order to investigate the binding strength of Bax-α1 onto membranes.

In the absence of vesicles, Bax-α1 displays an equal partition (~30%) between random coil and β-sheet structures in buffer solution (1mM NaCl present), as previously reported [21]. Addition of POPC/POPE SUV to Bax-α1 at low ionic strength, induces weak changes, mainly aggregation as β-sheet structures, with the characteristic low intensities of a broad minimum at ca 218 nm and a maximum at ca 195 nm (Figure 1 panel A), which reaches its maximum value (47%) at L/P 100:1 (table1). Increase in ionic strength does not change significantly the peptide structural behavior during titration with neutral lipid vesicles (Figure 1, panel B). Upon titration with CS mimicking lipid vesicles , the peptide undergoes a strong conformational transition into dominant helical features with the typical minima at 222 and 208 nm and a maximum at ca.190 nm (see Figure 1, panel C). The maximum amount of helical structure is obtained at a L/P molar ratio of 50:1 with 47±5% of α-helix (see table 1). As shown in Figure 1 (panel D), the presence of NaCl at 50mM has no pronounced consequences in the peptide structural behavior upon titration.

MAS ^{1}H NMR on OM and CS multilamellar vesicles interacting with Bax-α1

MAS ^{1}H NMR was applied to monitor the degree of perturbation across the whole membrane, as reflected in the different molecular segments of the lipid molecules: hydrophobic chains and headgroup region. MAS ^{1}H NMR results for Bax-α1 interacting with the two different vesicle systems are shown in Figure 2 where signals arising from the acyl chains region (right panels) and those arising from headgroups region (left panels) are separately displayed. Adding the peptide to OM mimicking vesicles induces two new components at 1.12 ppm and 1.53 ppm, while no additional spectral components or severe modifications are visible in CS mimicking vesicles. The effect is more

pronounced at 20:1 L/P molar ratio. In contrast, the peptide does not disturb significantly the headgroups region of OM mimicking vesicles while severe broadening and intensity loss appear in the CS mimicking vesicles with a remarkable effect on the glycerol C1 resonance (4.35 ppm) and especially on the choline α of cardiolipin (4.12 ppm). Again, the broadening effect is more pronounced at 20:1 L/P molar ratio.

Bax-α1 strongly binds to negatively charged membrane surfaces

In order to investigate in more detail the structural and dynamical changes in the lipid headgroup region when Bax-α1 is approaching the mitochondrial membrane interfaces, wideline and high resolution MAS solid state ^{31}P NMR spectroscopy was carried out on mitochondrial OM and on CS mimicking multilamellar membrane models. In Figure 3 (left panel), wideline ^{31}P NMR spectra of OM vesicles exhibit a typical pattern of lipid bilayers in a fluid lamellar phase with axial symmetry before and upon addition of Bax-α1 peptide at 35°C. Because the phosphate groups in POPC and POPE possess distinct chemical shift anisotropy (CSA) values, the lineshape exhibits superimposed spectra arising from both lipids with well resolved 90° ($\sigma_{\perp}$) and 0° ($\sigma_{//}$) edges, giving a CSA value ($\sigma_{//}$-$\sigma_{\perp}$) of ca. 45 and 36 ppm, respectively. Addition of Bax-α1 peptide does not change significantly the CSA at any L/P molar ratio investigated but a small loss in the 90° edge resolution and a higher intensity in the 0° edge occur as often reported from the onset of low frequency membrane motions as promoted by membrane proteins [32, 33].

The lipid MLVs containing cardiolipin produce the same typical NMR lineshapes of a lamellar membrane phase as clearly seen in Figure 2 (right panel). Once again, POPC, POPE and cardiolipin contribute to the total lineshape but a broadening of the whole spectrum is observed, making a separate characterization of the CSA for each lipid component delicate. The presence of cardiolipin clearly induces a marked change in mobility/orientation of the headgroups region as seen in the reduction of CSA to ca. 27 ppm (left panel, bottom line). Addition of Bax-α1 produces a further decrease in CSA down to 26 ppm at a 50:1 L/P and to 25 ppm at 20:1 L/P molar ratios. The lineshape is noticeably modified with the 0° edge resolution partially vanished and a reduction in the 90° edge. With the

decrease of L/P ratio, the spectra are more and more broadened which might be due to severe changes in the transverse relaxation T_2 (onset of slow motions as lipid diffusion or collective membrane motion), as reported for cationic peptide interacting with membrane [34].

To observe peptide induced changes for each lipid component separately, high resolution ^{31}P MAS NMR was performed, where the PC, PE and CL phosphate signals are separated by their different isotropic chemical shift (σ_i) values. At 6 kHz spinning speed, the CSAs for all lipids are entirely averaged out and only isotropic chemical shift contributions are visible as seen in Figure 4. The resonances (σ_i) of the OM vesicles are -0.81 ppm and -0.18 ppm for POPC and POPE, respectively. At L/P 50, there is no change in the σ_i for both lipids but a slight upfield shift occurs at L/P 20 to -0.85 ppm and -0.21 ppm, respectively. However, the linewidth (FWHH) is broadened with increase of the peptide amount (see Table 2). The lipid molar ratio (65:35) between the integrals of isotropic resonances is nearly constant independently of the L/P molar ratio.

Because incorporation of cardiolipin increases the negative surface potential of the membrane, in the absence of peptide, a typical upfield shift occurs as described previously [30]. Indeed, three isotropic chemical shifts can be resolved at -0.71, -0.14 and 0.21 ppm corresponding to POPC, POPE and cardiolipin, respectively, with areas representative of the molar ratios 43:36:21. In the presence of Bax-α1 at a 50:1 L/P molar ratio, the deconvolution of the spectrum required addition of a broad fourth component (see supplementary material, Figure 1). This required fourth component has been described previously as a lipid pool reflecting the overlapped spectral contribution from the lipids proportion interacting with the peptide [35]. It is not well understood yet, but one can see it as lipid complexed with the peptide (overlapped components) while part of the lipids remains unperturbed. The σ_i are approximately identical as for the free-peptide vesicles, the fourth component is sitting at -0.26 ppm (see table 2). From the deconvolution, the composition of the fourth component would represent 33% of the total area. The FWHHs are greatly affected by the presence of the peptide, as seen in table 2, with a higher broadening occurring for the cardiolipin. Addition of further peptide (L/P 20:1) increases significantly this effect, by even reducing further the σ_i to -0.78 (POPC), -0.15 (POPE) and particularly

the cardiolipin to 0.11 ppm, while the fourth component is shifted upfield to -0.22 ppm. Again, the FWHHs are considerably increased, especially for cardiolipin, while approximately constant for the fourth component (see table 2). Interestingly, the area of this later increased consequently, corresponding to 60% of the whole spectrum which supports the idea of partition between peptide-free and peptide-interacting lipid pools. Indeed, the cardiolipin depletion in the peptide-free lipid pool would move towards neutral membrane potential as reflected in the chemical shift and the opposite for the peptide-interacted lipid pool, nevertheless with less effect due to the peptide potential compensation.

Cardiolipin prevents deep insertion of Bax-α1 into the hydrophobic membrane core

To monitor the impact of Bax-α1 on the lipid hydrophobic core, we incorporated a small fraction (6.7%) of $^{2}H_{31}$-POPC lipid into these model bilayers. Although these NMR spectra are difficult to acquire, this procedure induced only very minor modification to the lipid/lipid and lipid/peptide initial ratios and the physico-chemical behavior of theses membranes. Pure spectra of $^{2}H_{31}$-POPC MLV were compared to the peptide-free ones (cardiolipin-containing or not) to check whether the deuterated lipid was well incorporated. Results (spectra not shown) lead to much lower splittings for pure $^{2}H_{31}$-POPC liposomes (23 kHz and 2.1 kHz for "plateau" – labeled carbon positions 2-8, near the interface - and chain end – methyl terminal at C16 - regions, respectively) than with POPC/POPE or POPC/POPE/CL containing MLV (see figure 5) and no overlap could be noticed meaning that no pure POPC liposomes were coexisting in solution.

As seen in figure 5 (left panel), at 35ºC the POPC/POPE membrane is entirely in the L_{α} fluid state and exhibits fast intra- and intermolecular axially symmetric motions with defined plateau and methyl group regions. The "plateau" region has a quadrupolar splitting of ca. 27.5 kHz, and the terminal methyl group a splitting of 3.1 kHz. Addition of Bax-α1 triggers a reduction for both the "plateau", from 27.5 kHz to 26 kHz, and methyl region, from 3.1 kHz to 2.6 kHz, at L/P ratio 20:1 while ratio L/P 50:1 shows slight perturbations. Addition of cardiolipin to POPC/POPE liposomes increases the $^{2}H_{31}$-POPC dynamics as observed by the reduced "plateau" quadrupolar splitting of 25.5 kHz (Figure

5, right panels). Further addition of Bax-α1 does not disturb significantly the plateau region (less than 0.5kHz reduction for both ratios) or the methyl region (rather identical splittings).

In order to conclude at a possible insertion of Bax-1 in OM mimicking membranes, polarized ATR was performed on Bax-α1 added to oriented lipid multibilayers of POPC/POPE (65:35, molar ratio) in ratio L/P 20:1 prepared in the same way as for NMR sample (see supplementary material, Figure 2). The dichroic ratios ($R^{ATR} = \frac{A_p}{A_s}$) of the 1620 cm^{-1} and 1680 cm^{-1} bands were used to evaluate the anti-parallel β-sheet orientation versus the normal of the bilayer. Values of 0.95±0.03 and 1.13±0.21, respectively, were found and correspond to angle values of 56°±10 versus the bilayer normal and 40°±10 versus the β-strand axis according to Tamm et al. [29]. However, it is not possible to distinguish between oriented and inoriented peptide population since these values represent an average.

Discussion

The major outcome of our experimental findings is summarized in Figure 6, where a molecular mechanism of Bax-α1 interacting with different mitochondrial target membranes is presented. Clearly the affinity of occurring lipid-peptide interactions depends on the membrane composition: Bax-α1 interacts with neutral membranes mimicking the outer mitochondrial membranes only at high concentration causing insertion and membrane disordering. However, cardiolipin promotes strong and preferential electrostatic interactions with Bax-α1 which is locked onto the negatively charged surface over the whole concentration range used. Bax-α1 also undergoes severe conformational changes with adopting α-helical features if cardiolipin containing membranes are present while it slightly aggregates as anti-parallel beta sheet structure into OM membranes. All these aspects will be discussed below, with implications for the potential regulative addressing of Bax protein in the mitochondrial apoptotic pathway.

Electrostatic versus hydrophobic forces driving Bax-α1 localisation

All NMR results which were obtained for three different reporter nuclei, support a small effect of Bax-α1 peptide on neutral OM membranes except at high concentration where insertion is promoted. Indeed, ^{1}H NMR and ^{2}H NMR showed a perturbation in the CH_2/CH_3 region while ^{31}P NMR indicated a weak perturbation of the OM membrane headgroup. The ratio dependence of the disordering effect of the hydrophobic core, seen by the reduction of the quadrupolar splittings in ^{2}H NMR, is due to an increase of the dynamics of the acyl chains; which indicates an increase of peptide population inserted into the membrane, as already observed for amphipathic peptides [36, 37] and might not be a specific feature of Bax-α1 property. However, the presence of negatively charged cardiolipin to the lipid bilayers mimicking CS clearly attracts Bax-α1 onto the surface. As seen in the ^{1}H NMR and ^{31}P NMR results, Bax-α1 interacts strongly with the headgroup region of the membrane and especially with cardiolipin, without any pronounced perturbation of the hydrophobic bilayer core. This observation can directly be connected to the fact the two phosphate groups of cardiolipin are exposed to the peptide, triggering a strong electrostatic interaction with the three positive charges of Bax-α1. Therefore, one can assume that cardiolipin has the possibility to trap Bax-α1. Inspecting the ^{31}P NMR resonance integrals, as summarized in Table 2, cardiolipin appears to be the most involved lipid in the 4th component population, the so-called peptide-interacting lipid pool. Only 24% of the total cardiolipin amount remains in a "free" phase compared to 42% or 44% for POPC or POPE, respectively. Bax-α1 preferential interaction with cardiolipin is further supported by the chemical shift of the "free" lipids towards a more neutral surface membrane [30]. Since the major difference between the two models is the presence of an anionic lipid, one can conclude that peptide insertion in OM is driven by a hydrophobic mechanism. The insertion is further supported by the ATR result at 20:1 L/P molar ratio that indicates an average peptide tilt inside the outer membrane core.

Peptide plasticity modulated by its environment

Neutral membranes promoted a 15% increase in β-sheet fraction of Bax-α1 which is most likely due to hydrophobic interactions during the insertion process. ATR experiments of the same peptide/membrane systems support the finding that Bax-α1 inserts in the membrane matrix as an anti-

parallel β-sheet at high concentration. Upon interaction with CS membranes, Bax-α1 is able to change its secondary structure between β-sheet and α-helix; an observation which is in accordance with our previous study where negatively charged membranes induced helical formation of Bax-α1 depending on the surface charge potential [21]. However, differences between DMPC and POPC/POPE are noticeable. Indeed, Bax-α1 seems to have less affinity for DMPC, inducing less structural changes, than with OM vesicles. It might come from a more compact and/or lower thickness of the hydrophobic core of DMPC membrane that would prevent the insertion of the peptide and therefore less structural changes, a phenomenon known as hydrophobic mismatch between membranes and spanning peptides [38, 39]. The remarkable ability of Bax-α1 to modify its secondary structure according to the lipid environment, the propensity of cardiolipin to trap the Nterm of Bax are two major findings for a further elucidation of the regulation of mitochondrial apoptosis and will therefore be discussed in the following section.

Potential biological implication for Bax targeting mitochondria

One of the key events in the regulation of apoptosis via the mitochondrial pathway is the translocation of Bax to the mitochondrion [7, 14, 40]. During this process pro- and anti-apoptotic proteins are strongly anchored at the mitochondrial membrane system in order to regulate the fate of the cell but one does not know how the regulation takes place. Indeed, there is a debate on whether Bax can form pores on its own or alternatively can interacts with native pores [41-44]. Furthermore, the NTerm *versus* the CTerm involvement in the Bax location is still versatile [15-17, 45]. However, there seems to be a consensus that a specific lipid environment is directly involved into insertion and/or regulation of the Bax protein [18, 42, 46-50].

We found that the potential addressing sequence of Bax has a low affinity for the OM membranes. But it has the ability to insert if a strong self-association occurs before entering in close contact. Interestingly, it has been shown that adding the first helix of Bax to a cytosolic protein lead to its translocation towards mitochondrial membranes. And not surprisingly, a L26G mutation decreased the association efficiency of Bax-α1-protein to mitochondria [45]. These findings agree with the results

presented here, since the mutation decreases the hydrophobicity of the Nterm and therefore reduces its insertion ability. Meanwhile, it stays unlikely that Bax recognizes the OM by its Nterm part considering that no strong auto-association of the full protein in solution has been found previously. However, we report that cardiolipin is required for the binding of the first helix of Bax protein to mitochondrial membrane which can be the first step in Bax addressing to mitochondria. It explains the given role of cardiolipin in apoptosis regulation. Indeed, CL was shown to be essential for Bax activation; depletion of CL in the OM would increase the cell resistance to apoptosis induction or that Bax-Bid-cardiolipin complexes are known to promote the release of cytochrome C or dextran molecules in membrane models [9, 18, 47, 51]. However, from our results, the insertion of Bax via its Nterm is either not promoted by interactions with contact sites or it is driven by another part of the protein. The Nterm could act as a pure targeting sequence as previously proposed, while the subsequent insertion steps would be promoted by other protein domains [16, 40, 52]. This would also explain recent contradictory findings that either the CTerm or the NTerm of Bax is responsible for its anchoring into mitochondria [16, 17, 45]. The specific interaction between cardiolipin and Bax-α1, as demonstrated herein, would then be required for addressing Bax to the correct location in the mitochondria, and the presence of cardiolipin in the OM could act as a strong signaling for Bax translocation.

Acknowledgements

We are grateful to Axelle Grelard, Bernard Desbat, (Université Bordeaux 1-ENITAB, France) and Göran Lindblom, Lennart Johansson and Eric Rosenbaum (Umeå University) for all their support. This work was supported by Knut and Alice Wallenberg Foundation, Carl Kempe Foundation, Swedish Research Council, Umeå University Insamlingsstiftelse and the Centre National de la Recherche Scientifique (CNRS). The Aquitaine region is acknowledged for equipment funding and the universities of Bordeaux 1 and Umeå for setting up a co-tutoring Ph.D. program.

Supporting Information Available

Figure S1, Deconvolution of ^{31}P MAS NMR of POPC/POPE/CL (43:36:21, molar ratio) with Bax-α1 added at a 50:1 L/P and at a 20:1 L/P molar ratios. Figure S2, polarized ATR spectra of Bax-α1 added to oriented POPC/POPE (65:35, molar ratio) membrane in ratio L/P 20:1.

Reference

[1] H. Okada, T.W. Mak, Pathways of apoptotic and non-apoptotic death in tumour cells, Nature Reviews Cancer 4 (2004) 592-603.

[2] C.B. Thompson, Apoptosis in the Pathogenesis and Treatment of Disease, Science 267 (1995) 1456-1462.

[3] J.F. Kerr, A.H. Wyllie, A.R. Currie, Apoptosis: a basic biological phenomenon with wide-ranging implications in tissue kinetics, British journal of cancer 26 (1972) 239-257.

[4] S. Cory, J.M. Adams, The BCL2 family: Regulators of the cellular life-or-death switch, Nature Reviews Cancer 2 (2002) 647-656.

[5] M.O. Hengartner, The biochemistry of apoptosis, Nature 407 (2000) 770-776.

[6] G. Kroemer, Mitochondrial control of apoptosis: an overview, Biochem. Soc. Symp. 66 (1999) 1-15.

[7] D.M. Finucane, E. Bossy-Wetzel, N.J. Waterhouse, T.G. Cotter, D.R. Green, Bax-induced caspase activation and apoptosis via cytochrome c release from mitochondria is inhibitable by Bcl-xL, J. Biol. Chem. 274 (1999) 2225-2233.

[8] E. Jacotot, P. Costantini, E. Laboureau, N. Zamzami, S.A. Susin, G. Kroemer, Mitochondrial membrane permeabilization during the apoptotic process, Ann N Y Acad Sci 887 (1999) 18-30.

[9] J.M. Jurgensmeier, Z. Xie, Q. Deveraux, L. Ellerby, D. Bredesen, J.C. Reed, Bax directly induces release of cytochrome c from isolated mitochondria, Proc. Natl. Acad. Sci. USA 95 (1998) 4997-5002.

[10] Y.T. Hsu, K.G. Wolter, R.J. Youle, Cytosol-to-membrane redistribution of Bax and Bcl-X-L during apoptosis, Proc. Natl. Acad. Sci. USA 94 (1997) 3668-3672.

[11] G. Kroemer, J.C. Reed, Mitochondrial control of cell death, Nat. Med. 6 (2000) 513-519.

[12] X. Roucou, J.C. Martinou, Conformational change of Bax: a question of life or death, Cell Death Differ. 8 (2001) 875-877.

[13] M. Suzuki, R.J. Youle, N. Tjandra, Structure of Bax: Coregulation of dimer formation and intracellular localization, Cell 103 (2000) 645-654.

[14] I.S. Goping, A. Gross, J.N. Lavoie, M. Nguyen, R. Jemmerson, K. Roth, S.J. Korsmeyer, G.C. Shore, Regulated targeting of BAX to mitochondria, J. Cell. Biol. 143 (1998) 207-215.

[15] P.F. Cartron, M. Priault, L. Oliver, K. Meflah, S. Manon, F.M. Vallette, The N-terminal end of Bax contains a mitochondrial-targeting signal, J. Biol. Chem. 278 (2003) 11633-11641.

[16] A.J. Valentijn, J.P. Upton, N. Bates, A.P. Gilmore, Bax targeting to mitochondria occurs via both tail anchor-dependent and -independent mechanisms, Cell Death Differ. (2008).

[17] L. Lalier, P.F. Cartron, P. Juin, S. Nedelkina, S. Manon, B. Bechinger, F.M. Vallette, Bax activation and mitochondrial insertion during apoptosis, Apoptosis 12 (2007) 887-896.

[18] S. Lucken-Ardjomande, S. Montessuit, J.C. Martinou, Contributions to Bax insertion and oligomerization of lipids of the mitochondrial outer membrane, Cell Death Differ. 15 (2008) 929-937.

[19] D. Ardail, J.P. Privat, M. Egret-Charlier, C. Levrat, F. Lerme, P. Louisot, Mitochondrial contact sites. Lipid composition and dynamics, J. Biol. Chem. 265 (1990) 18797-18802.

[20] M. Schlame, D. Rua, M.L. Greenberg, The biosynthesis and functional role of cardiolipin, Prog. Lipid Res. 39 (2000) 257-288.

[21] M.A. Sani, C. Loudet, G. Grobner, E.J. Dufourc, Pro-apoptotic bax-alpha1 synthesis and evidence for beta-sheet to alpha-helix conformational change as triggered by negatively charged lipid membranes, J. Pept. Sci. 13 (2006) 100-106.

[22] N. Sreerama, R.W. Woody, A self-consistent method for the analysis of protein secondary structure from circular dichroism, Anal. Biochem. 209 (1993) 32-44.

[23] N. Sreerama, R.W. Woody, Estimation of protein secondary structure from circular dichroism spectra: comparison of CONTIN, SELCON, and CDSSTR methods with an expanded reference set, Anal. Biochem. 287 (2000) 252-260.

[24] N. Sreerama, R.W. Woody, Estimation of protein secondary structure from circular dichroism spectra: Comparison of CONTIN, SELCON, and CDSSTR methods with an expanded reference set, Anal. Biochem. 287 (2000) 252-260.

[25] N. Sreerama, R.W. Woody, Analysis of protein CD spectra: Comparison of CONTIN, SELCON3, and CDSSTR methods in CDPro software, Biophys. J. 78 (2000) 334A-334A.

[26] E. Goormaghtigh, V. Cabiaux, J.M. Ruysschaert, Secondary Structure and Dosage of Soluble and Membrane-Proteins by Attenuated Total Reflection Fourier-Transform Infrared-Spectroscopy on Hydrated Films, Eur. J. Biochem. 193 (1990) 409-420.

[27] E. Goormaghtigh, V. Raussens, J.M. Ruysschaert, Attenuated total reflection infrared spectroscopy of proteins and lipids in biological membranes, Biochim. Biophys. Acta 1422 (1999) 105-185.

[28] E. Goormaghtigh, V. Cabiaux, J.M. Ruysschaert, Determination of soluble and membrane protein structure by Fourier transform infrared spectroscopy. III. Secondary structures, Subcell. Biochem. 23 (1994) 329-450.

[29] L.K. Tamm, S.A. Tatulian, Infrared spectroscopy of proteins and peptides in lipid bilayers, Q. Rev. Biophys. 30 (1997) 365-429.

[30] F. Lindstrom, P.T. Williamson, G. Grobner, Molecular insight into the electrostatic membrane surface potential by 14n/31p MAS NMR spectroscopy: nociceptin-lipid association, J. Am. Chem. Soc. 127 (2005) 6610-6616.

[31] J.H. Davis, Deuterium magnetic resonance study of the gel and liquid crystalline phases of dipalmitoyl phosphatidylcholine, Biophys. J. 27 (1979) 339-358.

[32] E.J. Dufourc, C. Mayer, J. Stohrer, G. Althoff, G. Kothe, Dynamics of Phosphate Head Groups in Biomembranes - Comprehensive Analysis Using P-31 Nuclear-Magnetic-Resonance Lineshape and Relaxation-Time Measurements, Biophys. J. 61 (1992) 42-57.

[33] E.J. Dufourc, C. Mayer, J. Stohrer, G. Kothe, P-31 and H-1-Nmr Pulse Sequences to Measure Lineshapes, T1z and T2e Relaxation-Times in Biological-Membranes, J. Chim. Phys. Pcb 89 (1992) 243-252.

[34] T.L. Pukala, M.P. Boland, J.D. Gehman, L. Kuhn-Nentwig, F. Separovic, J.H. Bowie, Solution structure and interaction of cupiennin 1a, a spider venom peptide, with phospholipid bilayers, Biochemistry 46 (2007) 3576-3585.

[35] B.B. Bonev, W.C. Chan, B.W. Bycroft, G.C. Roberts, A. Watts, Interaction of the lantibiotic nisin with mixed lipid bilayers: a 31P and 2H NMR study, Biochemistry 39 (2000) 11425-11433.

[36] P.C. Dave, E.K. Tiburu, K. Damodaran, G.A. Lorigan, Investigating structural changes in the lipid bilayer upon insertion of the transmembrane domain of the membrane-bound protein phospholamban utilizing 31P and 2H solid-state NMR spectroscopy, Biophys. J. 86 (2004) 1564-1573.

[37] E.J. Dufourc, J. Dufourcq, T.H. Birkbeck, J.H. Freer, Delta-haemolysin from Staphylococcus aureus and model membranes. A solid-state 2H-NMR and 31P-NMR study, Eur. J. Biochem. 187 (1990) 581-587.

[38] J.A. Killian, Hydrophobic mismatch between proteins and lipids in membranes, Biochim. Biophys. Acta. 1376 (1998) 401-415.

[39] J.A. Killian, I. Salemink, M.R. de Planque, G. Lindblom, R.E. Koeppe, 2nd, D.V. Greathouse, Induction of nonbilayer structures in diacylphosphatidylcholine model membranes by transmembrane alpha-helical peptides: importance of hydrophobic mismatch and proposed role of tryptophans, Biochemistry 35 (1996) 1037-1045.

[40] E. Er, L. Oliver, P.F. Cartron, P. Juin, S. Manon, F.M. Vallette, Mitochondria as the target of the pro-apoptotic protein Bax, Biochim. Biophys. Acta 1757 (2006) 1301-1311.

[41] C.P. Baines, R.A. Kaiser, T. Sheiko, W.J. Craigen, J.D. Molkentin, Voltage-dependent anion channels are dispensable for mitochondrial-dependent cell death, Nat. Cell Biol. 9 (2007) 550-555.

[42] G. Basanez, J.C. Sharpe, J. Galanis, T.B. Brandt, J.M. Hardwick, J. Zimmerberg, Bax-type apoptotic proteins porate pure lipid bilayers through a mechanism sensitive to intrinsic monolayer curvature, J. Biol. Chem. 277 (2002) 49360-49365.

[43] S. Shimizu, A. Konishi, T. Kodama, Y. Tsujimoto, BH4 domain of antiapoptotic Bcl-2 family members closes voltage-dependent anion channel and inhibits apoptotic mitochondrial changes and cell death, Proc. Natl. Acad. Sci. USA 97 (2000) 3100-3105.

[44] S. Shimizu, M. Narita, Y. Tsujimoto, Bcl-2 family proteins regulate the release of apoptogenic cytochrome c by the mitochondrial channel VDAC, Nature 399 (1999) 483-487.

[45] P.F. Cartron, C. Moreau, L. Oliver, E. Mayat, K. Meflah, F.M. Vallette, Involvement of the N-terminus of Bax in its intracellular localization and function, FEBS Lett. 512 (2002) 95-100.

[46] J.A. Yethon, R.F. Epand, B. Leber, R.M. Epand, D.W. Andrews, Interaction with a membrane surface triggers a reversible conformational change in Bax normally associated with induction of apoptosis, J. Biol. Chem. 278 (2003) 48935-48941.

[47] T. Kuwana, M.R. Mackey, G. Perkins, M.H. Ellisman, M. Latterich, R. Schneiter, D.R. Green, D.D. Newmeyer, Bid, Bax, and lipids cooperate to form supramolecular openings in the outer mitochondrial membrane, Cell 111 (2002) 331-342.

[48] R.F. Epand, J.C. Martinou, S. Montessuit, R.M. Epand, Transbilayer lipid diffusion promoted by Bax: implications for apoptosis, Biochemistry 42 (2003) 14576-14582.

[49] J. Jiang, Z. Huang, Q. Zhao, W. Feng, N.A. Belikova, V.E. Kagan, Interplay between bax, reactive oxygen species production, and cardiolipin oxidation during apoptosis, Biochem. Biophys. Res. Commun. 368 (2008) 145-150.

[50] B. Leber, J. Lin, D.W. Andrews, Embedded together: the life and death consequences of interaction of the Bcl-2 family with membranes, Apoptosis 12 (2007) 897-911.

[51] Q. Van, J. Liu, B. Lu, K.R. Feingold, Y. Shi, R.M. Lee, G.M. Hatch, Phospholipid scramblase-3 regulates cardiolipin de novo biosynthesis and its resynthesis in growing HeLa cells, Biochem. J. 401 (2007) 103-109.

[52] H. Arokium, N. Camougrand, F.M. Vallette, S. Manon, Studies of the interaction of substituted mutants of BAX with yeast mitochondria reveal that the C-terminal hydrophobic alpha-helix is a second ART sequence and plays a role in the interaction with anti-apoptotic BCL-x(L), J. Biol. Chem. 279 (2004) 52566-52573.

Figure Caption:

Figure 1

CD spectra of Bax-α1 peptide at 35^{o} C upon titration by vesicles composed of POPC/POPE (65:35, molar ratio) at 1mM NaCl (A) and 50mM of NaCl (B); by vesicles composed of POPC/POPE/CL (43:36:21, molar ratio) with 1mM of NACl (C) and 50mM NaCl (D) present. The lipid to peptide molar ratios (L/P) depicted in the four panels are 100 (triangle), 50 (circle), 20 (square) and pure peptide in HEPES buffer at pH 7 (solid line).

Figure 2

^{1}H MAS NMR spectra at 6kHz spinning speed at 35ºC of multilamellar vesicles composed of POPC/POPE (65:35, molar ratio) (top) and of POPC/POPE/CL (43:36:21, molar ratio) (bottom) at different region: acyl chain region (right panels) and headgroups region (left panels). Pure MLVs (bottom spectrum); Bax-α1 added at a 50:1 L/P (middle spectrum) and at a 20:1 L/P molar ratios (top spectrum).

Figure 3

Static ^{31}P NMR spectra of peptide-free MLVs composed of POPC/POPE (65:35, molar ratio) mimicking the outer membrane composition (left panel) and of POPC/POPE/CL (43:36:21, molar ratio) mimicking the contact site composition (right panel) at 35ºC. Pure MLVs (bottom) with Bax-α1 added at a 50:1 L/P (middle) and at a 20:1 L/P molar ratios (top).

Figure 4

^{31}P MAS NMR spectra at 6kHz spinning speed at 35ºC for peptide-free MLVs composed of POPC/POPE (65:35, molar ratio) mimicking the outer membrane composition (left panel) and of POPC/POPE/CL (43:36:21, molar ratio) mimicking the contact site composition (right panel). Pure MLVs (bottom) with Bax-α1 added at a 50:1 L/P (middle) and at a 20:1 L/P molar ratios (top).

Figure 5

Static ^{2}H NMR spectra of MLVs composed of POPC/POPE (65:35, molar ratio) (panel A, B) and of POPC/POPE/CL (43:36:21, molar ratio) (panel C, D) at 35ºC: full spectrum (top panels) and methyl group region (bottom panels). Pure MLVs (bottom spectrum) with Bax-α1 added at a 50:1 L/P (middle spectrum) and at a 20:1 L/P molar ratios (top spectrum).

Figure 6

Biophysical model of Bax-α1 interaction with two different mimicked mitochondrial locations. Hydrophobic interactions occurring at the outer membrane, mainly composed of the neutral lipid POPC and POPE, induce partition between β-sheet inserted structures (especially at high concentration) and random coil conformation remaining in solution of Bax-α1. Contact site mimicked membrane, where native pores are stabilized (show as an example here), are enriched by the anionic cardiolipin. The negatively charged surface locks the peptide onto the surface by electrostatic interaction and triggers α-helical secondary structure change.

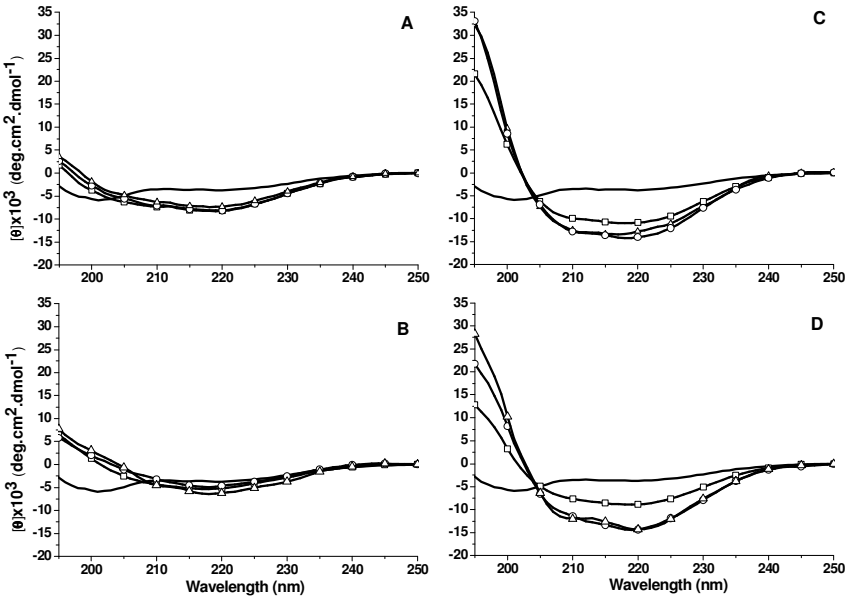

Fig 1 Sani et al.

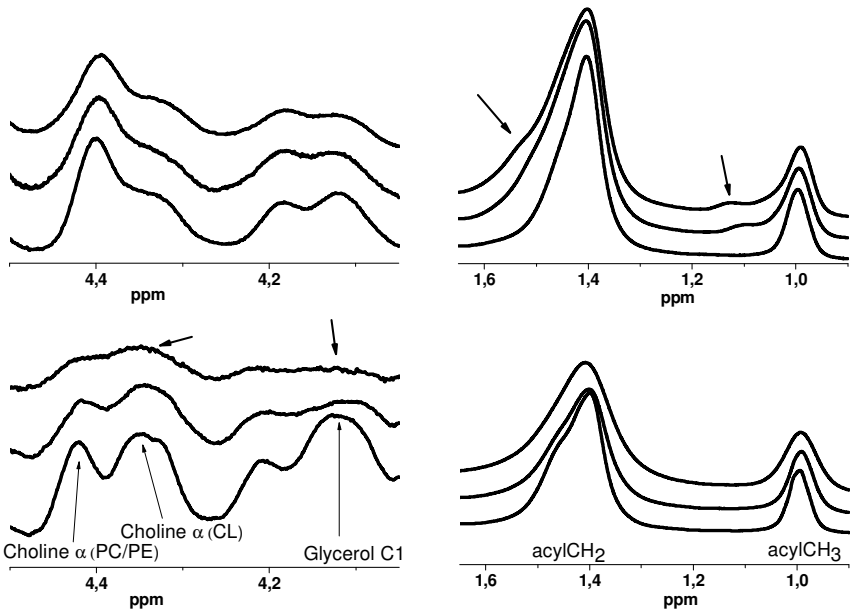

Fig 2 Sani et al.

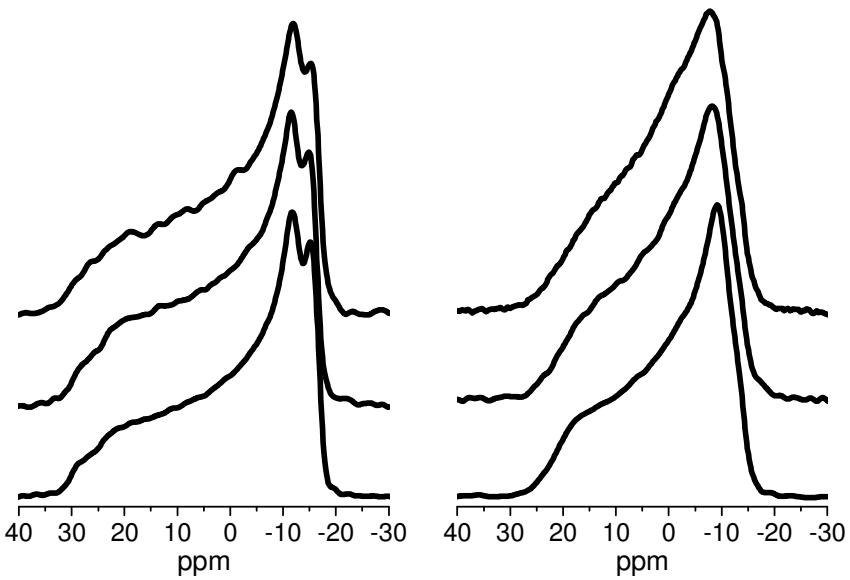

Fig 3 Sani et al.

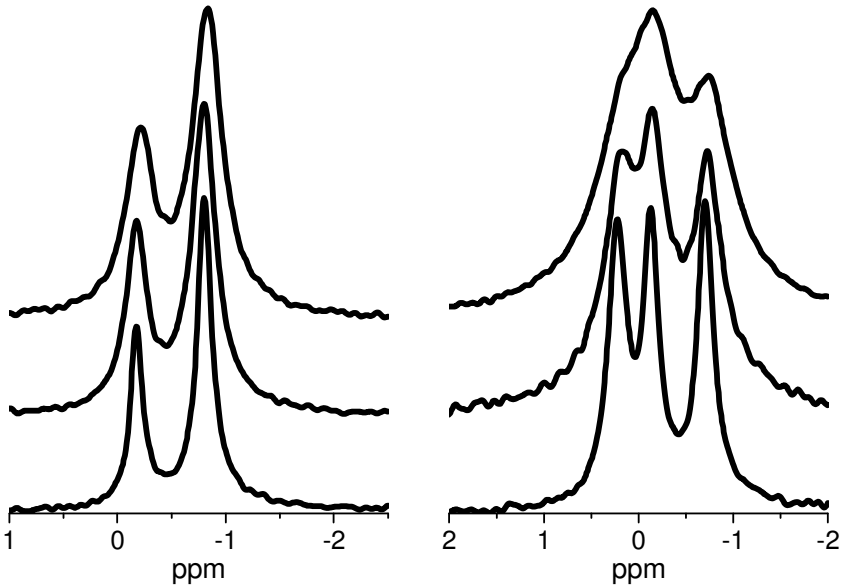

Fig 4 Sani et al.

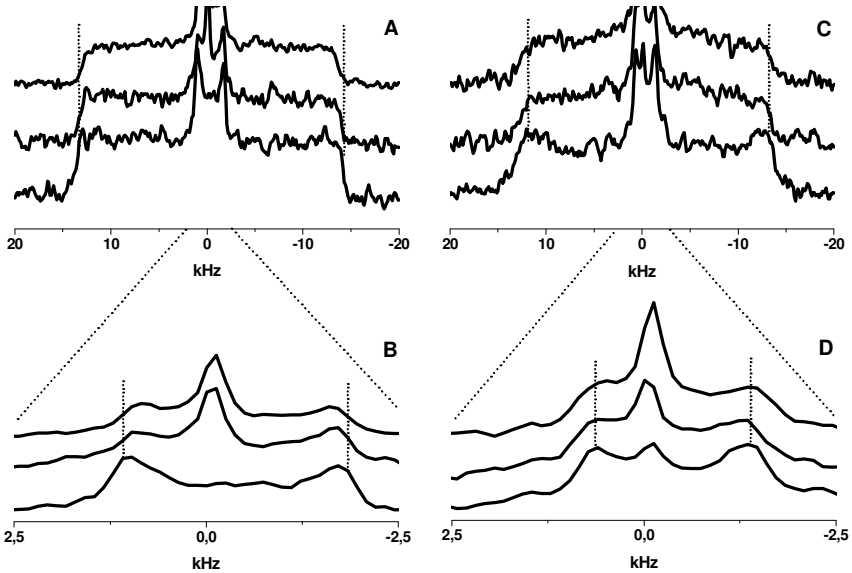

Fig 5 Sani et al.

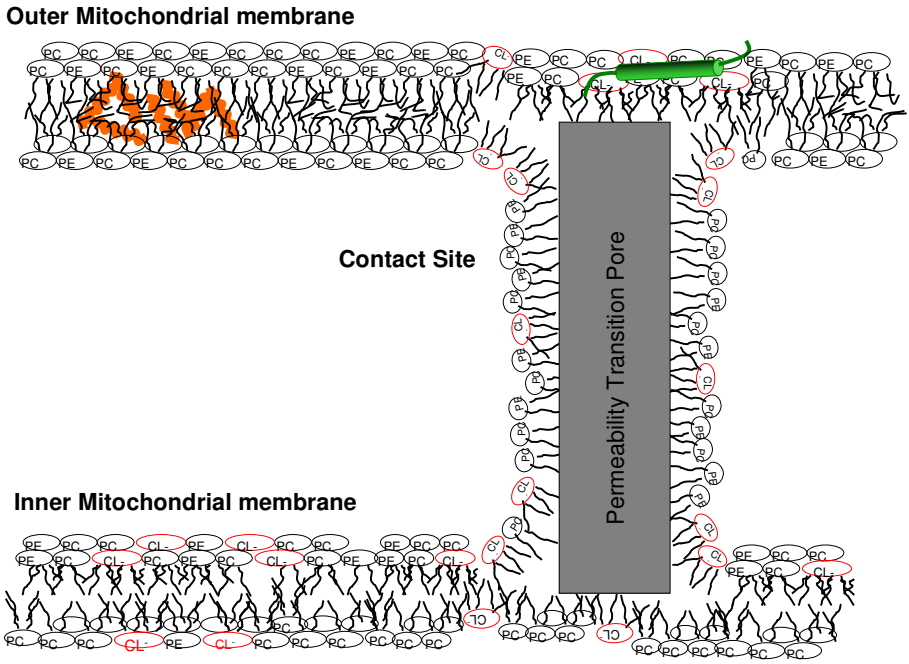

Fig 6 Sani et al.

V

Tracking lipid interactions in intact mitochondria under oxidative stress by *ex vivo* solid state ^{31}P NMR spectroscopy.

Marc-Antoine Sani [1,2]***, Olivier Keech***[3]***, Per Gardeström***[3]***, Erick J. Dufourc***[2]***, and Gerhard Gröbner*** [1*]

[1] Department of Chemistry, Umeå University, 90187 Umeå, Sweden

[2] UMR 5248 CBMN, CNRS - Université Bordeaux 1 - ENITAB, IECB, 33607 Pessac, France

[3] UPSC, Department of Plant Physiology, Umeå University, 901 87 Umeå, Sweden

Key words: *Ex vivo* solid-state NMR, isolated mitochondria, respiration, oxidative stress, membrane integrity, cardiolipin.

*Corresponding authors:

- Marc-Antoine Sani, Department of Chemistry, Umeå University, 901 87 Umeå, Sweden Tel/fax: +46 907865973/7779; UMR 5248 CBMN CNRS - Université Bordeaux 1 - ENITAB, IECB 2 rue Robert Escarpit, 33607 Pessac, France, Email: marco.sani@chem.umu.se
- Gerhard Gröbner, Department of Chemistry, Umeå University, 901 87 Umeå, Sweden tel/fax: +46 907866346/7779; e-mail: gerhard.grobner@chem.umu.se

We describe a non-invasive, high resolution solid state MAS NMR (Magic Angle Spinning Nuclear Magnetic Resonance) approach for tracking the behaviour of individual membrane components in fully functional biological systems during physiological processes. In the presented study we monitored, in atomic detail, responses of the main membrane phospholipids to external Ca^{2+} triggering programmed cell death (PCD) in live, isolated mitochondria, focusing on the fate of the mitochondrion-specific cardiolipin. The approach provided valuable insights into the complex mechanism of membrane-mediated programmed cell death. Furthermore, it could be easily applied in studies of other *ex vivo* responses of various organelles and cells to diverse physiological stimuli (drugs, signalling molecules, etc.).

Biological membranes and their constituents are involved in most essential processes in living organisms. These membranes have complex structures and features that enable them not only to act as cellular boundaries, but also to play crucial roles in cells' communications with their surroundings. For many years membrane lipids were seen as simple structural components, while membrane proteins were regarded as the functional units. However, evidence has recently emerged indicating that lipids play key roles in regulating numerous physiological activities, including signalling and programmed cell death [1]. However, unravelling in atomic detail the complex interactions involving lipids *in vivo* in their native biological membranes remains a severe challenge in modern structural biology.

Here, we propose a non-invasive, *ex vivo*, high-resolution solid state ^{31}P MAS NMR approach to track the behaviour of individual mitochondrial membrane lipids – in particular the mitochondrion-specific cardiolipin – in intact, active mitochondria, and the lipids' responses to external physiological stimuli such as induction of apoptotic stress by Ca^{2+} ions. We used fully functional, contaminant-free mitochondria from potato tubers as readily accessible, *ex vivo* proof-of-principle systems. After isolation in a Percoll gradient (Supplements), a fraction of pure mitochondria in a fully functionally state (Figure 1A), as demonstrated by respiratory controls (Supplementary Table 1), was loaded into an MAS NMR rotor. The survival and maintenance of integrity of these live

mitochondria under *ex vivo* MAS conditions (1 hour at 7°C and 3kHz spinning speed) was checked by examining wide-line ^{31}P NMR lineshapes (1 hour at 7°C after the MAS NMR experiments), as shown in Fig. 1A (lower spectrum), and oxygen consumption assays, in which the respiration rates obtained only slightly decreased under the applied NMR conditions (Supplementary Table 1).

In general, the observed wideline ^{31}P NMR spectrum of the isolated mitochondria showed the typical axially symmetric pattern of phospholipids organized in a lamellar liquid-crystalline membrane (Figure 1A, lower spectrum), as previously reported for isolated mammalian mitochondria [2]. However, information about individual phospholipid components and their behaviour is not accessible by static NMR. Therefore, we applied high resolution MAS ^{31}P NMR to detect the individual lipid components and track their behavior. The MAS NMR method simply separates overlapping static NMR spectra into distinct isotropic resonances, separated by characteristic lipid-specific chemical shift (σ_i) values [3], as seen in Fig. 1B (lower spectrum). The MAS NMR spectrum of whole mitochondria displays two strong resonances, at -0.79 ppm and -0.25 ppm, corresponding to the main mitochondrial lipid components, phosphatidylcholine (PC) and phophatidylethanolamine (PE), respectively. A third, but broad component, visible at 0.36 ppm, presumably indicates cardiolipin, the third major phospholipid of mitochondrial membranes [4,5]. This assumption is supported by the NMR control spectrum of protein-free vesicles composed of mitochondrial lipid extracts (supplements), in which the CL component is clearly visible as a sharp resonance at 0.05 ppm (Fig. 1B, upper spectrum). The broadening and down-field shift of the CL signals in intact mitochondria probably reflect its formation of strong complexes with proteins, especially the paramagnetic cytochrome c [6]. Interestingly, lipid extracts of these mitochondria are still able to assemble into bilayers with an intact membrane organization (Fig. 1A, upper spectrum), although the lipids display higher degrees of dynamic freedom in them, as reflected in reductions of CSA values from 34±1 ppm for intact mitochondrial membranes to 28±1 ppm.

To visualize losses of mitochondrial integrity in response to external stimuli by MAS NMR, we initially exposed intact mitochondria to harsh treatments (incubation for 24 h at room temperature or sonication for 15 min).

In both cases, the ^{31}P MAS NMR spectra indicated complete breakdown of the mitochondria's membrane integrity. Notably, narrow NMR resonances characteristic of PC, PE and CL components appeared at -0.16 ppm, 0.37 ppm and 0.74 ppm, respectively (Fig. 1C), indicating the presence of fast tumbling, smaller membrane fragments or micellar structures (also visible in static NMR spectra as isotropic components; spectra not shown). The loss of protein-lipid interactions was also apparent, most markedly for CL, for which the disintegration of its complex with cytochrome C (linebroadening) resulted in a clear, sharp resonance as found in pure lipid extracts (Fig. 1B). In addition, there was also a pronounced downfield shift in the NMR resonances of all lipids following the harsh treatments, probably due to differential packing of lipids in small fragments with high surface curvature accompanied by changes in the pKa of the lipids under these conditions [7,8].

Physiological fragmentation of mitochondria upon Ca^{2+} overload

Calcium ions play a major role in induction of the so-called mitochondrial permeability transition (MPT) [9,10], in which mitochondrial membranes swell and become substantially more permeable to low molecular weight substances (processes we can monitor using our NMR approach). Ca^{2+}-induced MPT can also lead to the release of cytochrome C and, ultimately, activation of PCD in both plants and animals [11,12].As the NMR spectra displayed in Fig. 2A (left panel) show, addition of calcium to intact, isolated mitochondria promoted severe membrane disruption and disintegration, accompanied by increases in the isotropic contributions of small fragments to the static NMR spectrum, e.g. from 5% to 31% following the addition of 10 mM Ca^{2+} (Figure 2B). In addition, the measured CSA of the remaining powder pattern declined from ca. 34 to ca. 21 ppm in the presence of 10 mM Ca^{2+}. High resolution ^{31}P NMR spectra were also acquired after adding calcium, to freshly prepared samples, at various concentrations, ranging from 0 to 10 mM (Fig. 2A, right panel). The PC and PE resonances at -0.79 ppm and -0.25 ppm became broader following additions of up to 1 mM Ca^{2+}, but at Ca^{2+} concentrations $\geq$ 1

mM, two new components appeared, at -0.05 ppm and 0.45 ppm, that became dominant at 10 mM Ca^{2+}.The overall shift observed is similar to that observed in our deliberately disrupted mitochondria (s. Figure 1C), thus the rearrangement of phospholipids into small vesicles is also promoted by calcium overload [13-15]. A low field peak can also be seen at around 2 ppm, originating from inorganic phosphate, which was added before the measurements to facilitate Ca^{2+} uptake. A progressive upfield shift was observed, especially at 5 mM Ca^{2+}, due to acidification arising from the internal proton gradient of the mitochondria. However, at 10 mM Ca^{2+}, the integrity of the mitochondria was severely compromised and Pi buffered the pH back to 7.2, resulting in a resonance close to 2 ppm.

Addition of Ca^{2+} decreased both the respiratory rates of the isolated mitochondria and their respiratory control ratios (RCRs), but did not inhibit their respiration completely (Supplementary Table 1), indicating that calcium induced leaks of the mitochondrial metabolites. Taken together with the absence of a free cardiolipin signal in corresponding NMR spectra, cardiolipin was presumably still tightly bound to the inner membrane under these conditions, although calcium-induced mitochondrial swelling had promoted partial disruption of the outer membrane and accelerated the lipid dynamics.

Conclusion

The high resolution ^{31}P MAS NMR approach presented here appears to be a valuable, non-invasive tool for investigating biological processes in conditions as close as currently possible to *in vivo* states. It enabled us to follow the behaviour of the mitochondrion-specific phospholipid cardiolipin – a major player in apoptosis – in fully intact, live mitochondria and to dissect the specific interactions of this lipid with proteins (mainly cytochrome c) during the course of their physiological responses to apopototic stimuli. Monitoring the response of mitochondrial membrane lipids by our approach can therefore provide valuable insights into the complex mechanisms of membrane-mediated programmed cell death at the mitochondrion level. Furthermore, the NMR approach could be extended to study membrane lipid components in many other intact biological

systems (organelles, whole cells and living tissues) and even – following *in vivo* isotopic labelling of specific membrane proteins – the structural behaviour of membrane proteins and their interactions under physiological conditions.

Acknowledgements

This work was supported by the Knut and Alice Wallenberg Foundation, Kempe Foundation, Swedish Research Council, Umeå University Insamlingsstiftelse and the Centre National de la Recherche Scientifique (CNRS). Financial support was provided by the Swedish Graduate Research School in Functional Genomics and Bioinformatics. Bordeaux 1 and Umeå Universities are acknowledged for establishing a co-tutoring PhD program.

Reference

1. M. R. Wenk, *Nat. Rev. Drug Discov*. **4** (7), 594 (2005).
2. B. De Kruijff, R. Nayar, and P. R. Cullis, *Biochim. Biophys. Acta* **684** (1), 47 (1982).
3. F. Lindstrom, P. T. Williamson, and G. Grobner, *J. Am. Chem. Soc.* **127** (18), 6610 (2005).
4. D. Ardail, J. P. Privat, M. Egret-Charlier et al., *J. Biol. Chem.* **265** (31), 18797 (1990).
5. K. Edman and I. Ericson, *Biochem. J.* **243** (2), 575 (1987).
6. K. Beyer and M. Klingenberg, *Biochemistry* **24** (15), 3821 (1985).
7. T. J. Pinheiro and A. Watts, *Biochemistry* **33** (9), 2451 (1994).
8. M. A. Swairjo, B. A. Seaton, and M. F. Roberts, *Biochim. Biophys. Acta* **1191** (2), 354 (1994).
9. S. Arpagaus, A. Rawyler, and R. Braendle, *J. Biol. Chem.* **277** (3), 1780 (2002).
10. F. Fortes, R. F. Castilho, R. Catisti et al., *J. Bioenerg. Biomembr.* **33** (1), 43 (2001).
11. G. R. Degasperi, J. A. Velho, K. G. Zecchin et al., *J. Bioenerg. Biomembr.* **38** (1), 1 (2006).
12. A. P. Halestrap and A. M. Davidson, *Biochem. J.* **268** (1), 153 (1990).
13. J. Balk, C. J. Leaver, and P. F. McCabe, *FEBS Lett.* **463** (1-2), 151 (1999).
14. M. T. Grijalba, A. E. Vercesi, and S. Schreier, *Biochemistry* **38** (40), 13279 (1999).
15. G. Petrosillo, F. M. Ruggiero, M. Pistolese et al., *J. Biol. Chem.* **279** (51), 53103 (2004).

Figure Legends

Figure 1

Solid-Sate *ex vivo* ^{31}P NMR spectroscopy of mitochondria isolated from a potato tuber. (A) A pure fraction of potato mitochondria was recovered by centrifugation, and their integrity was checked by respiratory measurements of controls (not shown) and static ^{31}P NMR spectroscopy (upper spectrum) at 7°C. Mitochondrial lipids were extracted in organic solvent and re-suspended in the extraction buffer (lower spectrum), showing an identical lamellar organization. (B) Signals from individual components resolved by mild magic angle spinning ^{31}P NMR at 3kHz, showing phosphatidylcholine (PC), phosphatidylethanolamine (PE) and cardiolipin (CL) to be the major components (upper spectrum), as detected for extracted lipids (lower spectrum). The integrity of the mitochondria was checked after the MAS measurements (1 h MAS + 1 h static NMR) at 7°C and only slight reductions in RCR values and respiratory rates were detected. (C) Following natural degradation (induced by incubating mitochondria at 37°C for 24 h, middle spectrum) or mechanical degradation (by sonication, upper spectrum), the membrane disintegrated into small isotropic vesicles, resulting in shifts in the lipids' resonances, as depicted by the schematic diagram.

Figure 2

Mitochondrial membrane responses to Ca^{2+} stress. (A) Solid-state *ex vivo* ^{31}P NMR spectra from isolated mitochondria in the presence of various concentrations of Ca^{2+}, under static (left spectra) and MAS (right spectra) conditions at 7°C. The dotted line shows the gradual resonance shift, as shown in Figure 1C, for degraded mitochondria. (B) Isotropic area as a proportion of the total spectral area as a function of Ca^{2+} concentration. Errors bars are plotted according to the signal to noise ratio. (C) Results of respiratory tests of pure isolated mitochondria (left trace) and mitochondria incubated in the presence of 1 mM Ca^{2+} (right trace).

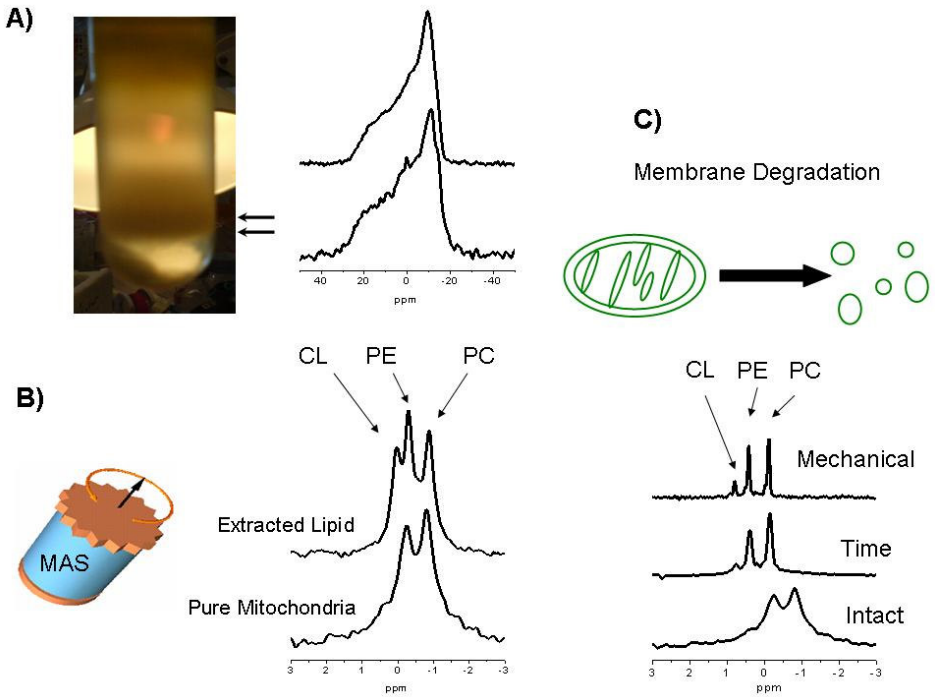
A)
40
20
0
-20
-40
ppm
C)
Membrane Degradation
B)
MAS
CL
PE
PC
Extracted Lipid
Pure Mitochondria
3
2
1
0
-1
-2
-3
ppm
CL
PE
PC
Mechanical
Time
Intact
3
2
1
0
-1
-2
-3
ppm

Figure 1

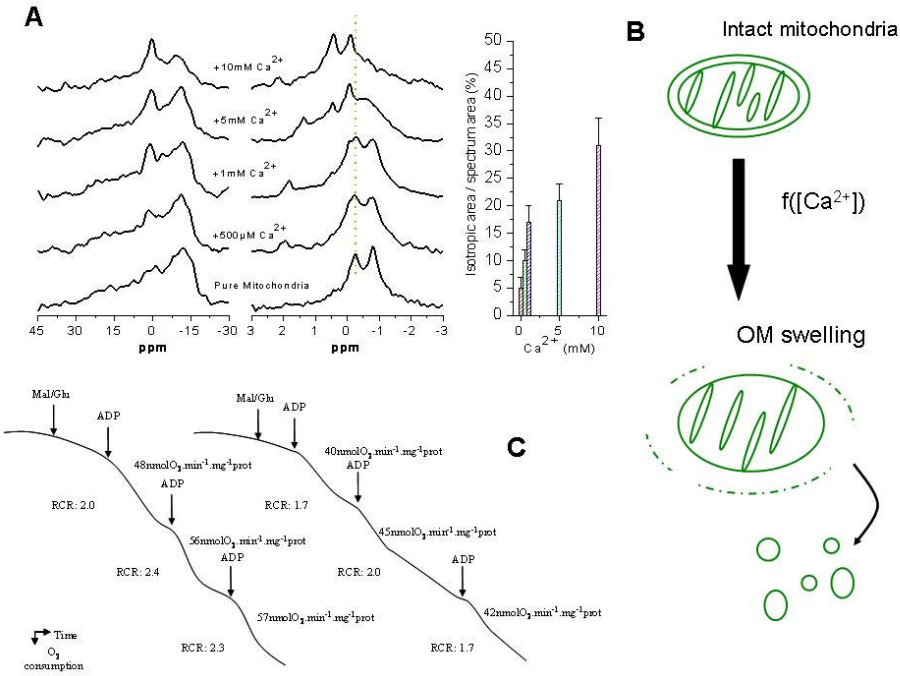
A
+10mM Ca2+
+5mM Ca2+
+1mM Ca2+
+500µM Ca2+
Pure Mitochondria
ppm
ppm
Isotropic area / spectrum area (%)
Ca2+ (mM)
B
Intact mitochondria
f([Ca2+])
OM swelling
C
Mal/Glu
ADP
48nmolO2.min-1.mg-1prot
RCR: 2.0
56nmolO2.min-1.mg-1prot
RCR: 2.4
57nmolO2.min-1.mg-1prot
RCR: 2.3
40nmolO2.min-1.mg-1prot
RCR: 1.7
45nmolO2.min-1.mg-1prot
RCR: 2.0
42nmolO2.min-1.mg-1prot
RCR: 1.7
Time
O2 consumption

Figure 2

Supplementary Material

Table 1 Respiratory rates and respiratory control ratios (RCRs) of mitochondria isolated from potato tubers

	Fresh mitochondria*	After NMR measurements
Respiratory rates ($nmolO_2.min^{-1}.mg^{-1}$)	41 ±3	37 ±5
RCRs**	3 ±0.2	1.8 ±0.2

* Measurements performed after extraction.
** Significantly different from control values (T-test) at $p<0.01$

Experimental Procedures

Isolation of pure mitochondria

Potato (*Solanum tuberosum* L.) tubers were purchased from local producers, and mitochondria were isolated from them, at 4°C, largely according to Petit et al (1987). Briefly, 2 kg of potato tubers were ground with a juice machine in extraction buffer (KOH-adjusted pH, 7.5) containing 30 mM MOPS, 0.3 M mannitol, 1 mM EDTA, 0.5% PVP-40, 0.5% BSA and 8 mM cysteine. After two differential centrifugations (2500 g for 5 min and 12000 g for 12 min), mitochondria were pelleted, then resuspended in 1 mL of washing buffer and finally loaded on top of 28% (v/v) Percoll gradients in Percoll/washing buffer containing 10 mM MOPS and 0.3 M mannitol (KOH-adjusted, pH 7.2). The gradients were centrifuged for 40 min at 40 000 g and purified mitochondria were collected, from close to the bottom of the gradients, with a Pasteur pipette, diluted 20-fold with the Percoll/washing buffer and subjected to a final centrifugation at 12000 g for 15 min to pellet the pure mitochondria. The buffer was discarded and approximately 400µL of isolated mitochondrial pellet at *ca.* 150 $mg.mL^{-1}$ of proteins (quantified as described below) were finally recovered and stored at 4°C

Respiratory measurements

Mitochondrial suspensions with a final volume of 1 mL were prepared for the respiratory measurements, containing the cofactor NAD (nicotinamide adenine dinucleotide) to avoid loss of activity during the NMR experiments, and both malate and glutamate as substrates to stimulate respiratory complexes of the mitochondrial electron transport chain and avoid accumulation of OAA (oxaloacetic acid) in the mitochondrial matrix. Mitochondrial respiration was then stimulated by adding 100 µM ADP and oxygen consumption was recorded. Proteins were quantified using a *DC* protein assay kit from Bio-Rad (Hercules, CA, USA).

Lipid extraction from isolated mitochondria

Lipids were extracted from the mitochondria isolated from potato tubers following the Folch method. Briefly, isolated mitochondria were homogenized in a sonication bath for approximately 3 min with chloroform/methanol (2:1) to a final dilution of the extract of 20:1. The homogenate was passed through a paper filter, the crude extract was washed with 20% of its volume with water, the resulting phases were separated by centrifugation and the upper phase was removed. The organic solvents were evaporated under vacuum, then milli-Q water was added and the resuspended lipid vesicles were freeze-dried overnight. From 200 µL of isolated mitochondria suspension (containing ca. 150 mg/mL of proteins), approximately 7.5 mg of lipids was extracted.

Solid State Nuclear Magnetic Resonance Spectroscopy (NMR)

^{31}P NMR measurements were carried out using a 400 MHz Infinity spectrometer (Chemagnetics, USA) with either a 4 mm or 5 mm double resonance CP-MAS probe (inner volume; 100 or 150 µL, respectively). ^{31}P MAS NMR data were acquired under proton decoupling (40 kHz) using a single $\pi/2$-pulse with 7 µs duration and 3 kHz spinning speed. A Hahn echo sequence was applied for static wide-line ^{31}P static measurements with an interpulse delay of 50 µs and Lorentzian line broadening of 100 Hz was used prior to Fourier transformation. All ^{31}P NMR spectra were referenced externally to -0.9 ppm [3], using DMPC vesicles at 35°C. 1200 transients were added with a repetition time of 3 s. Spectra were deconvoluted using an internal Spinsight module

(Varian/Chemagnetics, Fort Collins, CO), and both isotropic and full spectrum areas were determined using the OriginPro 7.5 integration module (OriginLAb corporation, USA). The temperature was maintained at 35°C ±1 °C.